University of Zurich[UZH]

Lecture 3: Experimental techniques

ISAPP 2024: Particle Candidates for Dark Matter
Scuola Galileiana di Studi Superiori
Padova, July 4, 2024

Laura Baudis
University of Zurich

Content

- Cryogenic experiments at mK temperatures
    - Principles of phonon mediated detectors
    - Detection of fast and thermalised phonons
    - Temperature measurements: thermistors, SC transition sensors
    - Phonon and charge/light detectors
    - Examples
- Sodium Iodide Detectors
- Bubble chambers
- Ionisation detectors
- New technologies

Content

- Noble liquids
  - Properties of noble liquids as radiation detection media
  - The ionisation and scintillation processes in noble liquids
  - Electronic and nuclear recoils
  - Scintillation and ionisation yields
  - Electron attachment and electron drift lifetime, purity monitors
  - Energy calibration and resolution, the W-value
  - Pulse shape discrimination
- Single-phase detectors; examples
- Time projection chambers and detection principles; examples
- Summary

Cryogenic experiments at mK

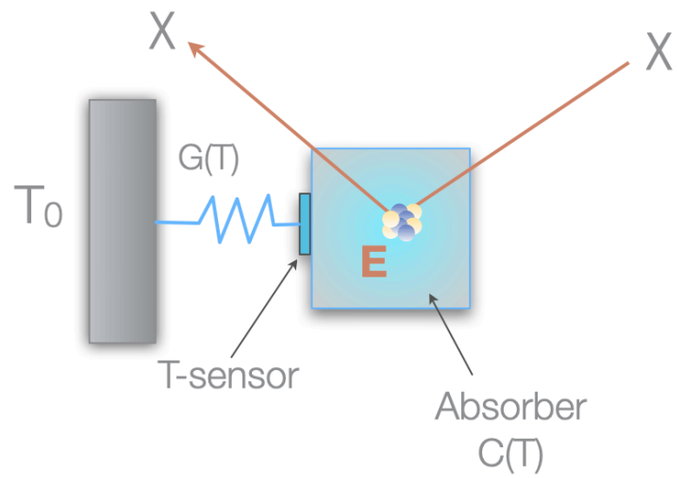

Cryogenic Experiments at mK Temperatures

- Principle: phonon (quanta of lattice vibrations) mediated detectors
- **Motivation:** increase the energy resolution + detect smaller energy depositions (lower the threshold); use a variety of absorber materials
- The energy resolution (W = FWHM) of a semiconductor detector (N = nr. of e^--h excitations)

$$W_{stat} = 2.35\sqrt{F\epsilon E} \qquad \frac{\sigma(E)}{E} = \sqrt{\frac{F}{N}} = \sqrt{\frac{F\epsilon}{E}} \qquad W_{stat} = 2.35\,\sigma(E)$$

- E = deposited energy, F = Fano factor; N = E/ε; in Si: ε = 3.6 eV/e^--h pair (band gap is 1.2 eV! - where does 70% of the energy go?), F→ the energy loss in a collision is not purely statistical (=0.13 in Ge; 0.11 in Si)
- Example: maximum phonon energy in Si: 60 meV
  - **many more phonons are created than e^--h pairs!**
- For dark matter searches:
  - **thermal phonon detectors (measure an increase in temperature)**
  - **athermal phonon detectors (detect fast, non-equilibrium phonons)**
- Detector made from superconductors: the superconducting energy gap 2Δ~ 1 meV
  - binding energy of a Cooper pair (equiv. of band gap in semiconductors); 2 quasi-particles for every unbound Cooper pair; these can be detected → in principle large improvement in energy resolution

Basic Principles of mK Cryogenic Detectors

- A deposited energy E (ER or NR) will produce a temperature rise ΔT given by:

$$\Delta T = \frac{E}{C(T)} e^{-\frac{t}{\tau}} \qquad \tau = \frac{C(T)}{G(T)}$$

C(T) = heat capacity of absorber

G(T) = thermal conductance of the link between the absorber and the reservoir at temperature T_0

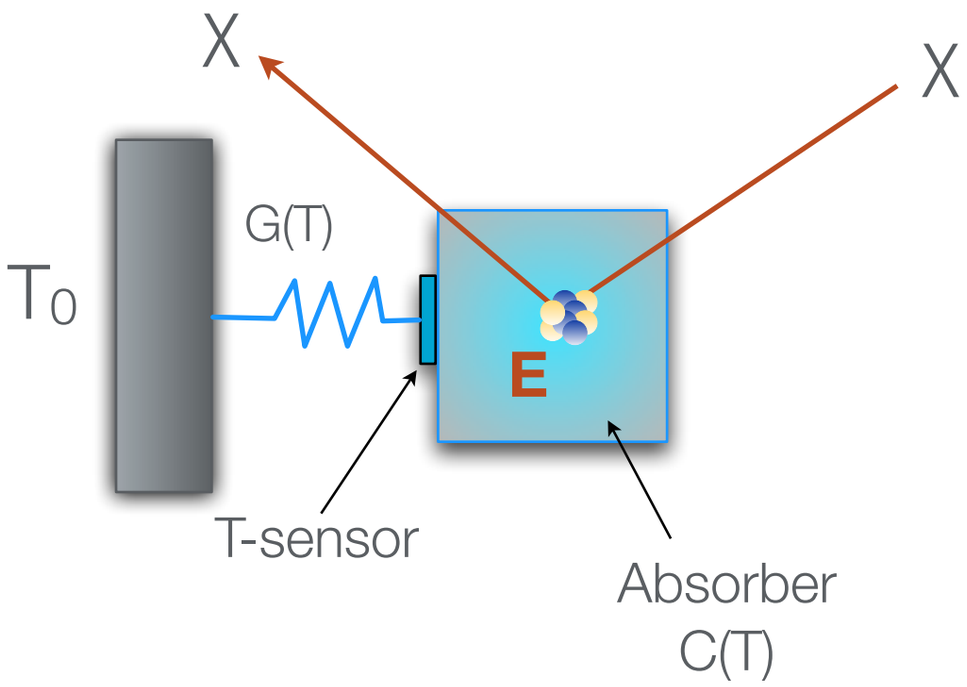

Normal metals: the electronic part of C(T) ~ T, and dominates the heat capacity at low temperatures

Superconductors: the electronic part is proportional to $\exp(-T_c/T)$

(T_c = superconducting transition temperature)

and is negligible compared to lattice contributions for $T \ll T_c$

Basic Principles of mK Cryogenic Detectors

- For pure dielectric crystals and superconductors at $T \ll T_c$, the heat capacity is given by:

$$C(T) \sim \frac{m}{M}\left(\frac{T}{\theta_D}\right)^3 \ \mathrm{J\,K^{-1}}$$

m = absorber mass

M = molecular weight of absorber

Θ_D = Debye temperature (at which the highest frequency gets excited) $\theta_D = \frac{h\nu_m}{k}$

➡ the lower the T, **the larger the ΔT per unit of absorbed energy**

➡ in thermal detectors E is measured as the temperature rise ΔT

- **Example:** at T = 10 mK, a 1 keV energy deposition in a 100 g detector increases the temperature by:

$$\Delta T \approx 1\,\mu K$$

➡ this can be measured!

Thermal Detectors

- Ideal case of a perfect calorimeter: all the energy is converted into heat and the resulting T-rise is measured
- For a superconductor as absorber: a fraction of the energy goes into breaking of Cooper pairs creating electronic excitations called *quasiparticles*, which will not all recombine on the timescale to be measured as a thermal pulse (also, the phonons are far from equilibrium and must first decay to lower energy phonons and become thermalised, before ΔT can be measured)
- For a finite thermalisation time τ_{th}, the time behaviour of the thermal pulse is given by:

$$T(t) = T_0 + \frac{E}{C(T)} \frac{\tau}{\tau - \tau_{th}} \left[e^{-t/\tau} - e^{-t/\tau_{th}} \right] \qquad \tau = \frac{C(T)}{G(T)}$$

- Rise time of the pulse: in general at least 1 μs (limited by detector physics)
- Decay time: several ms ⇒ < few Hz counting rates for thermal detectors

Thermal Detectors

- The intrinsic energy resolution (as FWHM) of such a calorimeter is given by (k_B is the Boltzmann constant):

$$W = 2.35\xi\sqrt{k_B T^2 C(T)} \qquad \frac{C(T)}{k_B} = \text{number of phonon modes}$$

$$\xi = 1.5 - 2$$

Info about the sensor. the thermal link and the T-dependance of C(T)

- Example for the theoretical expectation of the intrinsic energy resolution:
  - a 1 kg Ge crystal operated at 10 mK could achieve an energy resolution of about 10 eV ⇒ two orders of magnitude better than Ge ionisation detectors
  - a 1 mg of Si at 50 mK could achieve an energy resolution of 1 eV ⇒ two orders of magnitude better than conventional Si detectors

Temperature Sensors

- Semiconductor thermistor: a highly doped semiconductor such that *the resistance R is a strong function of temperature* (NTD = neutron-transmutation-doped Ge - uniformly dope the crystal by neutron irradiation)
- Superconducting (SC) transition sensor (TES/SPT): thin film of superconductor *biased near the middle of its normal/SC transition*

- In both cases, an energy deposition produces a change in the electrical resistance R(T). The response can be expressed in terms of the logarithmic sensitivity:

$$\alpha \equiv \frac{d\log(R(T))}{d\log(T)}$$

Typical values:

α = -10 to -1 for semiconductor thermistors

α ~ $+10^3$ for TES/SPT devices

→ the sensitivity of TES/SPTs can be extremely high (depending on the width of the SC/normal transition)

→ however, the temperature of the detector system must be kept very stable

Example: Thermal Detector with SPT-sensor

- The *change of resistance* due to a particle interaction in the absorber is detected by a superconducting quantum interference device (SQUID) (by the change in current induced in the input coil of the SQUID)

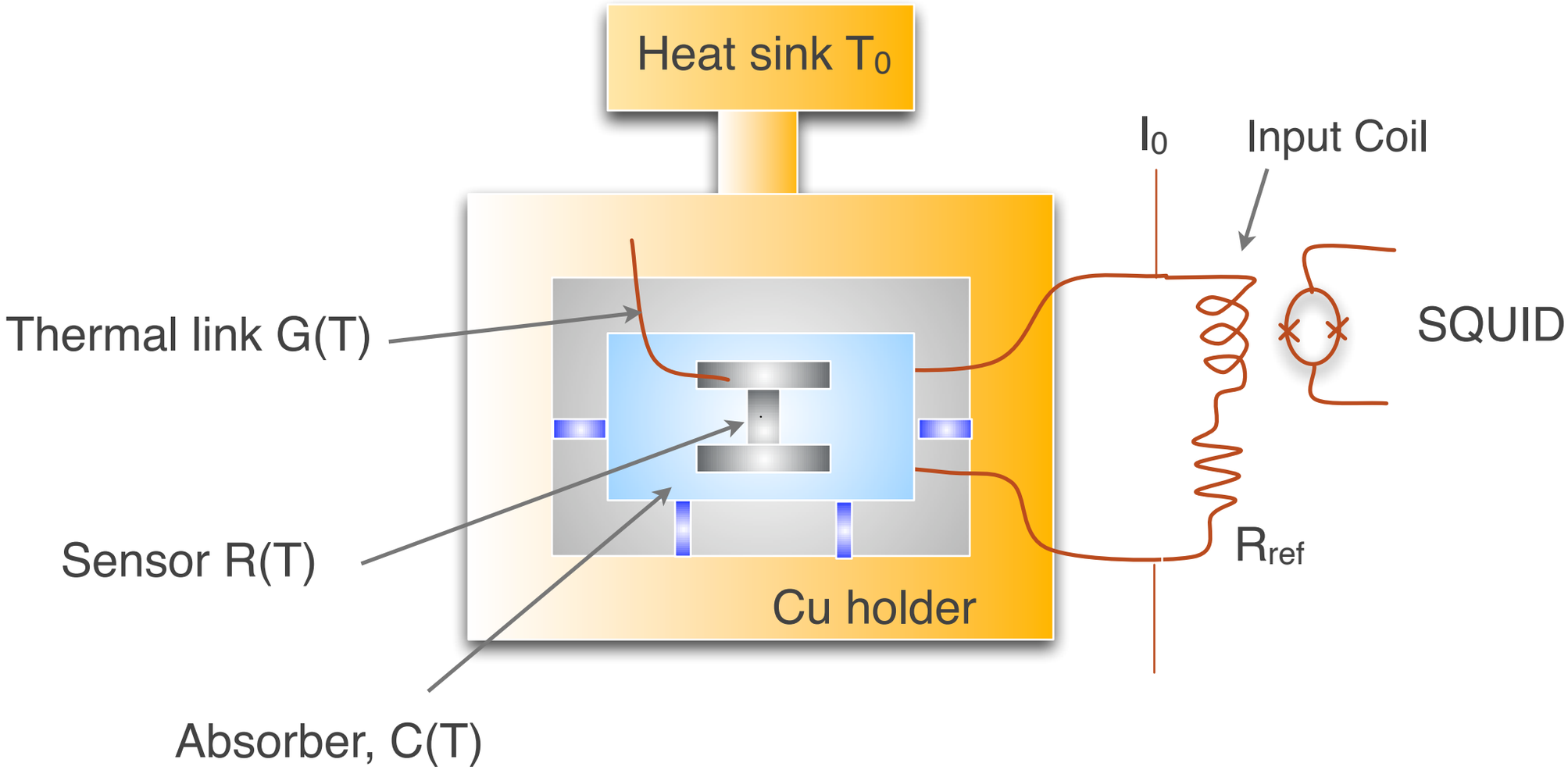

- Thermal detectors: slow → ms for the phonons to relax to a thermal distribution
- TES: can be used to detect fast, athermal phonons → how are these kept stable?

TES with Electrothermal-Feedback

- $T_0 \ll T_C$: substrate is cooled well below the SC transition temperature T_C

- A voltage V_B is placed across the film (TES)

  and equilibrium is reached when ohmic heating of the TES by its bias current is balanced by the heat flow into the absorber

  When an excitation reaches the TES

  → the resistance R increases

  → the current decreases by ΔI

  ⇒ this results in a reduction in the Joule heating

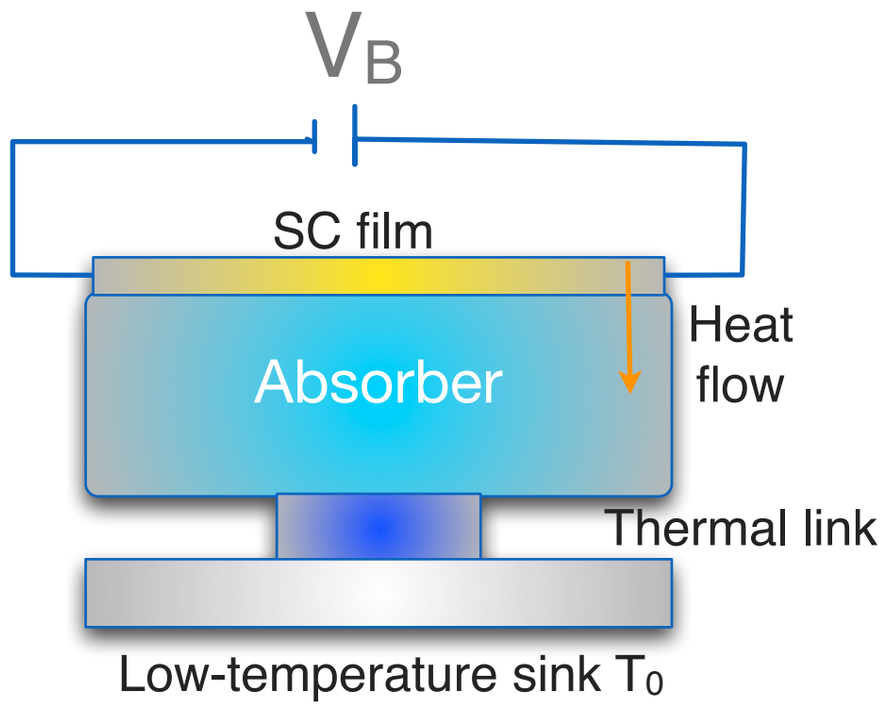

The feedback signal = the change in Joule power heating the film $P=IV_B=V_B^2/R$

The energy deposited is then given by: $E = -V_B \int \Delta I(t) dt$

⇒ the device is self-calibrating

TES with Electrothermal-Feedback

- By choosing the voltage V_B and the film resistivity properly

  ⇒ one achieves a stable operating T on the steep portion of the transition edge

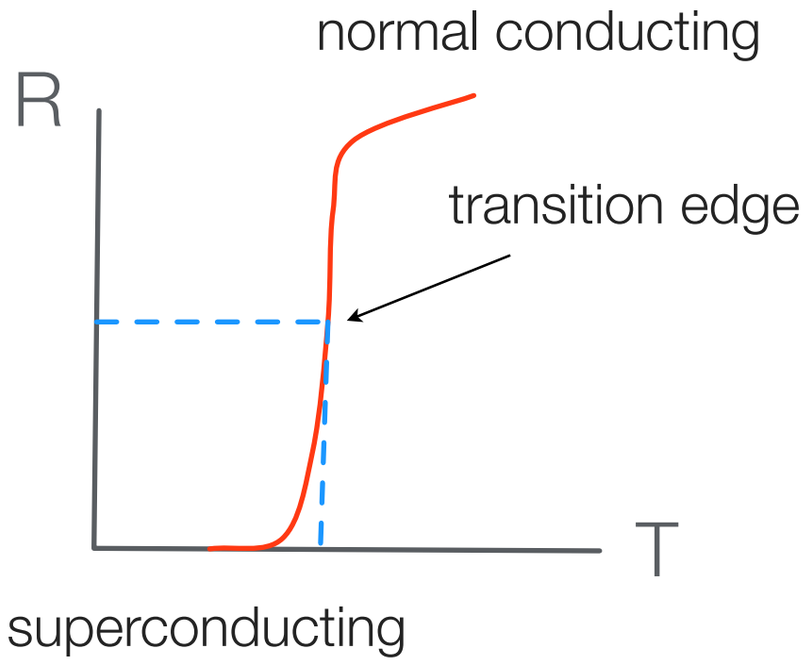

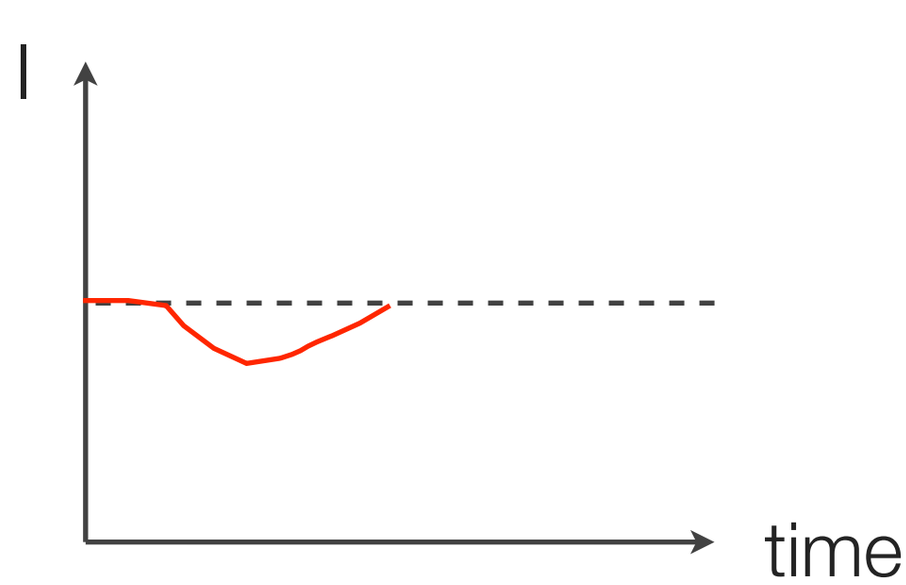

ET-feedback: leads to a thermal response time 10^2 faster than the thermal relaxation time
+ a large variety of absorbers can be used with the transition edge sensor

Cryogenic bolometers

- Sub-keV (< 100 eV) energy thresholds
- Phonons and/or ionisation/light ⇒background discrimination
- Optimised to **probe sub-GeV DM**

CRESST at LNGS

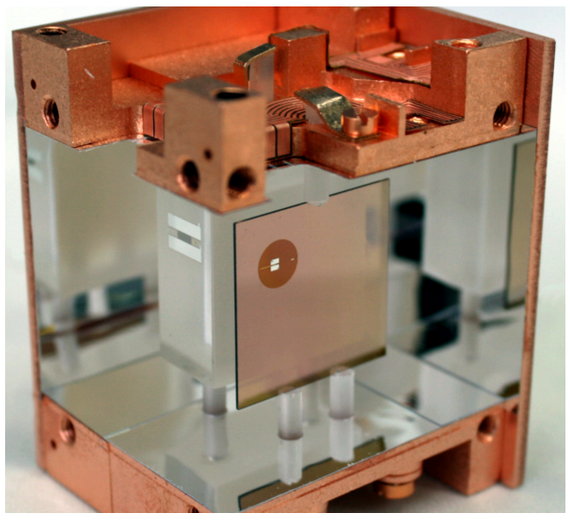

$CaWO_4$, $LiAlO_2$, Al_2O_3, Si

EDELWEISS at Modane

Ge

Super-CDMS at SNOLAB

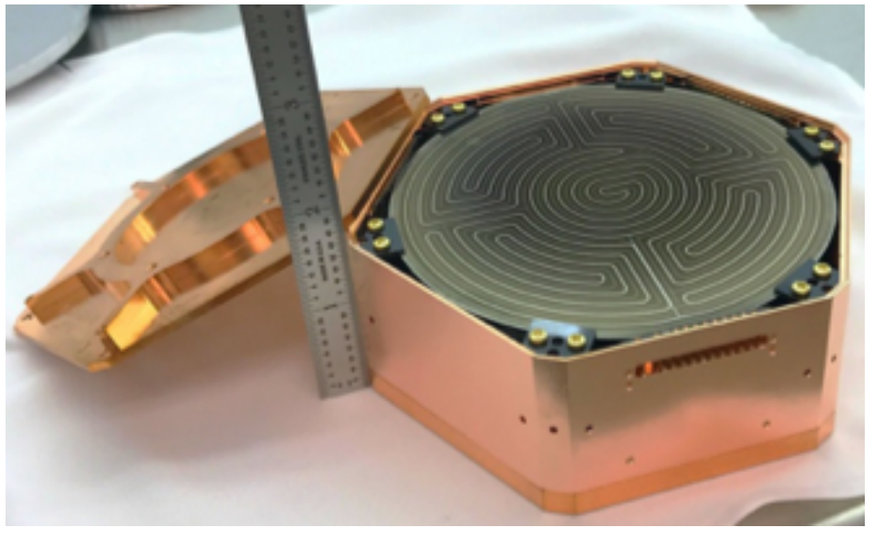

Ge, Si

Cryogenic bolometers

- Sub-keV (< 100 eV) energy thresholds
- Phonons and/or ionisation/light ⇒background discrimination
- Optimised to **probe sub-GeV DM**

CRESST at LNGS

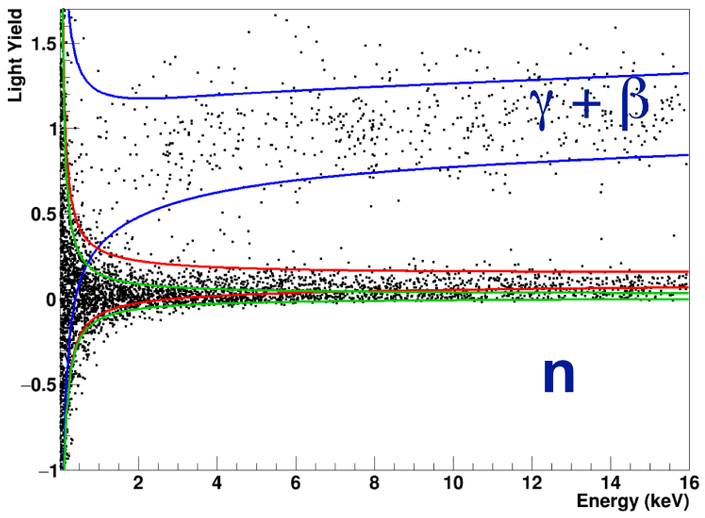

$CaWO_4$, $LiAlO_2$, Al_2O_3, Si

EDELWEISS at Modane

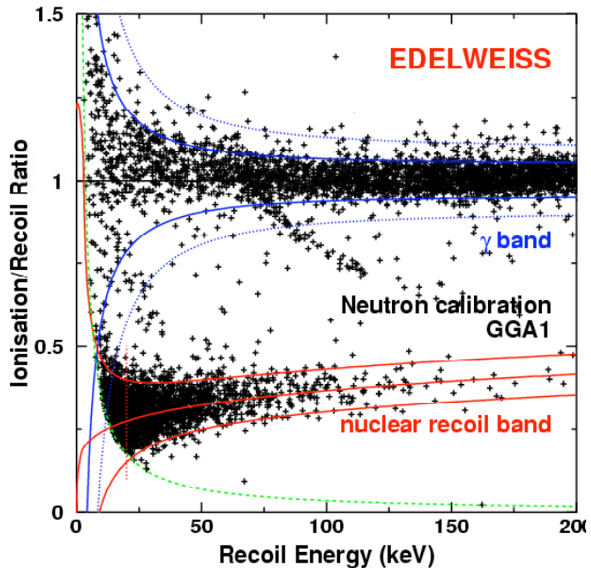

Ge

Super-CDMS at SNOLAB

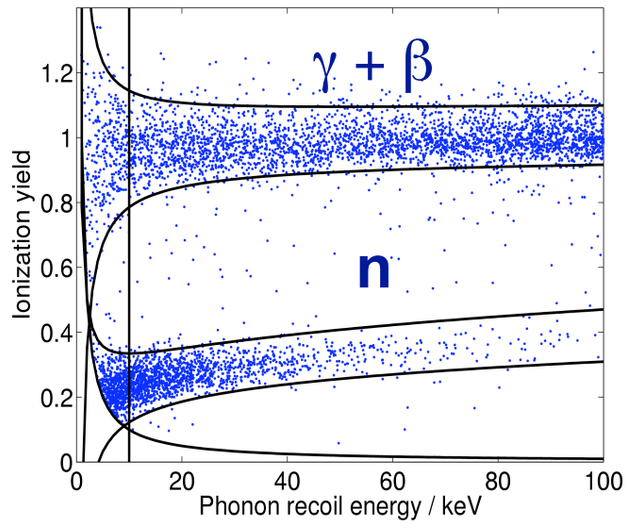

Ge, Si

Cryogenic bolometers: current status

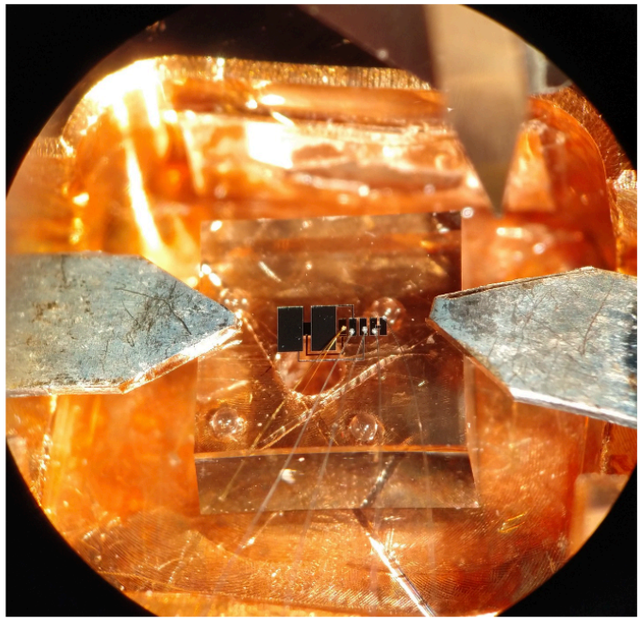

CRESST: new diamond crystal with high potential for sub-GeV DM search (0.175 g with 17 eV NR energy threshold)

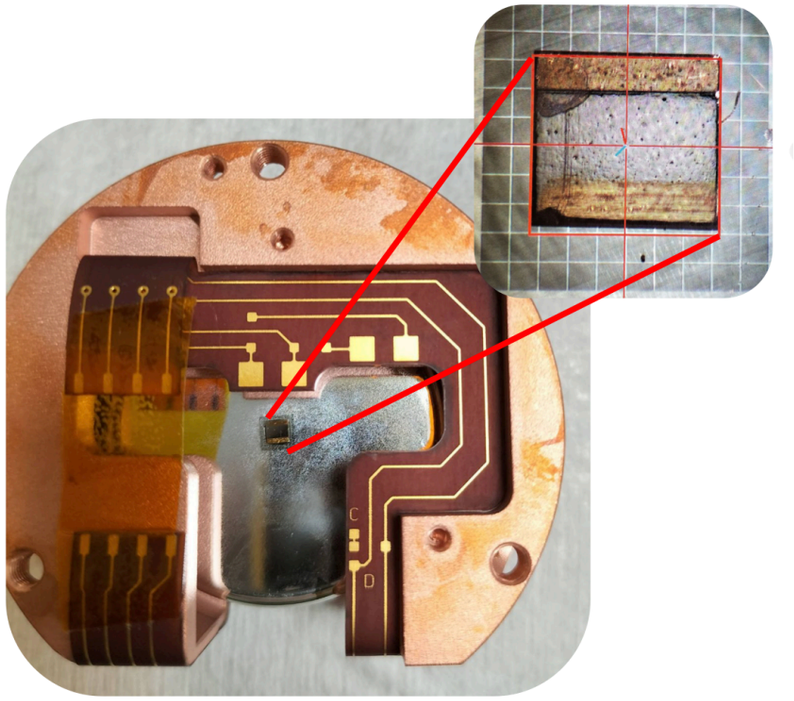

EDELWEISS →
CRYOSEL: 40 g Ge detectors with NTDs and new small sensors (superconducting single electron device) to tag single charges

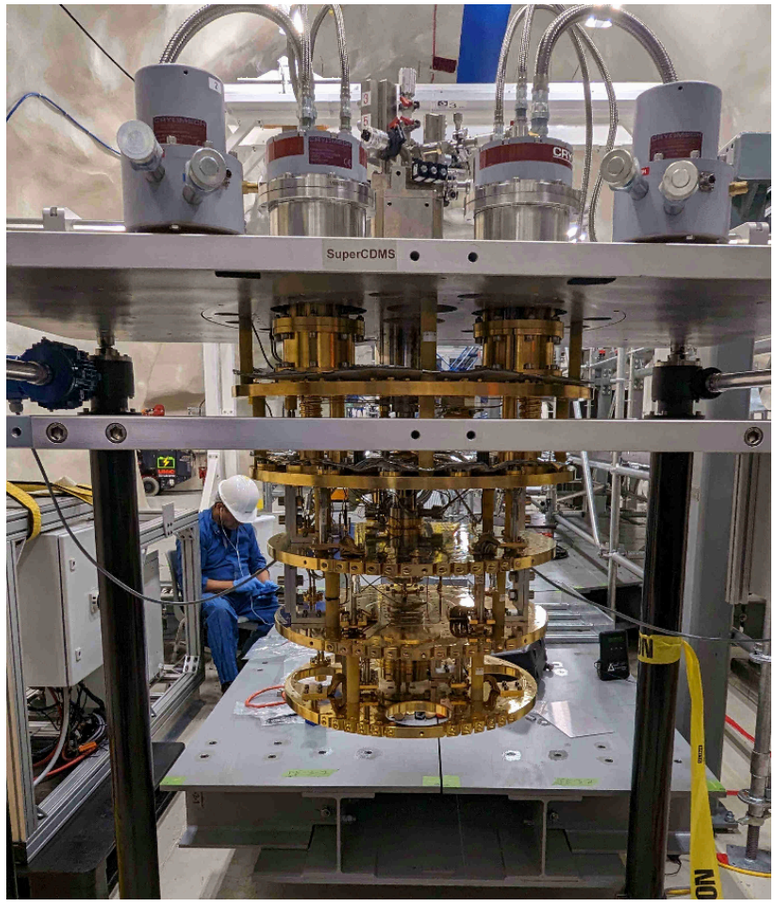

Super-CDMS: in construction at SNOLAB, several detector types (iZIP and HV; initial payload: 18 Ge, 6 Si detectors)

Cryogenic bolometers: science reach

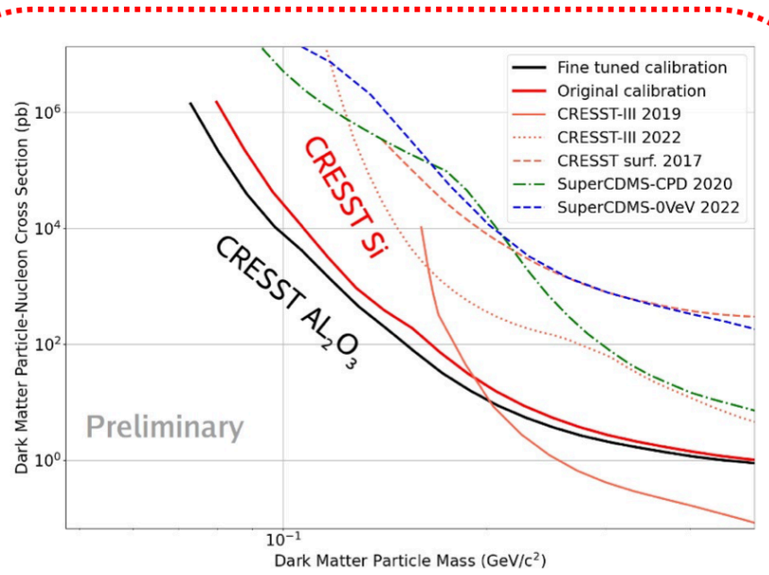

Reach to DM masses <100 MeV/c²

with low threshold detectors

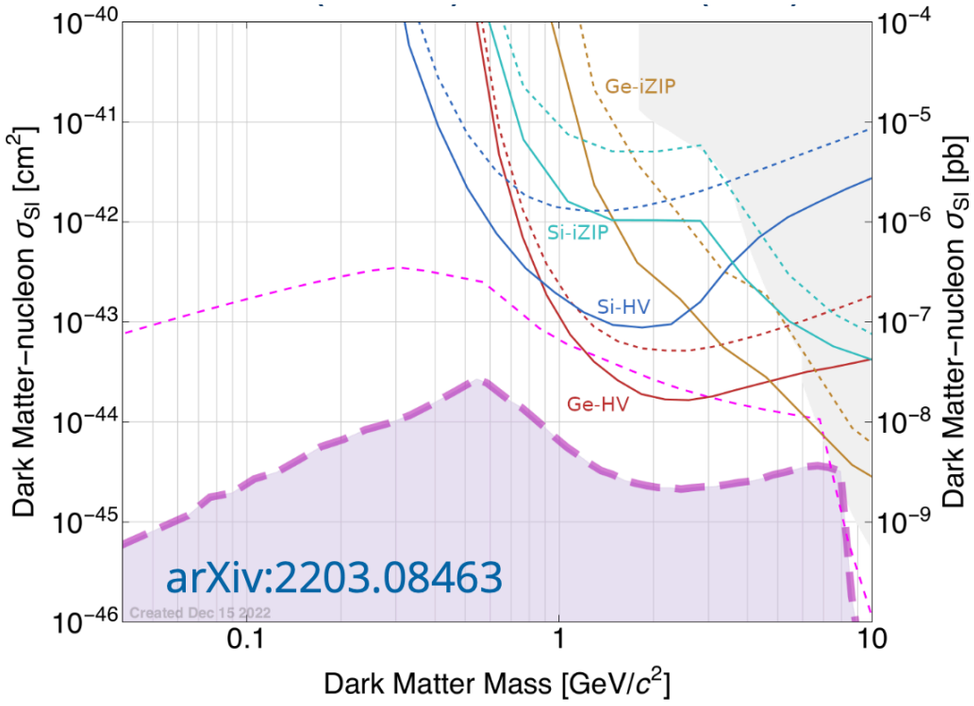

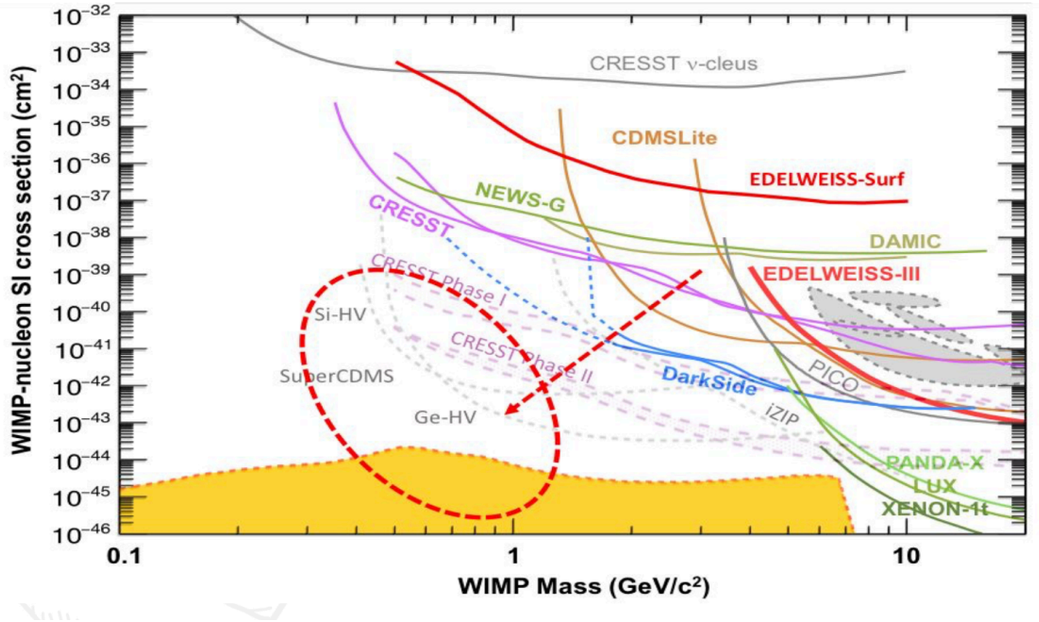

The low-energy excess

- Observed by all experiments: sharply rising energy spectrum <200 eV, high count rate; limits the sensitivity to light dark matter and to CEvNS
- Large community effort: understand the origin and mitigate, e.g., EXCESS workshops and publication (10.21468/SciPostPhysProc.9.001)
- Likely cause: long-lived metastable states releasing energy in small bursts in the systems

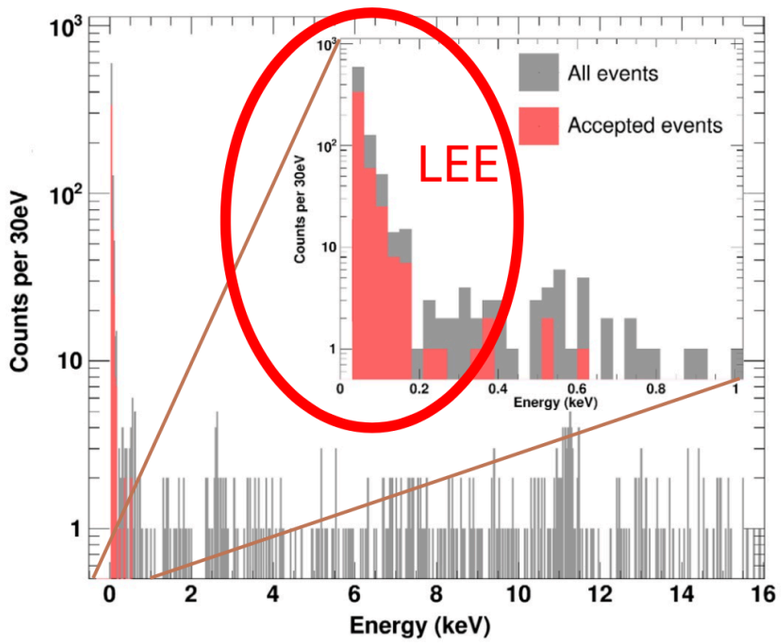

Example: CRESST, TAUP2023

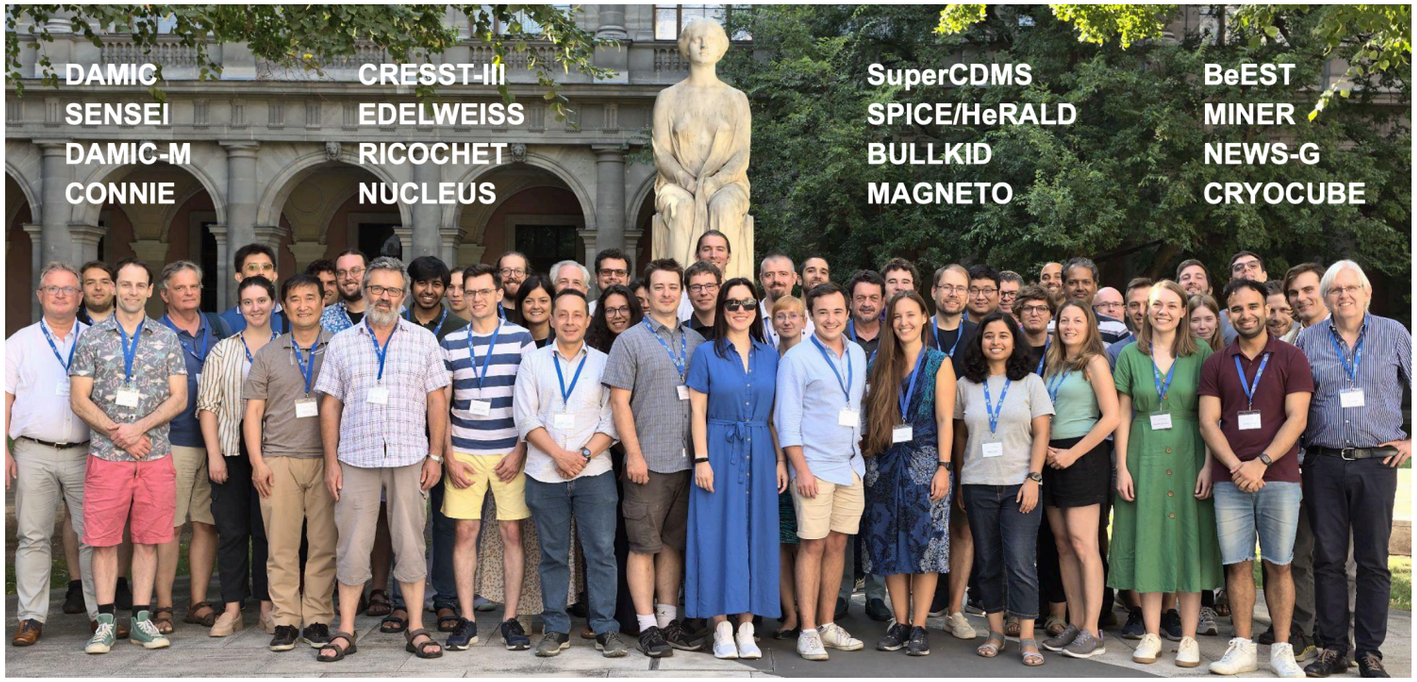

EXCESS workshop 2023

Bubble chambers

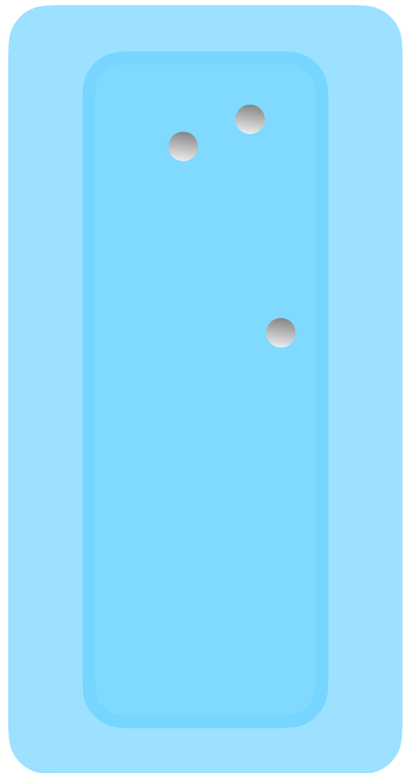

Bubble chambers

- Principle: detect single bubbles induced by high dE/dx nuclear recoils in heavy liquid bubble chambers (with acoustic, visual or motion detectors)
- Advantages
  - large ‘rejection factor’ for MIPs (> 10^{10}): in fact ‘blind’ to these type of particles
  - can be easily scaled to large masses
  - nuclei with and without spin ⇒ sensitivity to SD and SI interactions
  - C_3F_8, CF_3I, CF_3Br, C_4F_{10} etc
  - high spatial granularity (reject neutrons ⇒ multiple interactions)
  - low costs and room temperature operation
- Challenge: reduce α-emitters in fluids to acceptable levels

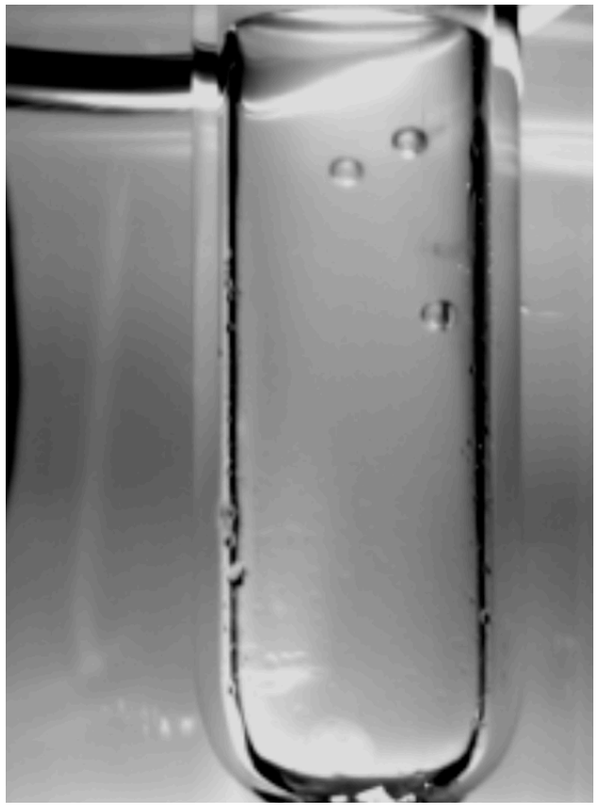

Bubble chambers

- PICO: superheated liquid C_3F_8 octafluoropropane
  - Acoustic + visual readout : impressive background rejection
  - PICO-40L: new design with bellows at the bottom, 3D position reconstructions with 2 mm spatial resolution
  - Started physics run at SNOLAB

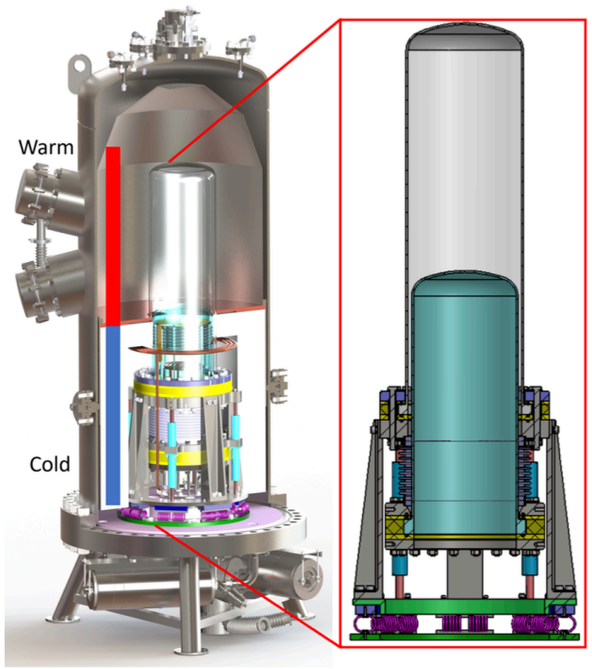

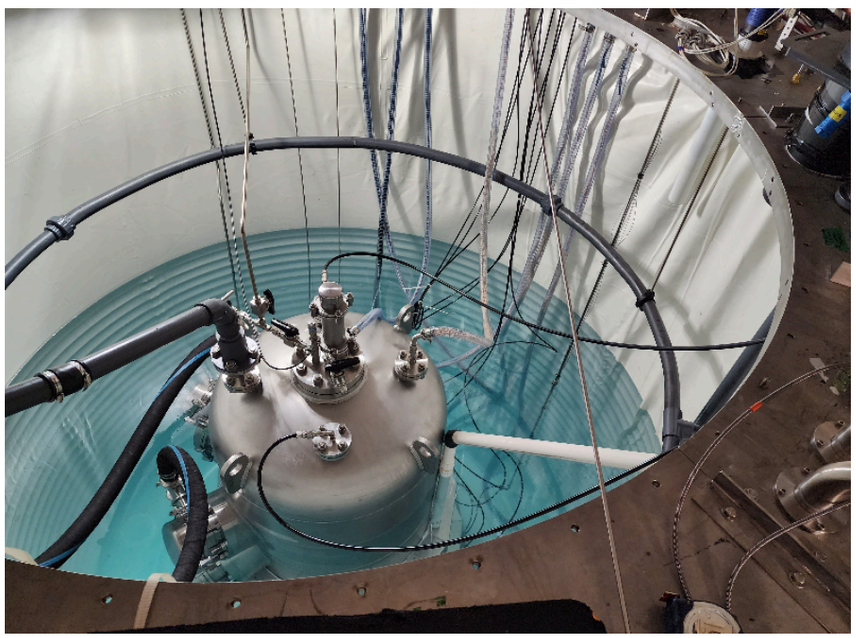

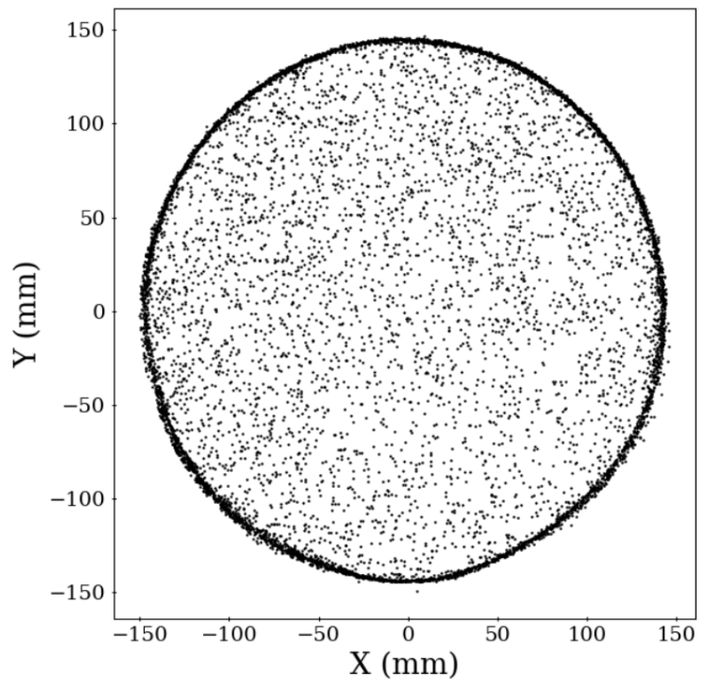

Bubble chambers

- PICO: superheated liquid C_3F_8 octafluoropropane
  - Acoustic + visual readout : impressive background rejection
  - PICO-500: 250 l of C_3F_8
  - In preparation in Cube Hall at SNOLAB

PICO-500 in Cube Hall

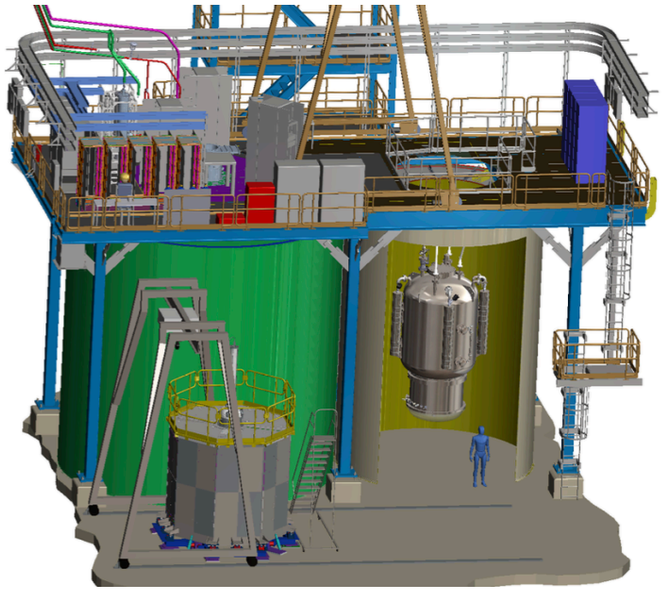

Spin-dependent WIMP interactions

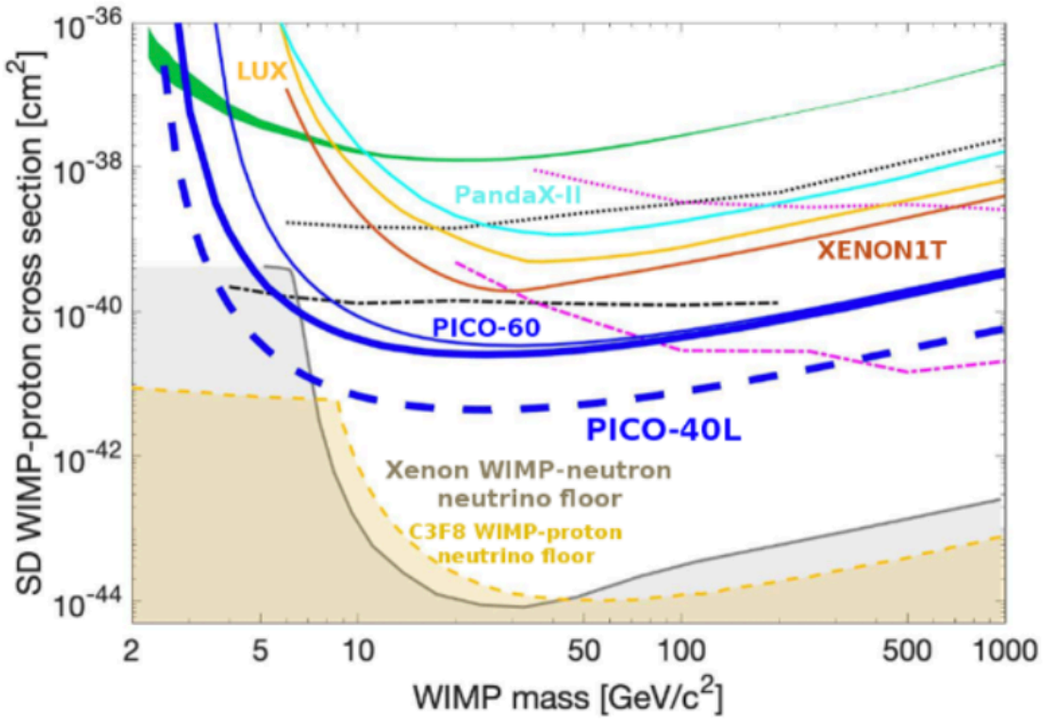

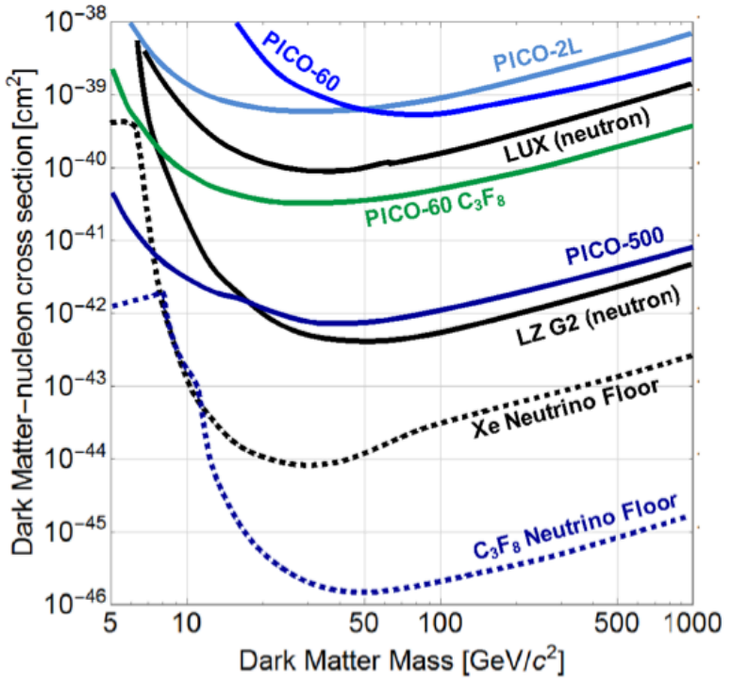

Sodium Iodide Experiments

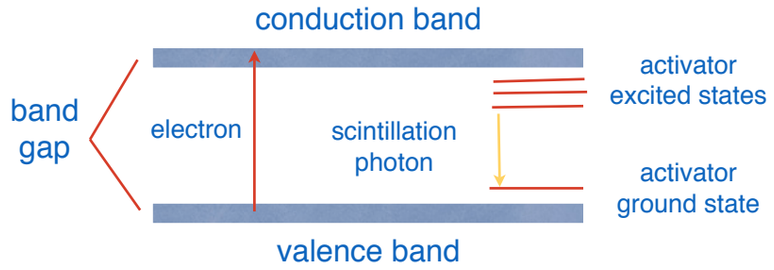

Room temperature scintillators

- Detection of scintillation light produced in various materials is a very old technique in particle physics

- **Ideally, the material should:**
  - convert the kinetic energy of the particle into light with high efficiency, and the conversion should be linear
  - be transparent to its own emission λ for good light collection
  - have a short decay time for the induced luminiscence for fast detectors
  - have an index of refraction near that of glass (1.5) for coupling to a PMT or another type of light sensor

- **For dark matter searches:**
  - mostly inorganic alkali halide crystals, NaI(Tl), operated at room temperature
  - best light output and linearity
  - can be produced as high-purity crystals

Room temperature scintillators

- To enhance the probability of visible light emission: add impurities = “activators”

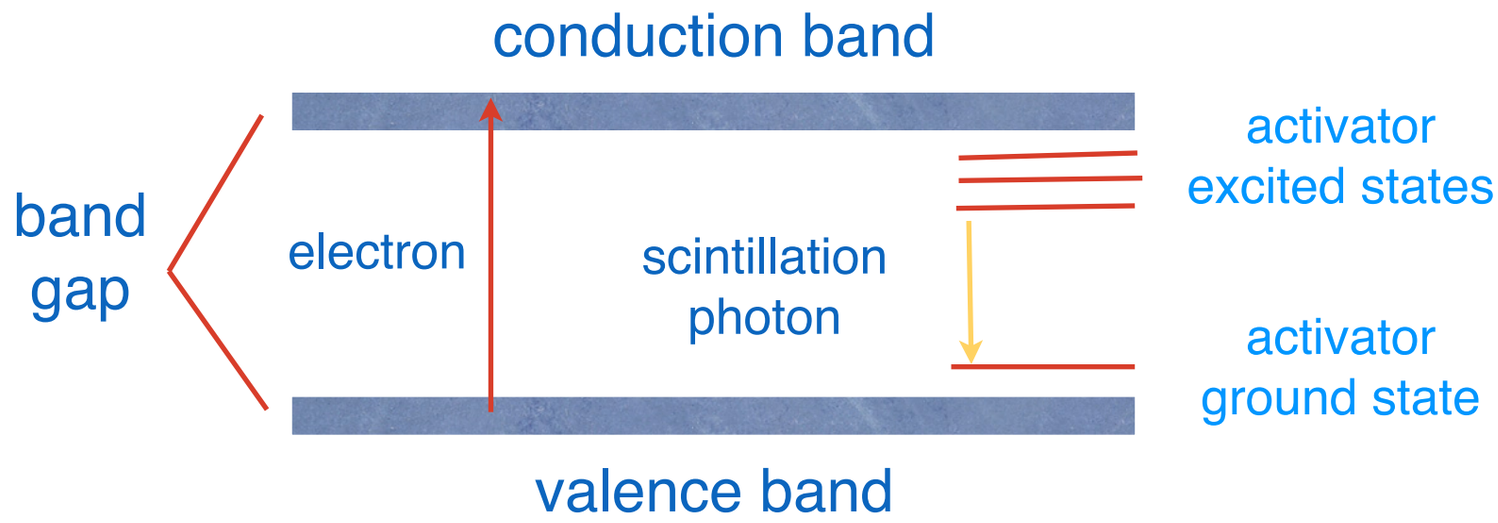

- NaI (Tl): 20 eV to create e^--hole pair, scintillation efficiency ~ 12%
  - 1 MeV yields 4 x 10^4 photons, with average energy of 3 eV
  - dominant decay time of the scintillation pulse: 230 ns, λ_{max} = 415 nm

- **No discrimination between electron- and nuclear recoils on event-by-event basis**

Sodium Iodide Experiments

- Test the DAMA/LIBRA annual modulation signal with sodium iodide crystals: NaI(Tl)
- ANAIS, COSINE, COSINUS, SABRE, PICO-LON
- So far: no evidence for annual modulation from ANAIS-112 (600 kg y exposure) and COSINE-100 (6 y of data, concluded in March 2023)
- **In construction:** COSINUS, SABRE and COSINE-200

ANAIS, TAUP2023

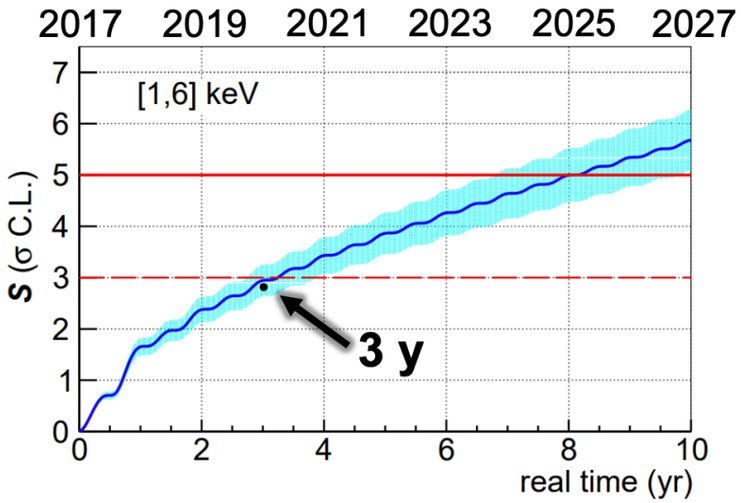

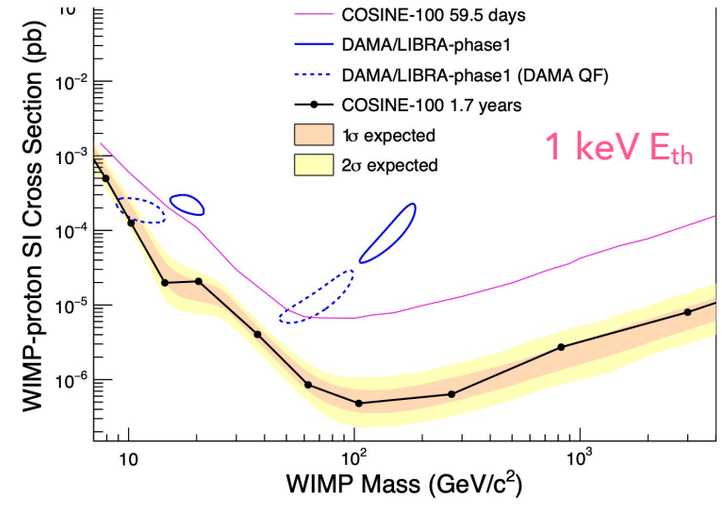

COSINE-100, arXiv:2104.03537


ANAIS at Canfranc


COSINE-100 at Yangyang

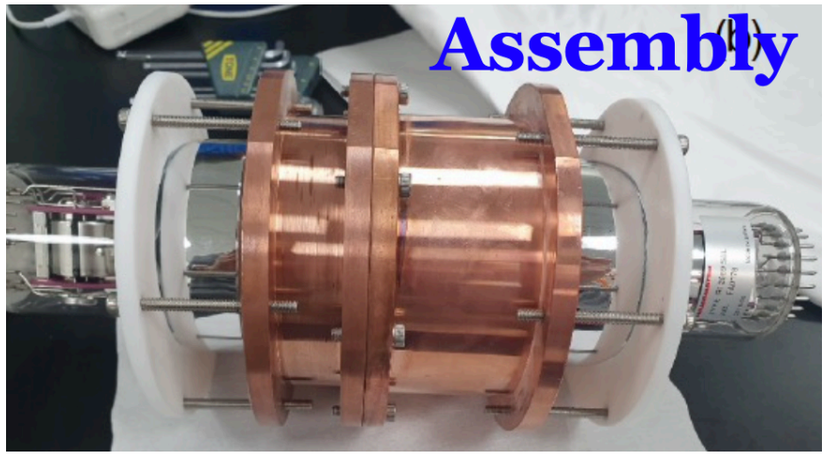

Sodium Iodide Experiments

- **SABRE** at LNGS and SUPL: detector deployments in 2024
- **COSINE-200** at Yemilab: in-house crystal growing, improved light yields; preparation to move to Yemilab ongoing
- **COSINUS** at LNGS: detects also phonons in un-doped NaI (apart from scintillation) at few mK, for active background rejection

SABRE design

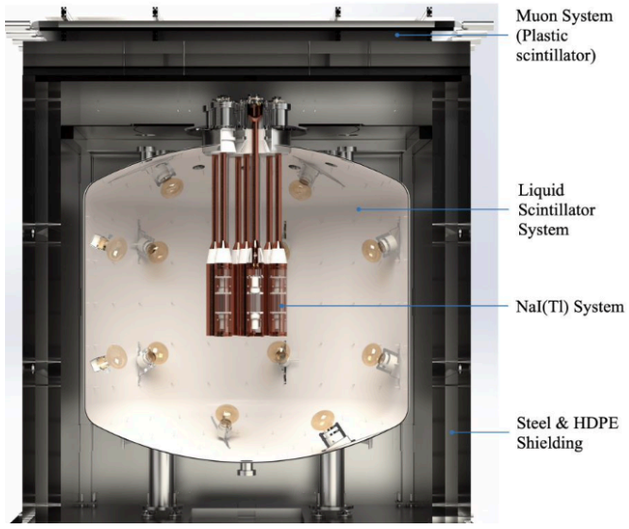

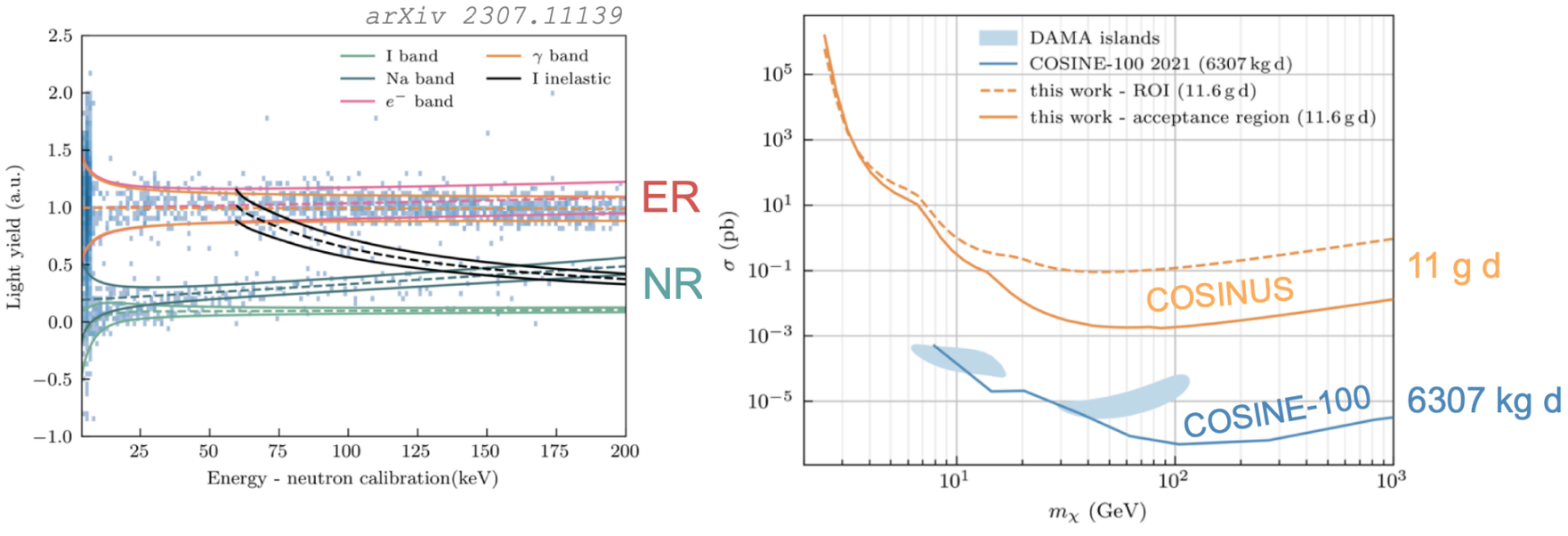

COSINUS: discrimination and goals

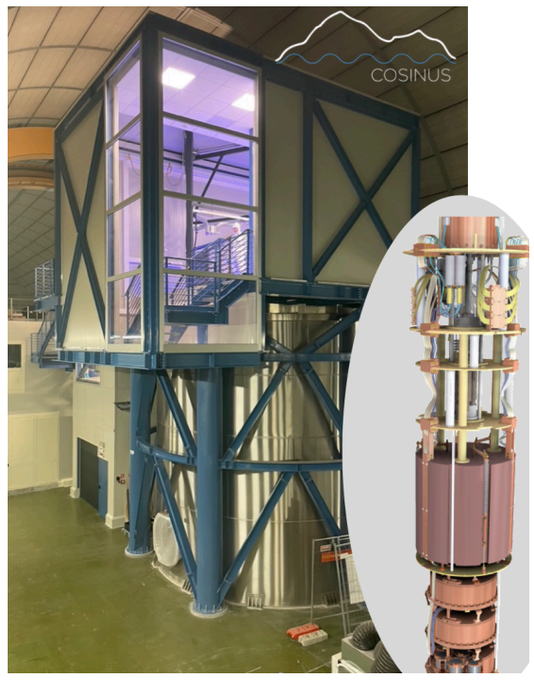

COSINUS at LNGS

Directional detectors

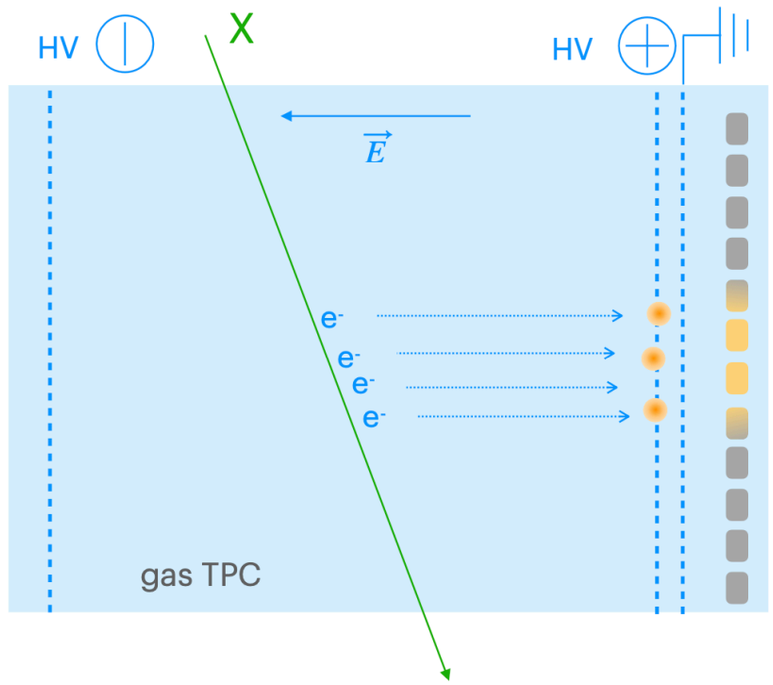

Directional detectors

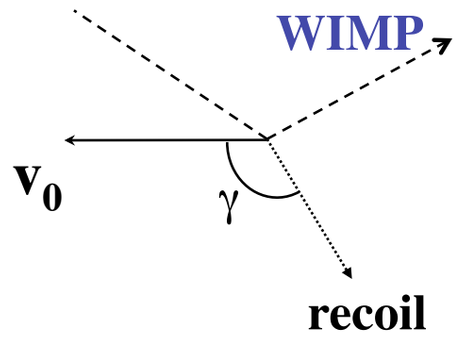

- **Low-pressure gas, nuclear emulsion and graphene detectors:** to measure the recoil direction (30° & 13° res) correlated to galactic motion towards Cygnus
- **Challenge:** good angular resolution plus head/tails at low recoil energies
- **Cygnus:** proto-collaboration to coordinate R&D efforts for gas based (He-CF_4) TPCs with ~ 1 keV threshold

F. Mayet et al., Physics Reports 627(2016)

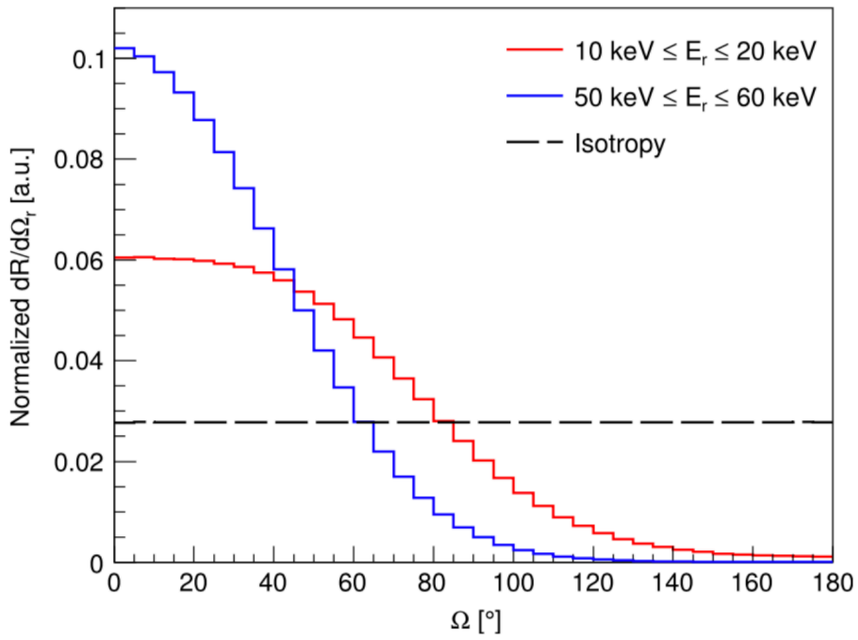

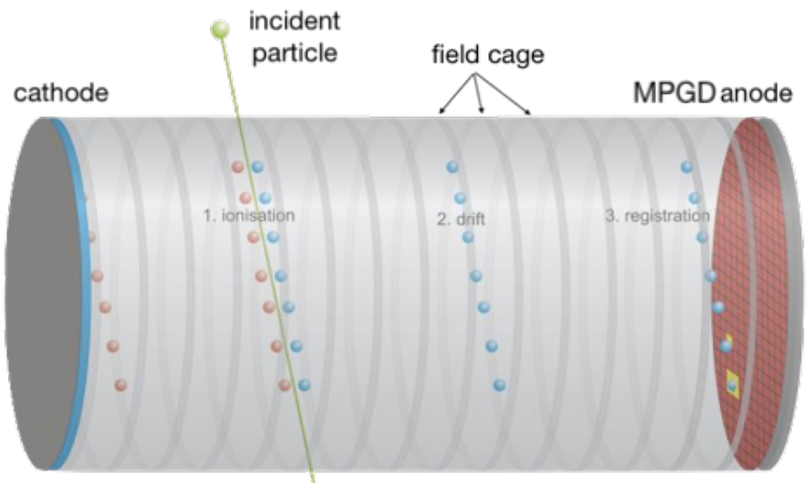

Cygno schematic view

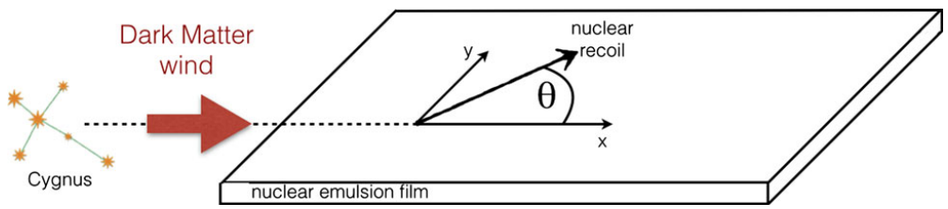

NEWSdm:
nuclear emulsions: target and tracking devices

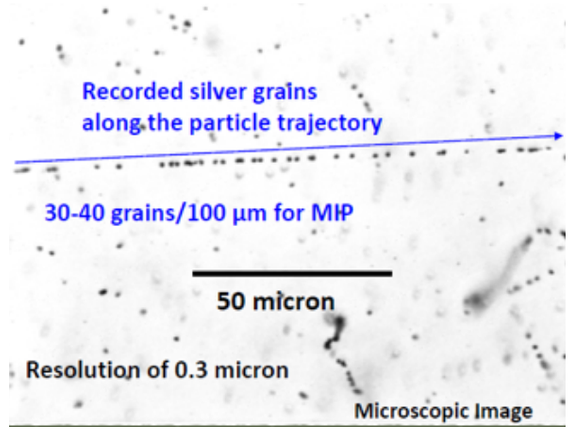

NEWSdm, EPJ-C 78, 2018

Ionisation detectors

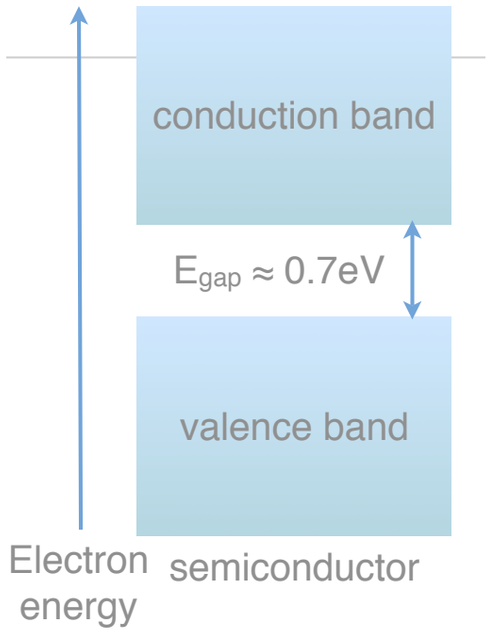

Ionisation detectors

- **Si CCDs**: low ionisation energy, low noise, and particle tracks for background reduction ⇒ particle ID (DAMIC-M, SENSEI). **DAMIC-M**: Installation and commissioning of kg-scale detector at Modane at the end of 2024. **Oscura**: next-gen detector 10 kg active Si mass, construction starting 2025 at SNOLAB
- **Point contact HPGe detectors**: low energy threshold and potentially large total mass; **CDEX**, 50 kg detector array immersed in liquid nitrogen, in construction at CJPL

DAMIC-M

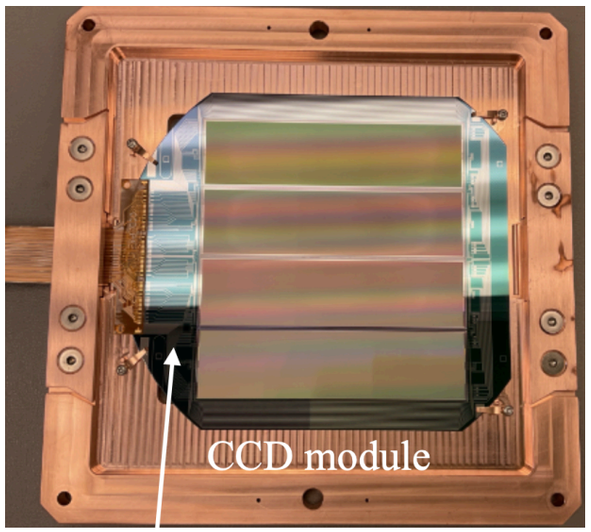

First constraints on DM-electron int. DAMIC-M, PRL. 130, 2023

Light mediator

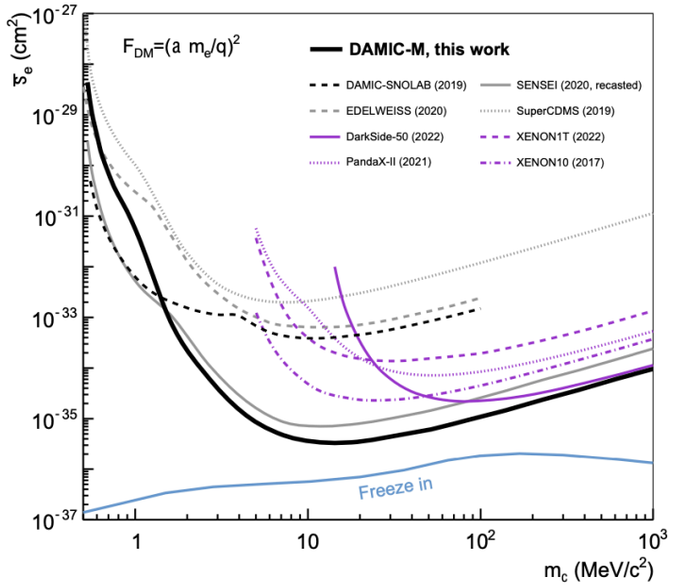

Heavy mediator

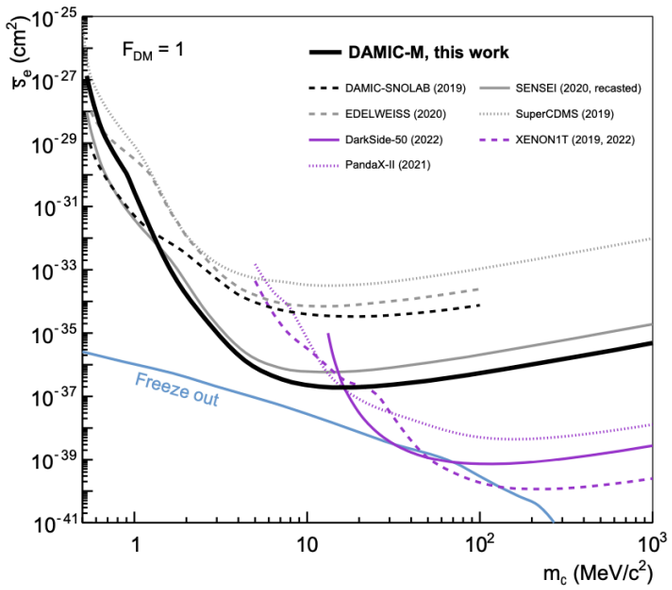

New technologies

- (Looking Beyond *Classical* Billiard Ball Nuclear Recoil)

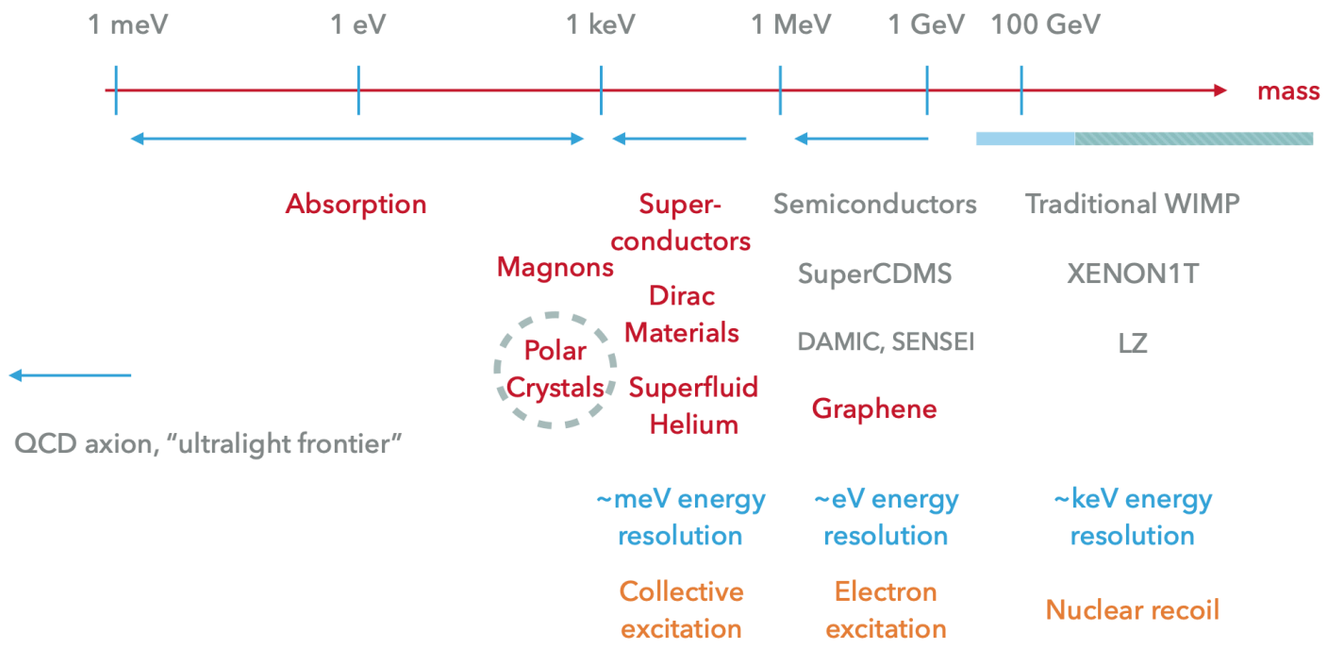

Kathryn Zurek, DM Nobel Symposium, August 2023

New technologies

- Light DM: materials with small band gaps for e^- excitations: superconductors, Dirac materials (graphene, etc), superfluid He, polar crystals,...
- Condensed matter effects become important
- Example: TESSERACT - multi-target cryogenic experiment, all sensors share TES readout; recently approved to be built in the Modane underground lab

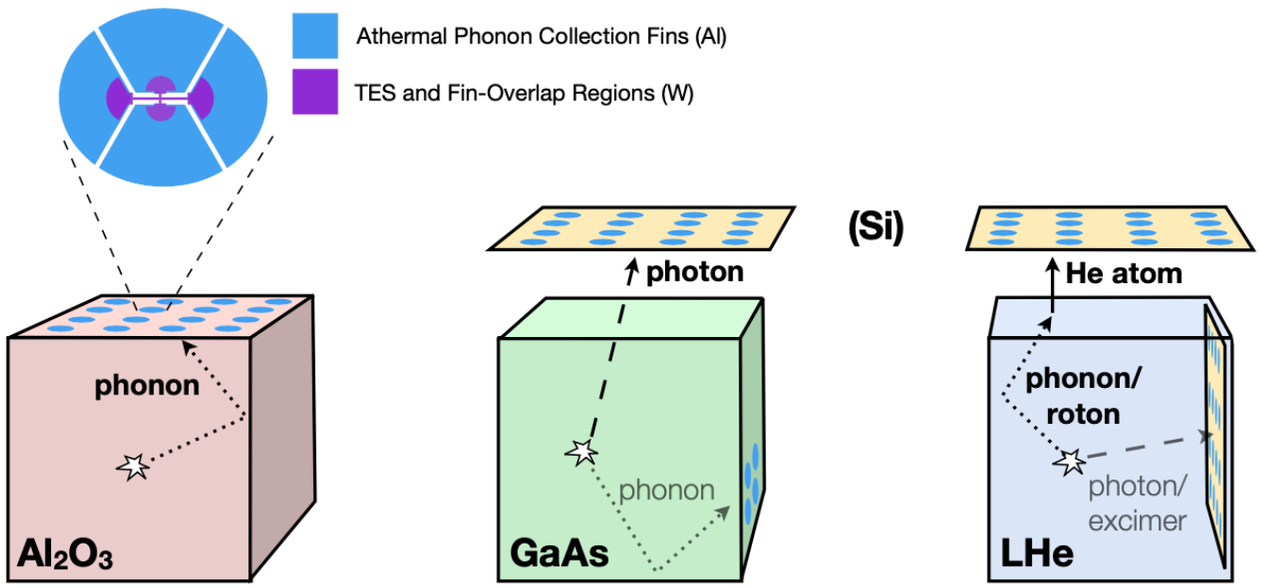

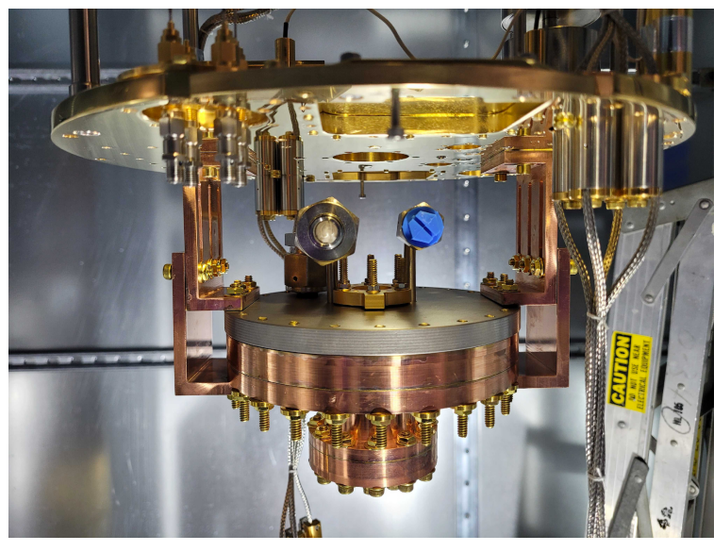

Matt Pyle, Dan McKinsey, et al., GaAs + Sapphire; liquid He

Example: Qrocodile

- Quantum Resolution-Optimised Cryogenic Observatory for Dark matter Incident at Low Energy

- **Newly formed collaboration:**
  - condensed matter/astroparticle experiment/quantum sensing/particle theory
- **Goal:** use SC nanowires as both target and sensor for sub-GeV DM particles (scatters on electron and absorption)

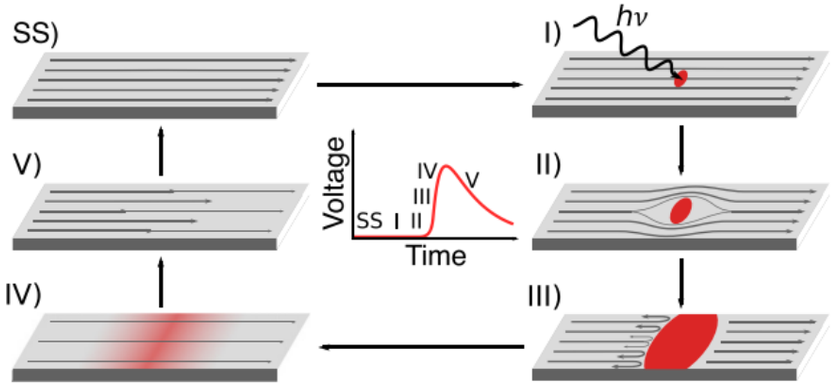

Appl. Phys. Lett. 118, 190502 (2021)

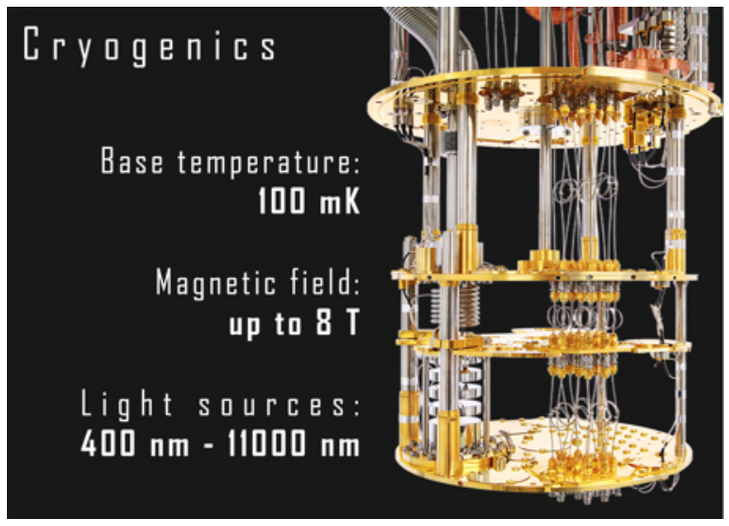

Universität Zürich[UZH]

Massachusetts Institute of Technology

האוניברסיטה העברית בירושלים
THE HEBREW UNIVERSITY OF JERUSALEM

Example: Qrocodile

- **Location:** at UZH, in the future possibly underground (LNGS, Modane, Boulby,...)
- **UZH groups** (LB, I. Charaev, T. Neupert, A. Schilling)
  - sensor development, production, testing
  - background characterisation, MC simulations, material radio-assay with Gator at LNGS
  - condensed matter theory
- **MIT:** B. Lehmann, **Jerusalem:** Y. Hochberg
  - particle physics theory: DM interaction rates, based on the dielectric response of the target

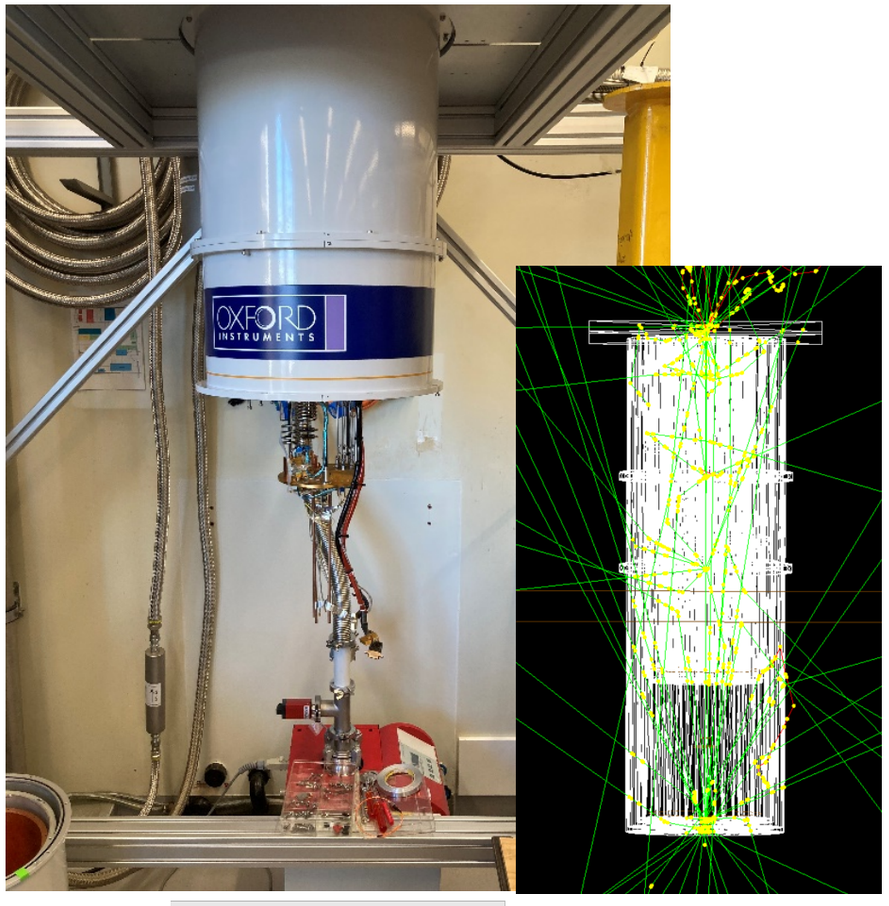

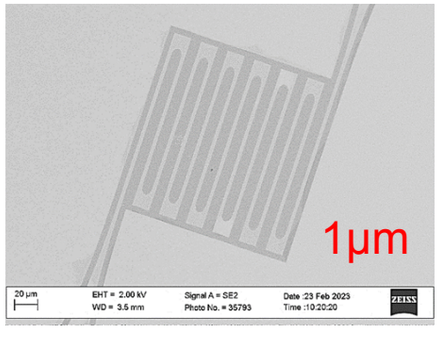

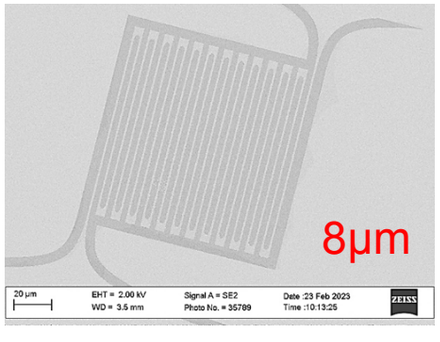

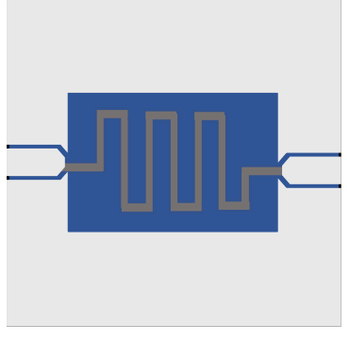

Patterned WSi nanowires with e- beam lithography and reactive ion etching

Example: Qrocodile

- **Presently**
  - running at surface, 400 × 400 μm^2 active area, 98% detection efficiency at 1.55 μm (0.8 eV)
  - 15 counts in ~ 16 d
  - test impact of radioactive sources
  - probe the energy threshold (with lasers at 5 μm and 11 μm)

- **Plans**
  - scale-up the SNSPDs detector mass with areas of ~ cm^2 and beyond
  - extend the energy threshold to the fundamental limit
  - understand and reduce backgrounds

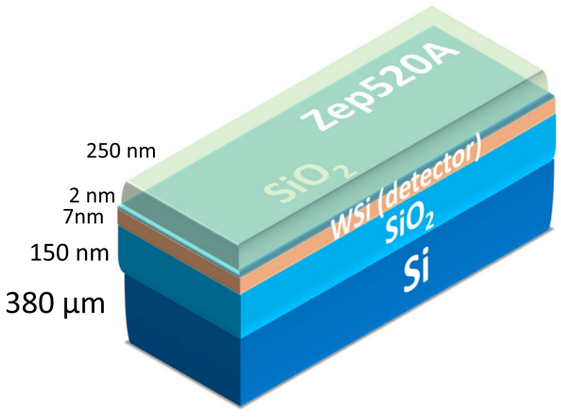

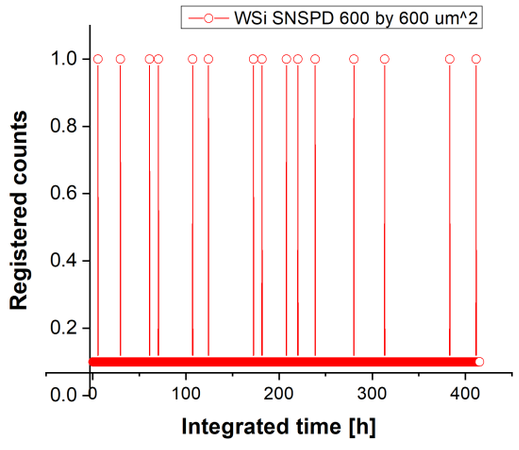

DM-electron scattering

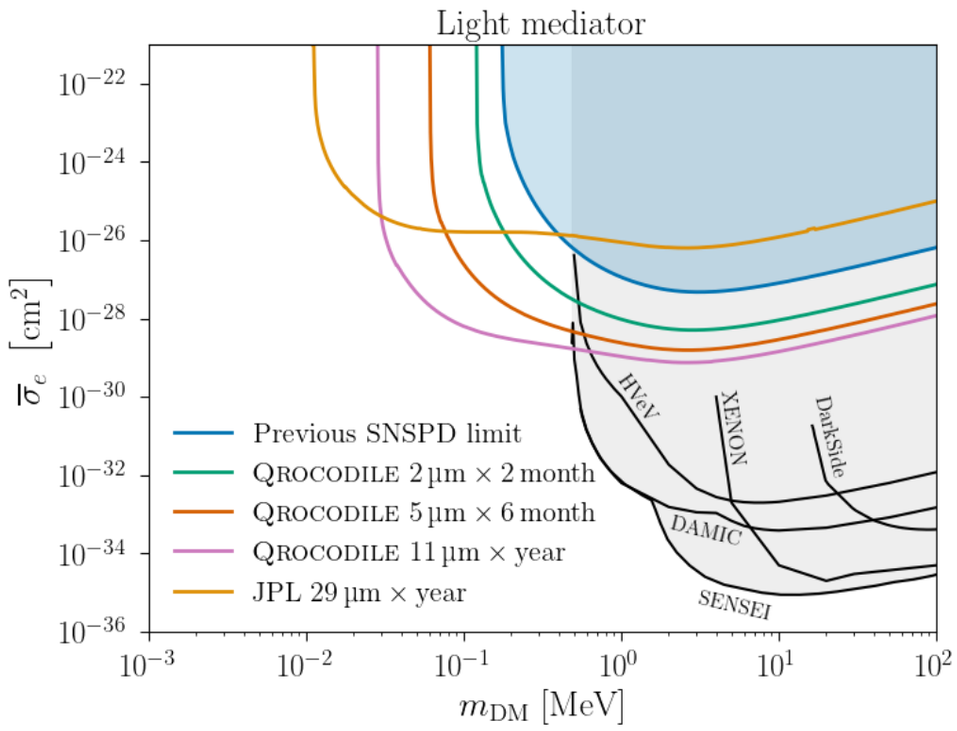

Projections: **0.73 eV (1.6 μm)**, **0.5 eV (2 μm)** thresholds

Previous: Y. Hochberg et al., PRD 106, 2022

Events: pulses with amplitude ~1 mV, few ns long, for absorbed energies 0.1 meV - 10 eV.

Liquefied noble gases

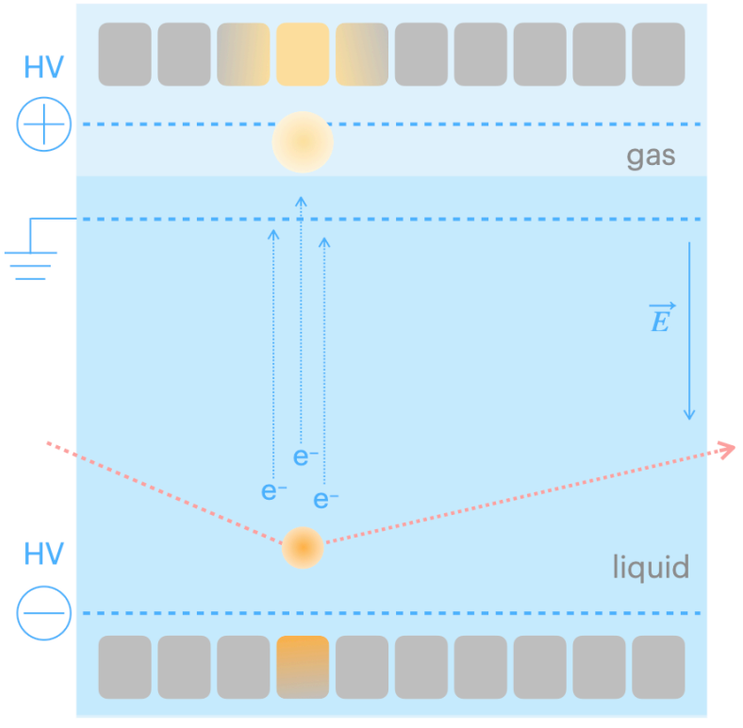

Noble gases

- Discovered by William Ramsay, student of Bunsen and professor at UC London (1904 Nobel prize in chemistry)

- W. Ramsay: "These gases occur in the air but sparingly as a rule, for while argon forms nearly 1 hundredth of the volume of the air, neon occurs only as 1 to 2 hundred-thousandth, helium as 1 to 2 millionth, krypton as 1 millionth and xenon only as about 1 twenty-millionth part per volume. *This more than anything else will enable us to form an idea of the vast difficulties which attend these investigations*"

- Argon - "the inactive one"; neon - "the new one", krypton - "the hidden one", xenon - "the strange one"

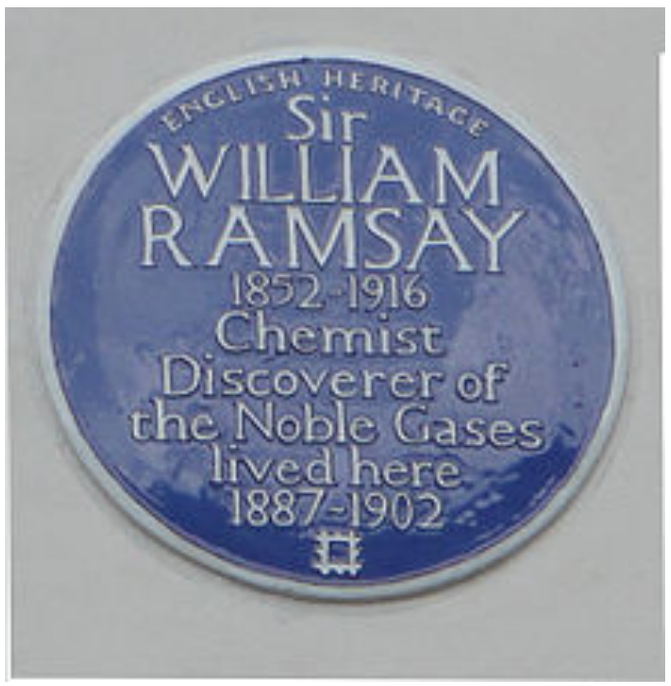

"in recognition of his services in the discovery of the inert gaseous elements in air, and his determination of their place in the periodic system".

Noble gases in the Earth's atmosphere

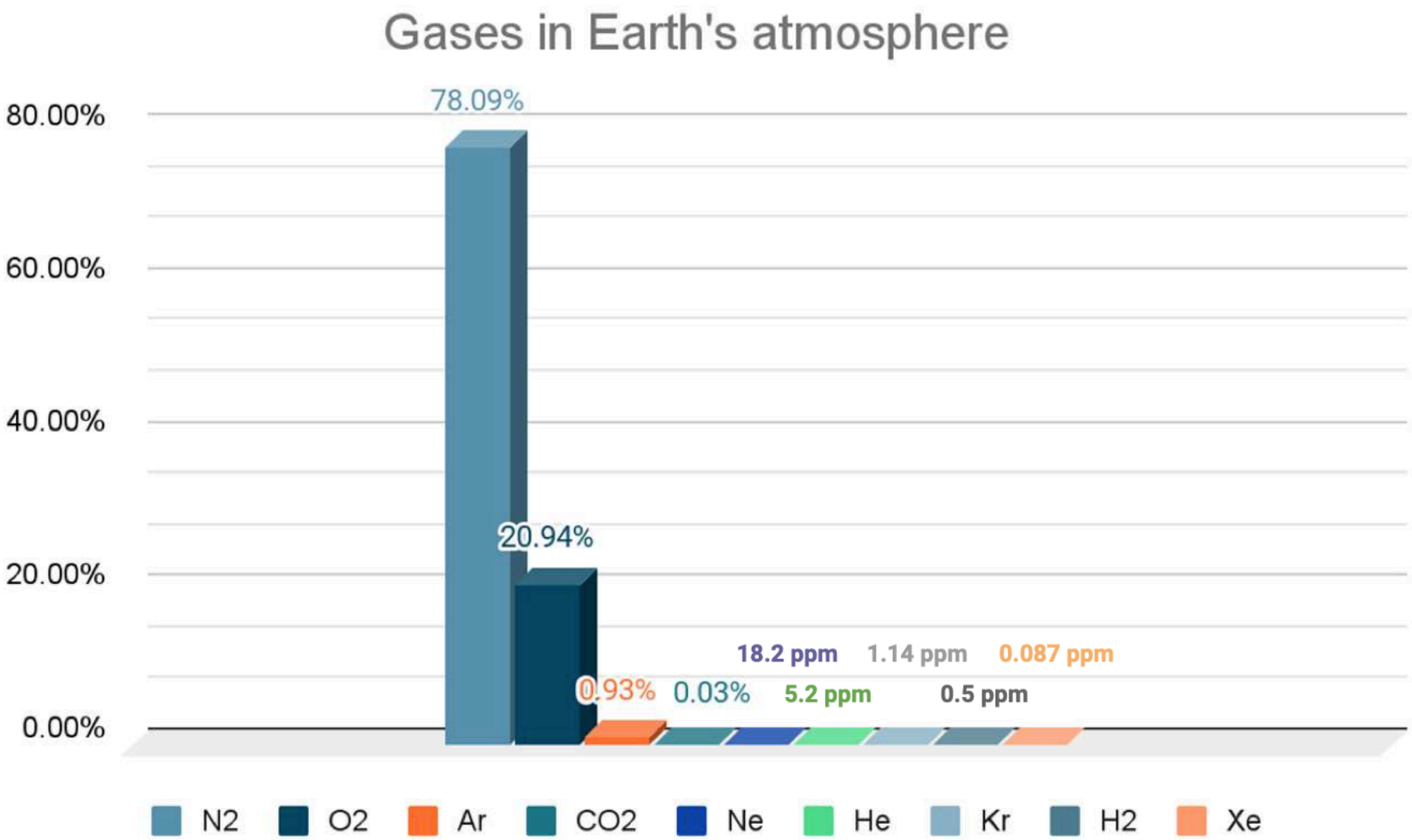

Gaz	Abundance
N2	78,09 %
O2	20,94 %
Ar	0,93 %
CO2	350 ppm
Ne	18,2 ppm
He	5,2 ppm
Kr	1,14 ppm
H2	0,5 ppm
Xe	**0,087 ppm**

Properties of noble gases for radiation detectors

- Rare-event search experiments: mostly argon and xenon are used (helium and neon detectors also proposed)
- **Liquefied noble gases allow for:**
  - dense, homogeneous targets for ionising radiation
  - detectors with self-shielding and fiducialisation
  - large detector masses with ultra-low levels of radioactivity

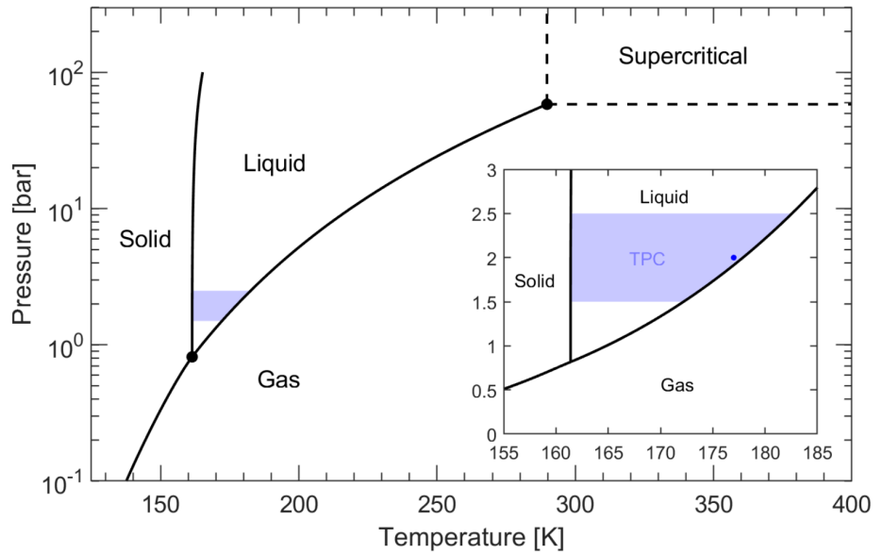

Properties [unit]	**Xe**	**Ar**	**Ne**
Atomic number:	54	18	10
Mean relative atomic mass:	131.3	40.0	20.2
Boiling point T_{b} at 1 atm [K]	165.0	87.3	27.1
Melting point T_{m} at 1 atm [K]	161.4	83.8	24.6
Gas density at 1 atm & 298 K [$\mathrm{g\,l^{-1}}$]	5.40	1.63	0.82
Gas density at 1 atm & T_{b} [$\mathrm{g\,l^{-1}}$]	9.99	5.77	9.56
Liquid density at T_{b} [$\mathrm{g\,cm^{-3}}$]	2.94	1.40	1.21
Dielectric constant of liquid	1.95	1.51	1.53
Volume fraction in Earth's atmosphere [ppm]	0.09	9340	18.2

Example - phase diagram for xenon (fig by F. Girard, data from NIST): at atm pressure, the liquid phase extends over a narrow range of T

Cryogenic noble liquids

- Suitable materials for detecting ionisation tracks
  - do not attach electrons; inert, non flammable, very good dielectrics
  - can be obtained commercially, and purified
  - dense, homogeneous targets for ionising radiation, with high charge and light yields

Element	Z (A)	BP (T_b) at 1 atm [K]	liquid density at T_b [g/cc]	dielectric constant	ionisation [e^-/keV]	scintillation [photon/keV]
He	2 (4)	4.2	0.13	1.06	39	15
Ne	10 (20)	27.1	1.21	1.53	46	7
Ar	18 (40)	87.3	1.40	1.51	42	40
Kr	36 (84)	119.8	2.41	1.66	49	25
Xe	54 (131)	165	2.95	1.95	64	46

The ionisation process in noble liquids

- Energy loss (E_0) of an incident particle: shared between ionisation, excitation and sub-excitation electrons (E_{kin} < energy of first excited level) liberated in the ionisation process:

$$E_0 = N_i E_i + N_{ex} E_{ex} + N_i \epsilon$$ Platzmann equation

- N_i, N_{ex} = mean number of ionised and excited atoms; E_i, E_{ex} = mean energies to ionise and excite the atoms; ε = average kin. energy of sub-excitation electrons *(energy eventually goes into heat;* ε ~ 6 eV in LAr, ε ~ 5 eV in LXe*)*
- In their condensed states: noble liquids exhibit a band-like structure of electronic states
- The atomic ionisation potential should thus be replaced by the *band-gap energy* E_g - we divide all terms by E_g and define the *W_i-value* as the energy required to produce an electron-ion pair:

$$W_i \equiv \frac{E_0}{N_i}$$

- to obtain:

ratio of W-value to the ionisation potential, or band-gap energy

$$\frac{W_i}{E_g} = \frac{E_i}{E_g} + \frac{N_{ex}}{N_i} \times \frac{E_{ex}}{E_g} + \frac{\epsilon}{E_g}$$

The ionisation process in noble liquids

- The average energy loss in ionisation is slightly larger than the ionisation potential or the band gap energy E_g, because it includes multiple ionisation processes
  - as a result, the ratio of the W_i-value to the ionisation potential or band gap energy is:

$$W_i / E_g = 1.6 - 1.7$$

- about 40-60% of absorbed energy is converted into free charge carriers

Material	Ar	Kr	Xe
Gas			
Ionisation potential [eV]	15.75	14.00	12.13
W-value [eV]	26.4	24.2	22
Liquid			
Gap energy [eV]	14.3	11.6	9.3
W-value [eV]	19.5±1.0	18.4±0.3	13.7±0.2

- the W-value in the liquid phase is smaller than in the gaseous phase
- the W-value in xenon is smaller than the one in liquid argon, and krypton (and neon)
- the ionisation yield is highest in liquid xenon (of all noble liquids)

The scintillation process in noble liquids

- Two distinct processes; in the first process:
  - excited atoms R^* (excitons) and ions R^+, both produced by ionising radiation
  - direct excitation: less than 1 ps after the excitation, the excited atom (exciton, R^*) forms a bound state with a stable atom (R): *a bound dimer state, called excimer*
  - the excited dimer is de-excited to the dissociative ground state

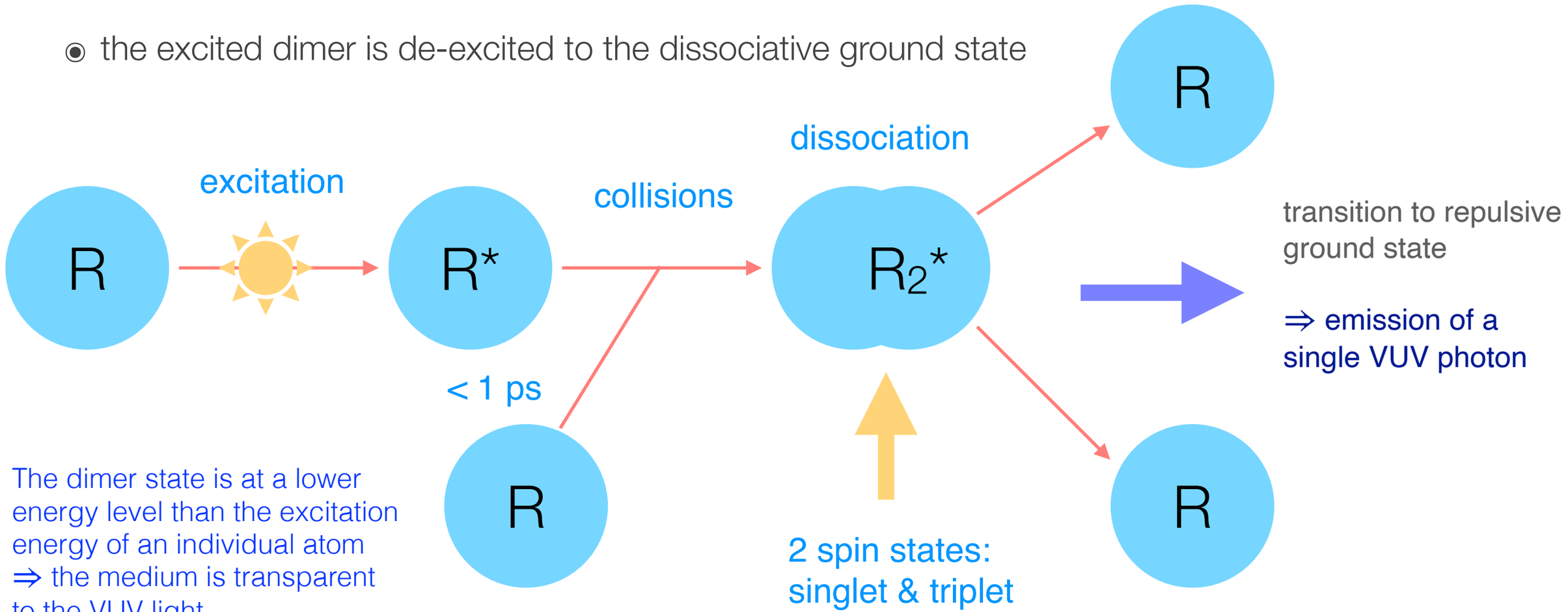

★ The dimer state is at a lower energy level than the excitation energy of an individual atom
⇒ the medium is transparent to the VUV light

★ the two spin states refer to the combined spin state of the electron and the angular momentum due to the molecular orbit

The scintillation process in noble liquids

Kubota et al.,
PRB 20, 1979

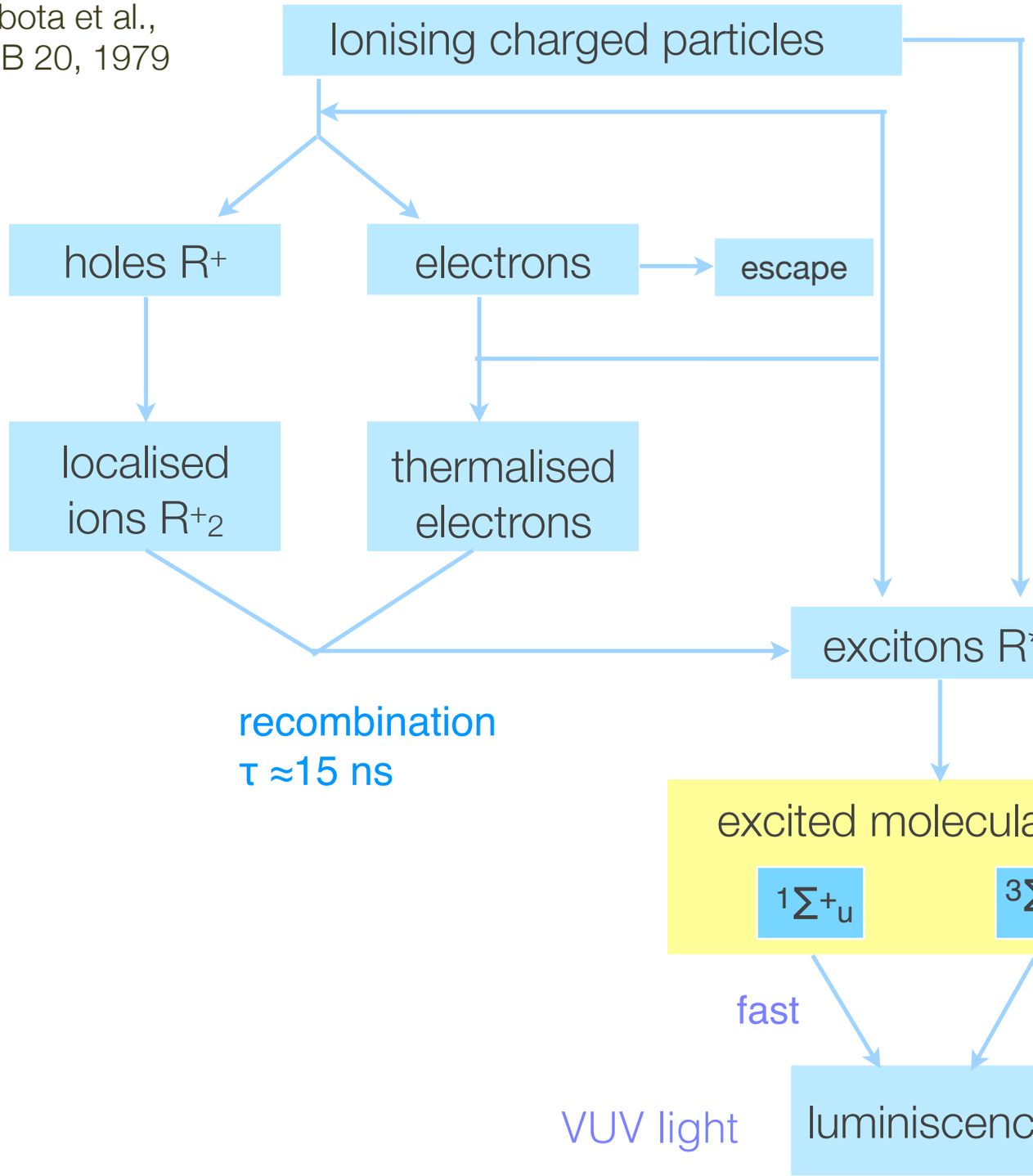

Second process producing scintillation light:

- A fraction of the ionisation e^- recombines with ions and produce a scintillation photon in a process called recombination
- Electrons that thermalise far from their parent ion may escape recombination
- A mechanism called “bi-excitonic quenching” can reduce the scintillation yield in very dense tracks:

$$R^* + R^* \longrightarrow R_2^{**} \longrightarrow R + R^+ + e^-$$

Bi-excitonic quenching (or Penning quenching): two excitons combine to form an electron-ion pair and a ground-state atom:

⇒ only a single e^- or photon (in case of recombination) is produced, instead of two

The excitation process and the photon energy

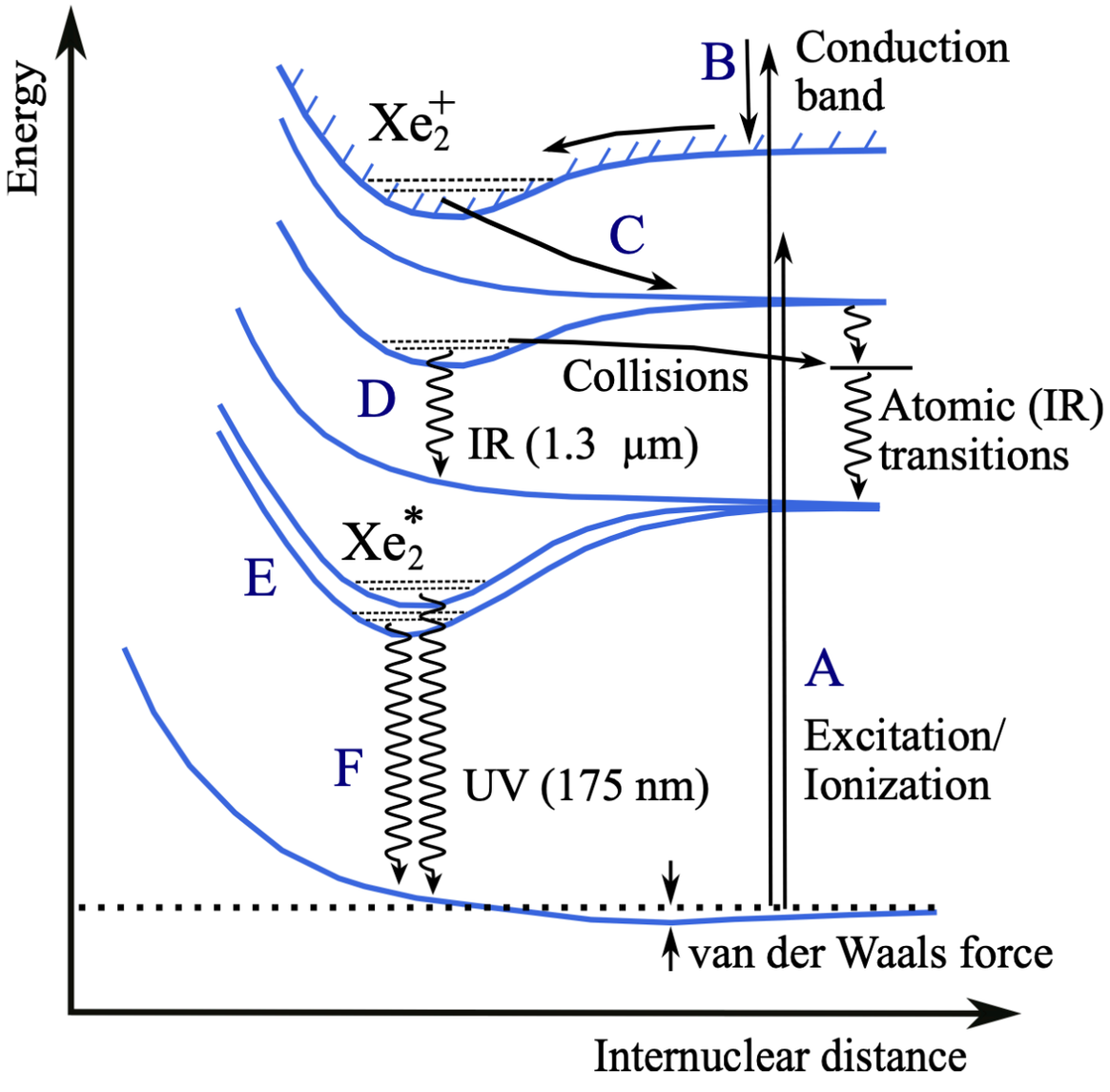

Example for xenon, from arXiv:2303.09344: different processes, which end at the lowest lying exited dimer states, which decay with emission of VUV photons

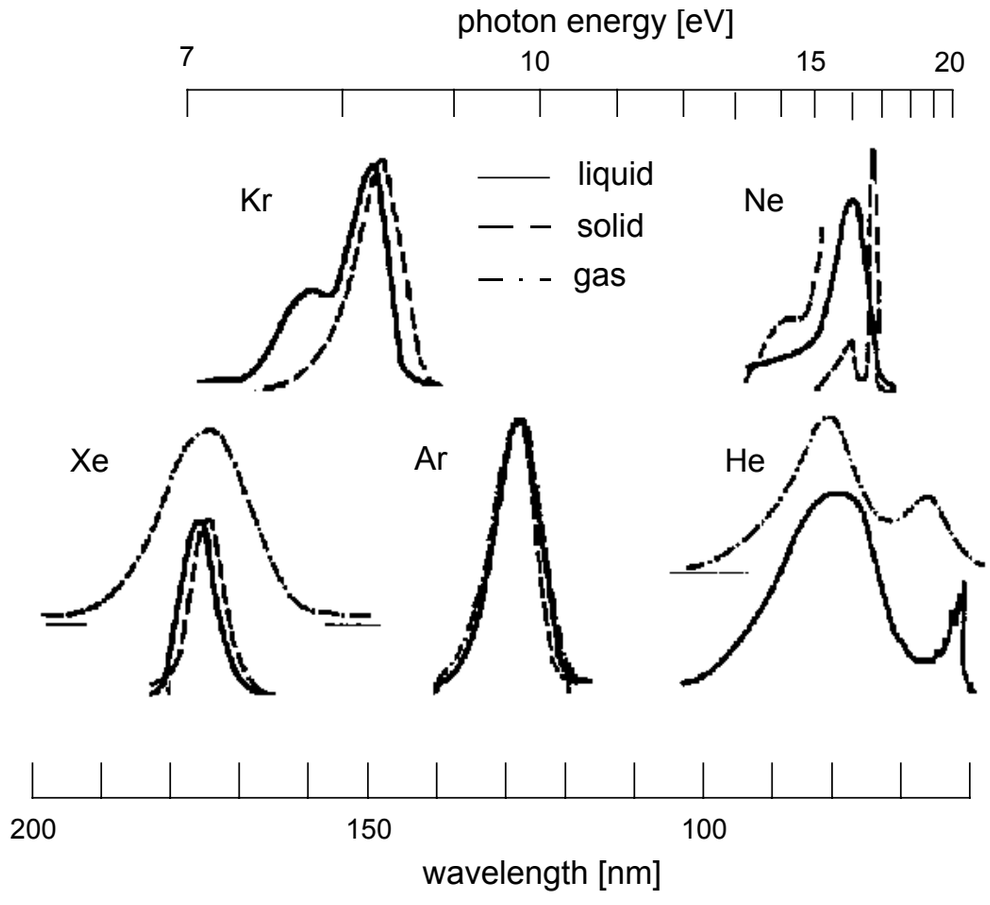

The dimer (or exciton) can not exist in the ground state (the transition from the lowest electronic excited states to the ground state occurs at short distances, where the ground state potential is repulsive):

⇒ the photon emission has practical applications in dense, noble scintillators

The scintillation process in noble liquids

- We define W_{ph} as the average energy required to produce a single photon:

$$W_{ph} = \frac{E_0}{N_{ex} + N_i} = \frac{W_i}{1 + N_{ex}/N_i} = \frac{W_i}{1 + \alpha}$$

Doke at al, 2002

E_0 = energy loss, N_{ex}, N_i = mean number of excitons and electron-ion pairs; E_i, E_{ex} = mean energies to ionise and excite the atoms; α = ratio N_{ex}/Ni (~0.2 for LAr, and ~ 0.2 for LXe)

- We assume the efficiencies for exciton and electron-ion pair creations are unity, namely:

$$N_{ph} = N_{ex} + r \cdot N_i$$

with r = recombination fraction

- If an electric field is applied, one can measure the electrons which do not recombine, with the amount of extracted charge defined as:

$$N_q = (1 - r) \cdot N_i$$

The scintillation process in noble liquids

- With the previous equations we can define the recombination-independent sum:

$$E_0 = (N_q + N_{ph}) \cdot W_{ph}$$

- The recombination-independent energy required to produce a single detectable quantum, N_q or N_{ph} is also called the W-value (*note that $N_q + N_{ph} = N_i + N_{ex}$ for any value of r*)

- We will thus use $W_{ph} = W$ (this assumes that each recombining electron-ion pair produces an exciton, which leads to a photon)

- The W-value can be measured, e.g., at fixed energy interactions, by varying the electric field, or using lines at different energies, for a given drift field

Material	Ar	Xe
W-value [eV]	19.5±1.0	13.7±0.2 11.5±0.2

The scintillation process in noble liquids

- The distribution of the total number of emitted scintillation photons between different excitation channels depends on the type of particle which interacts *(and thus on the linear energy transfer, LET)*
- It can be used to discriminate between different type of interactions:
  - Example for fast electrons (with energies 0.5 MeV - 1 MeV) and α-particles; R = recombination; Ex = direct excitation ⇒ distribution of the number of emitted photons between different excitation channels
  - LXe: the fast component for e^- only observed with an E-field (to suppress recombination); alphas: high LET, no difference in time decay constants between R and Ex; LET ~ 100 higher than for e^-, higher densities of ionised and excited species along the tracks, thus stronger and faster recombination

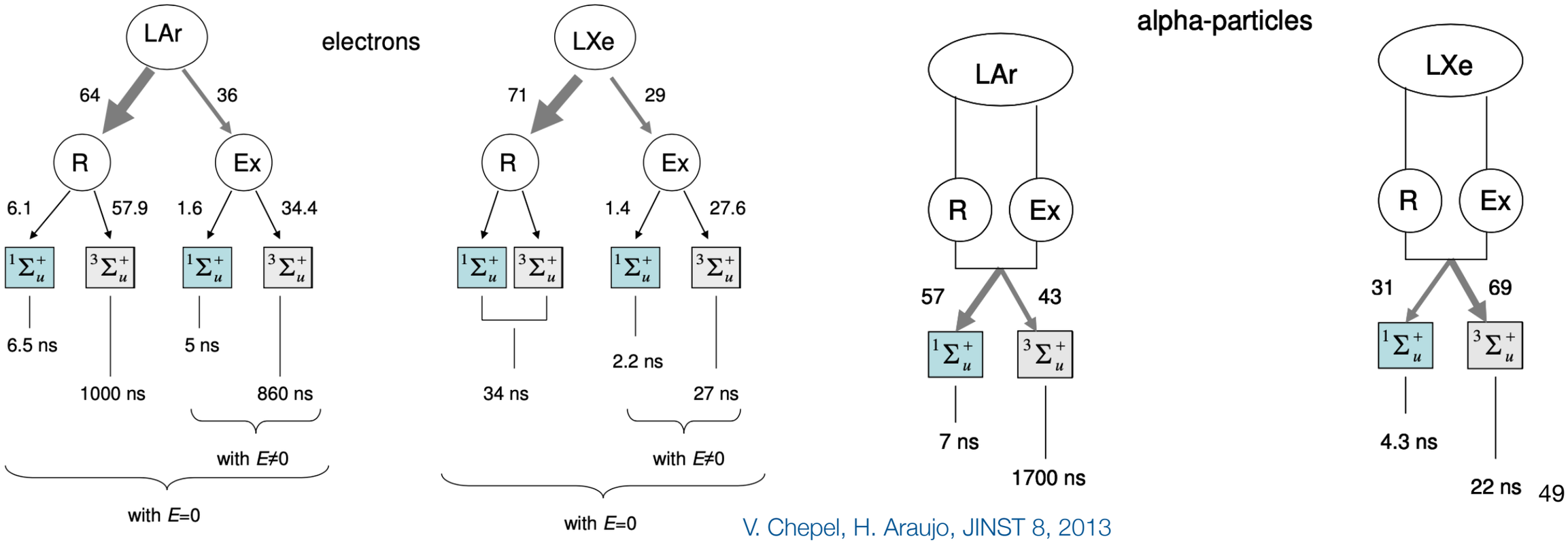

V. Chepel, H. Araujo, JINST 8, 2013

Scintillation light yield in Ar and Xe

- Light yield - as photons/keV - as a function of LET (dE/dx) for various particles
- Data shown in green (LAr) and blue (LXe)

V. Chepel, H. Araujo, JINST 8, 2013

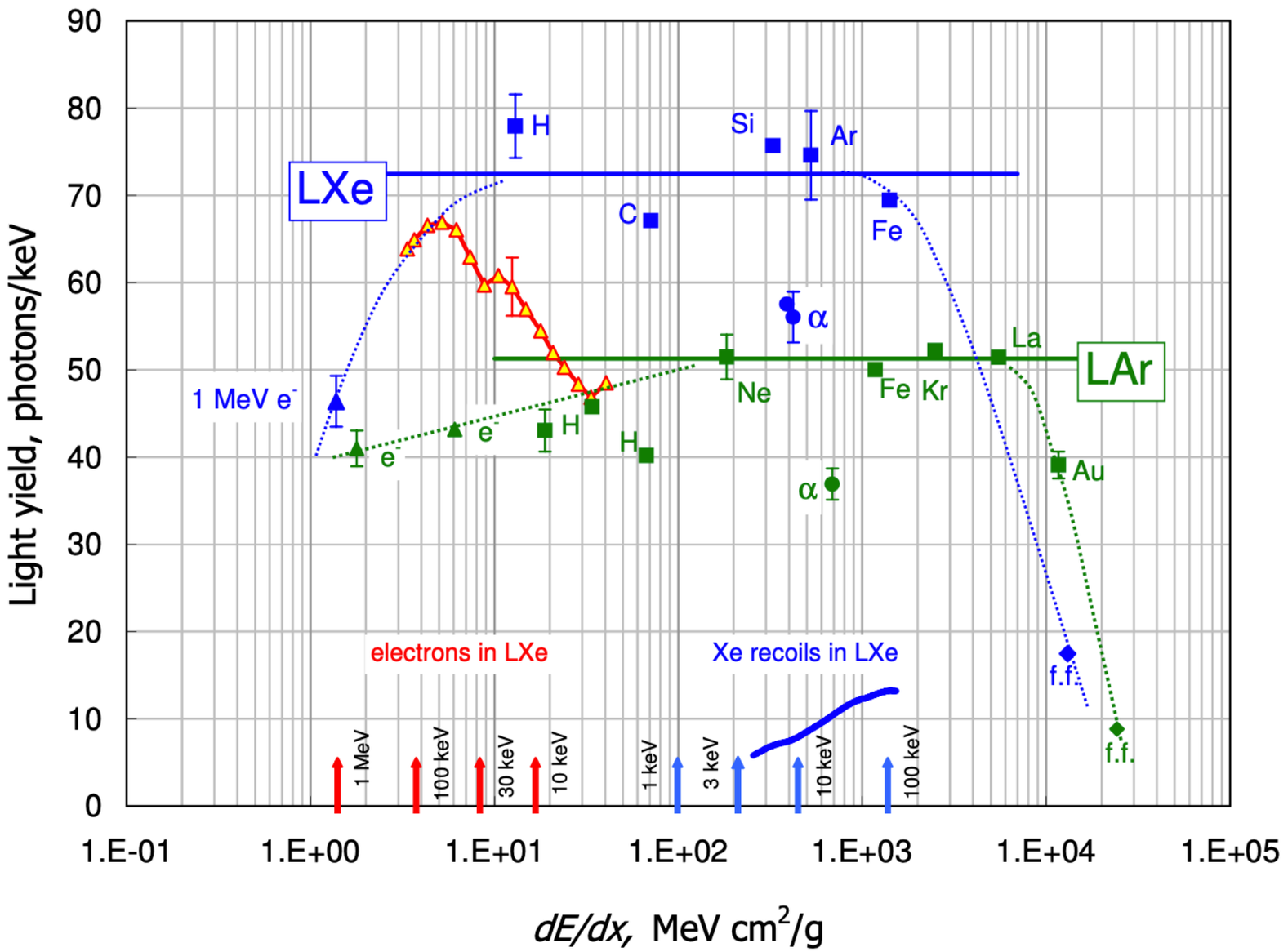

The scintillation pulse shape

- The scintillation light from pure noble liquids has *two decay components* due to the de-excitation of the singlet and triplet states of the excited dimer:

$$R_2^* \longrightarrow 2R + h\nu$$

- Figure:
  - Alphas and fission fragments: the shorter decay time comes from the de-excitation of singlet states, the longer from triplet states
  - Relativistic electrons: only one decay component
- The difference in pulse shape between different type of particle interactions is used to discriminate among the various particles via PSD

Time constants:

- Ne: few ns versus15.4 μs
- Ar: 10 ns versus 1.5 μs
- Xe: 4 ns versus 27 ns Xe

- e^-: the decay times dominated by a slow, recombination component
- alphas, fission fragments: the recombination is very fast, does not affect the decay times

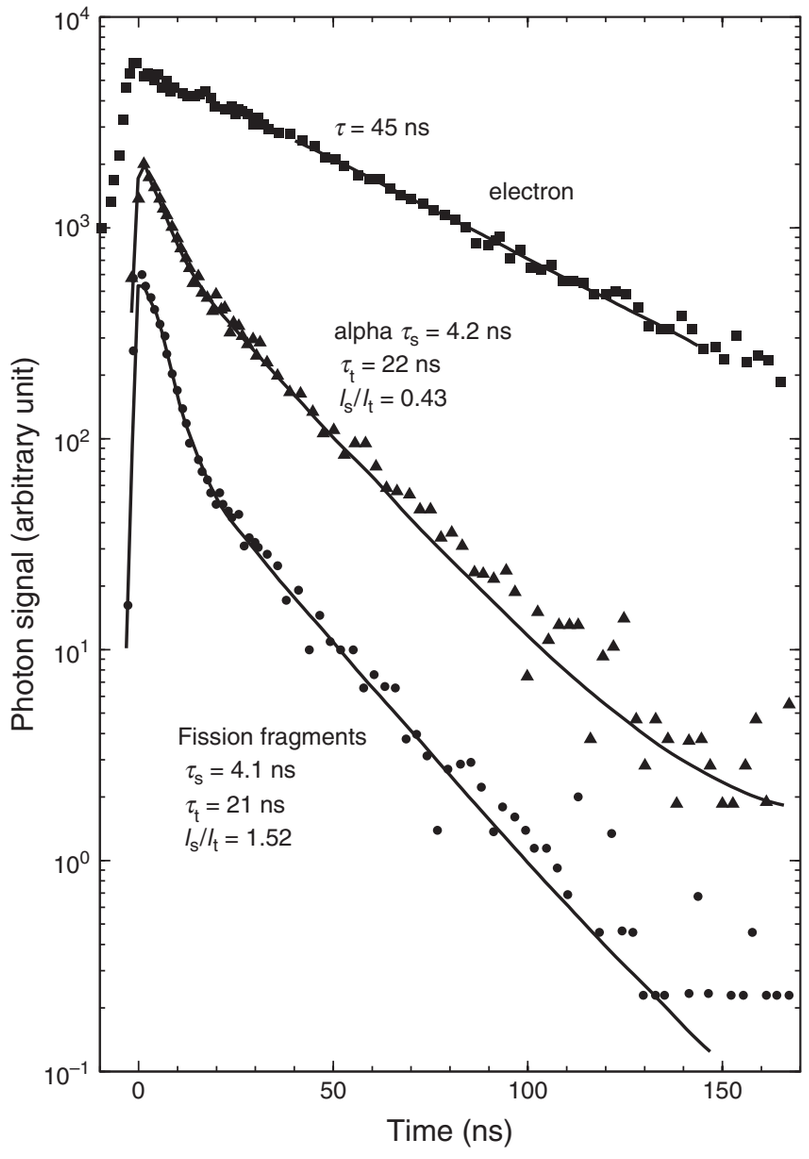

Fig. 21.1. Decay curves of luminescence from liquid xenon excited by electrons, α-particles and fission fragments, without an external electric field [1109; 1283].

Electronic and nuclear recoils in noble liquids

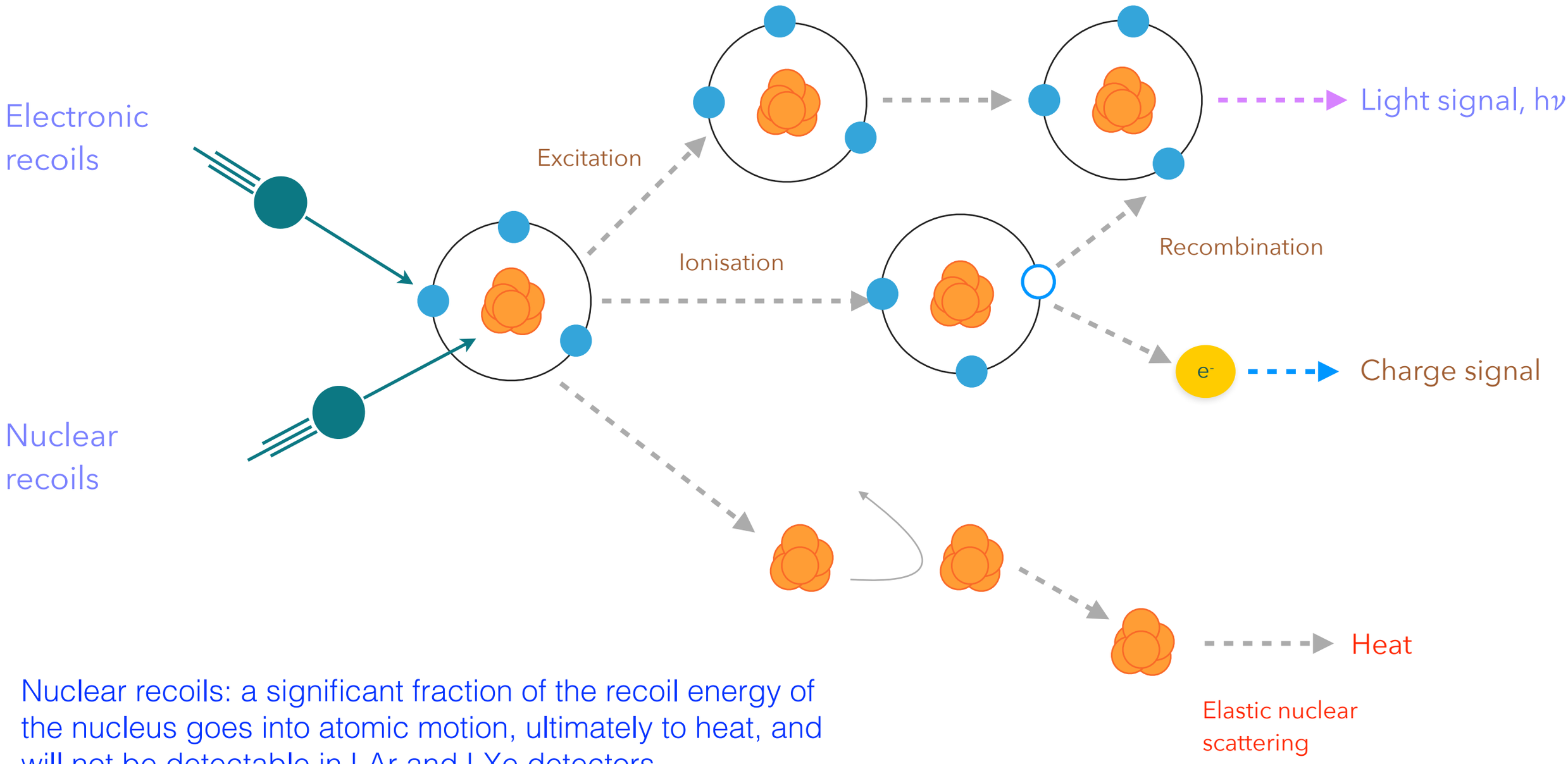

Nuclear recoils: a significant fraction of the recoil energy of the nucleus goes into atomic motion, ultimately to heat, and will not be detectable in LAr and LXe detectors

Scintillation yield in noble liquids

- An energetic particle looses energy through:
  - inelastic interactions with electrons in the medium (electronic stopping)
  - elastic collisions with nuclei (nuclear stopping)
- Electrons, gamma rays and fast ions loose most of their energy through electronic stopping
- Nuclear recoils loose a considerable fraction of their energy via nuclear stopping (nuclear quenching, q_{nc})
- The lower scintillation yield of alpha tracks is attributed to bi-excitonic quenching (electronic quenching, q_{el}) and nuclear recoils will also suffer from this effect

Liquid argon quenching factor for ions:
A. Hitachi, Instruments 2021, 5

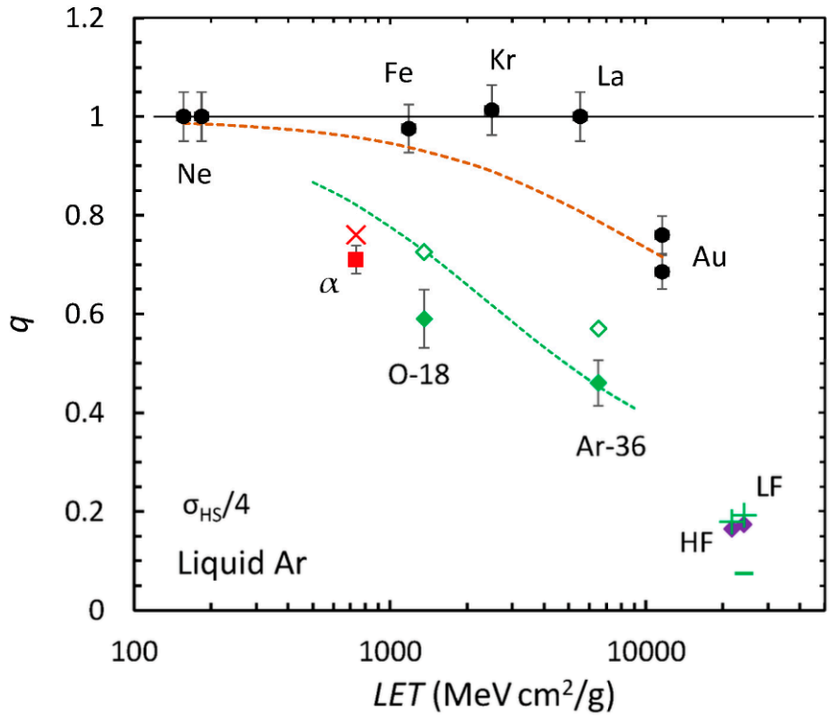

Liquid xenon relative scintillation yield:
T. Doke at al., Jpn J. Appl. Phys, 2002, 41

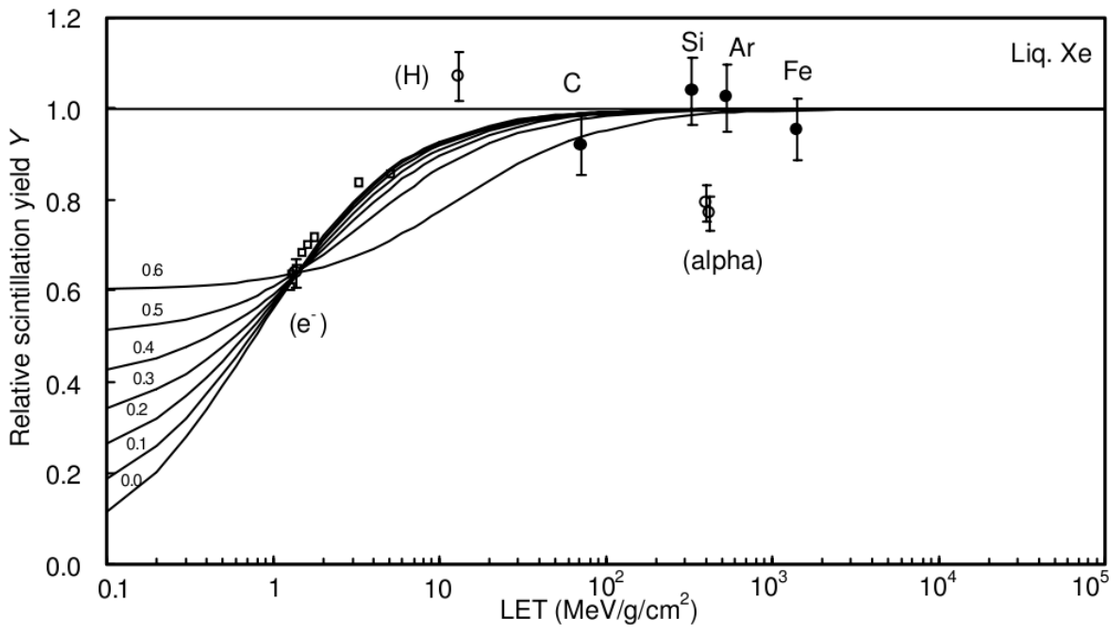

The Lindhard factor

- Lindhard computed the fraction of the initial recoil energy lost to electronic excitation, f_n
- His theory describes quite well the ionisation signals in semiconductors:

$$f_n = \frac{kg(\epsilon)}{1 + kg(\epsilon)}$$

$$\epsilon = 11.5\, E_R(\mathrm{keV}) Z^{-7/3}$$

$$k = 0.133\, Z^{2/3} A^{-1/2}$$

$$g(\epsilon) = 3\epsilon^{0.15} + 0.7\epsilon^{0.6} + \epsilon$$

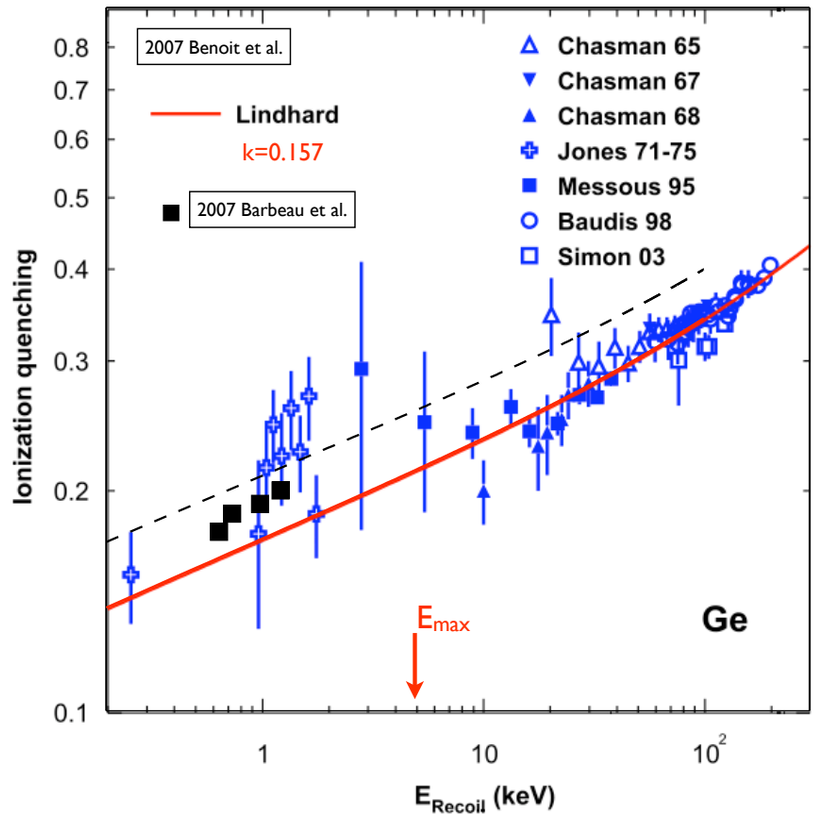

- ε: reduced energy = dimensionless deposited energy, with Z = atomic number of nucleus
- k = proportionality constant between the electronic stopping power dE/dx and the velocity of the projectile (which is the recoiling atom)
- g(ε): proportional to the ratio of electronic stopping power to nuclear stopping power

The Lindhard factor in noble liquids

- Historically, the measured values of the scintillation efficiency in noble liquids were considerably lower than the Lindhard prediction (k = 0.165 for xenon, k = 0.144 for argon)
- It was believed that this may be due to electronic quenching and possibly to escape electrons

Liquid xenon

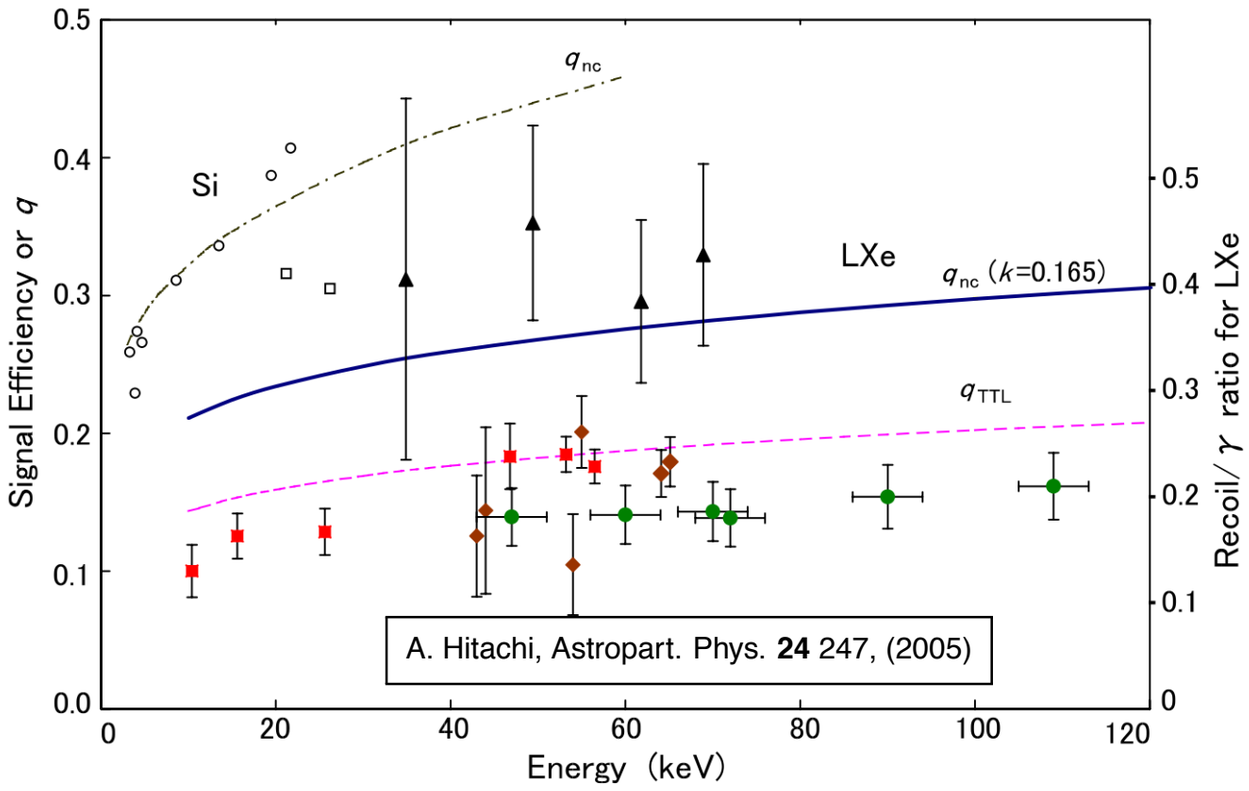

Liquid argon

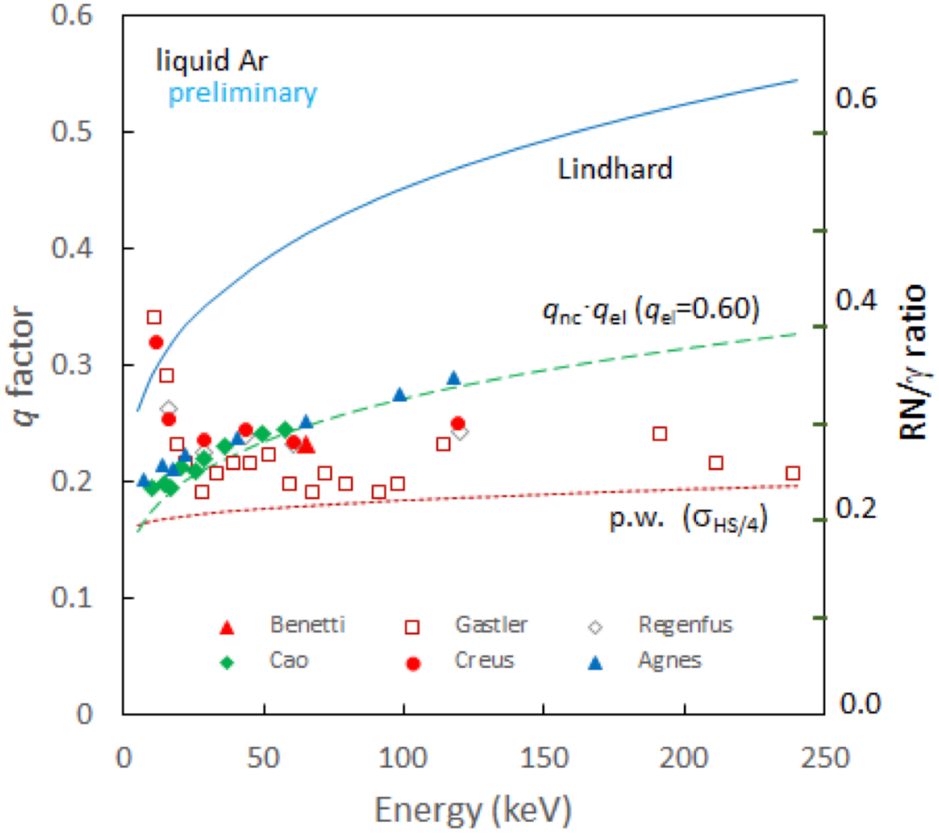

A. Hitachi. A. Mozumder, arXiv:1903.05815, 2019

The Lindhard factor in noble liquids

- More recently: the Lindhard prediction seems to apply if the nuclear recoil energy is reconstructed using both scintillation and ionisation signals (hence the total quanta, for example in two-phase TPCs, more on this later in the lecture), the so-called “combined energy scale”:

$$E_{ER} = W \cdot (N_{ph} + N_q)$$

$$E_{NR} = W \cdot (N_{ph} + N_q) \cdot \frac{1}{f_n}$$

$$f_n = \frac{W \cdot (N_{ph} + N_q)}{E_{NR}}$$

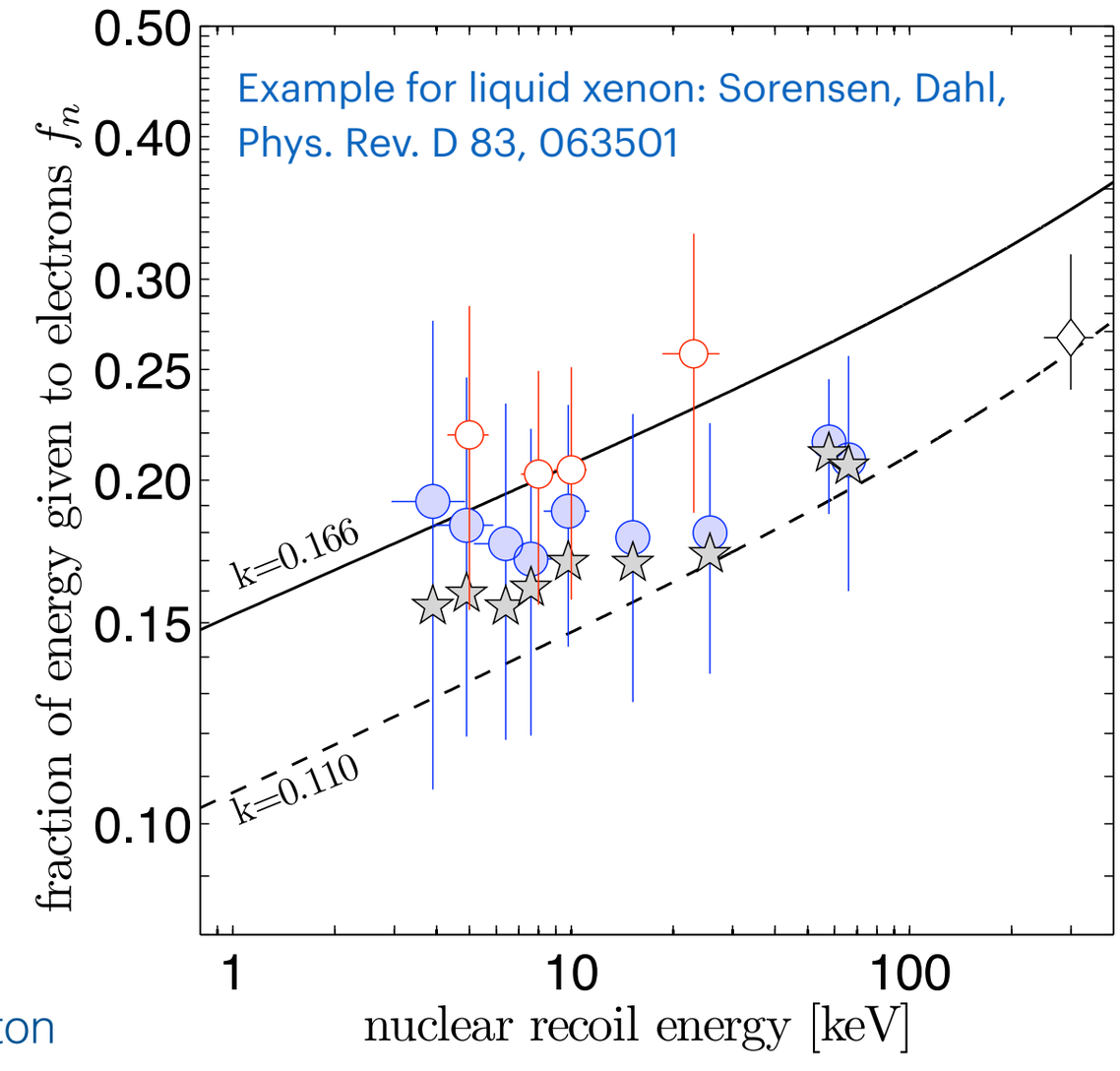

- N_q = nr. of primary electrons
- N_{ph} = nr of primary UV photons
- W = average energy to produce an electron or a photon

Light and charge yields of NRs

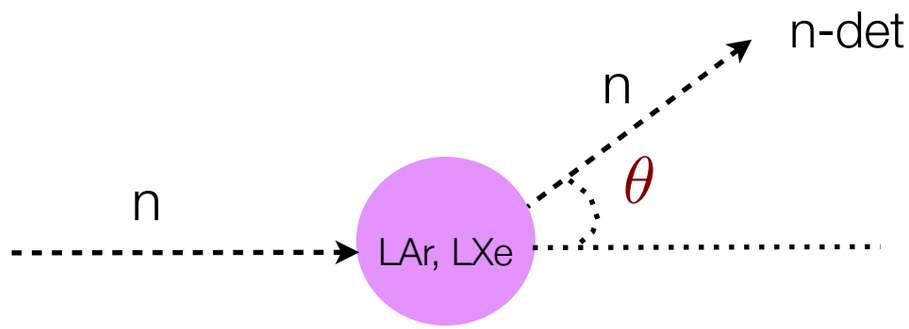

- Must be determined based on NR data, using two methods
  - direct: observe mono-energetic neutrons scatters which are tagged with n-detectors
  - indirect: measure energy spectra from calibration n-sources, compare with MC predictions

P. Agnes et al., Phys. Rev. D 104, 2021

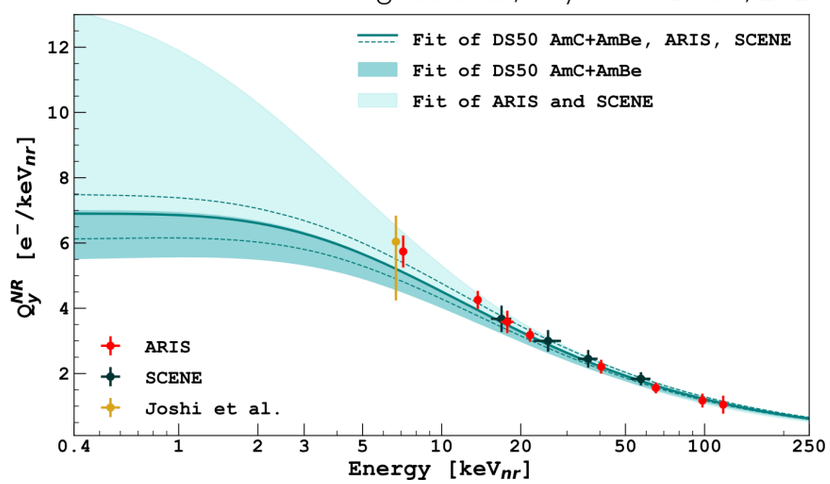

- LAr: charge yield measured down to ~ 0.5 keV$_{NR}$ (≡ 3 ionisation electrons)

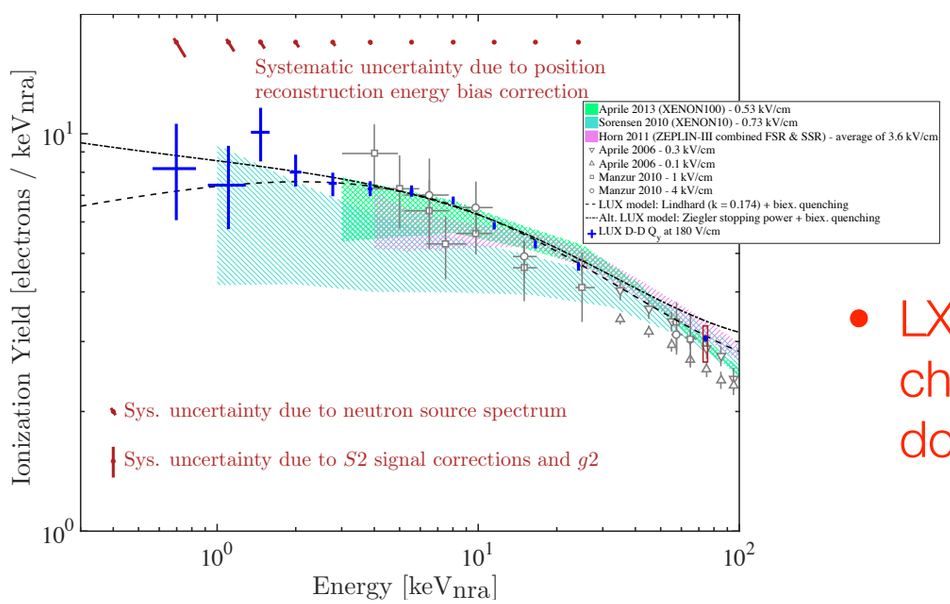

- LXe: here data from LUX; charge yield measured down to 0.7 keV$_{NR}$

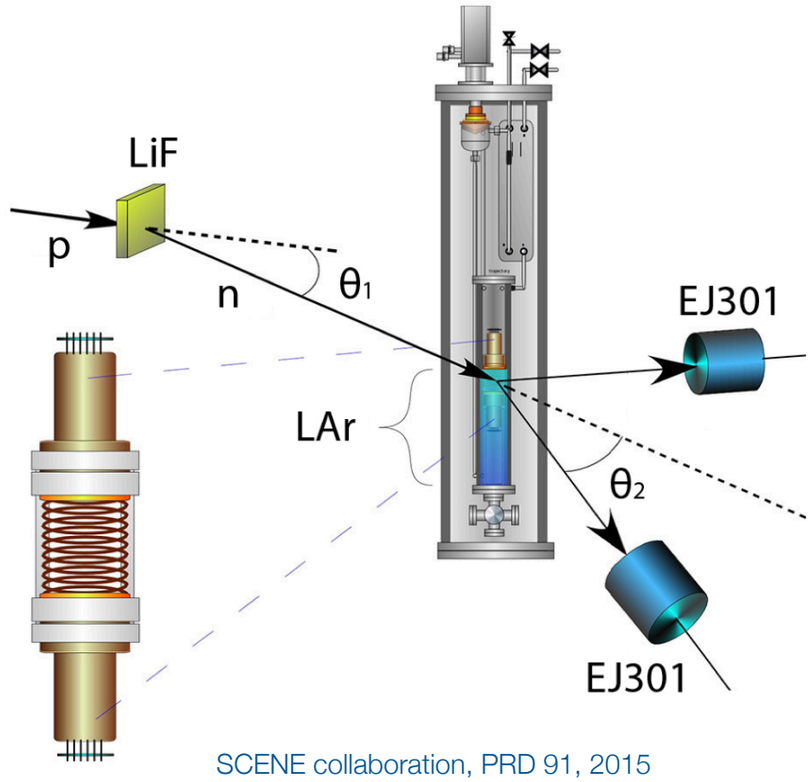

SCENE collaboration, PRD 91, 2015

Light and charge yields from NEST

- NEST (Noble Element Simulation Technique): a MC simulation framework that allows for parametrisation of excitation, ionisation and the corresponding scintillation and electroluminscence processes in noble liquids
  - based on semi-empirical models; as a function of incoming or deposited energy, electric field, interaction type (electronic and nuclear recoils, alpha particles)
  - calculates average light and charge yields, recombination and simulates actual energy deposits in a detector
  - models are validated against real data and updated when new data becomes available
- Primary code in C++, bindings available to use in Python; available for xenon and argon

Ar

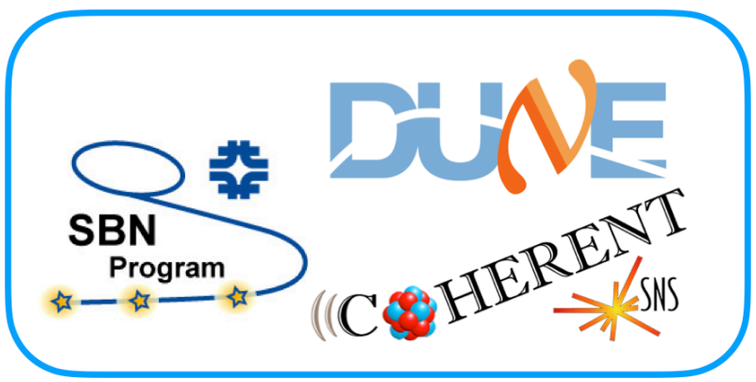

Xe

Figure by Sophia Andaloro

https://nest.physics.ucdavis.edu

Light and charge yields from NEST

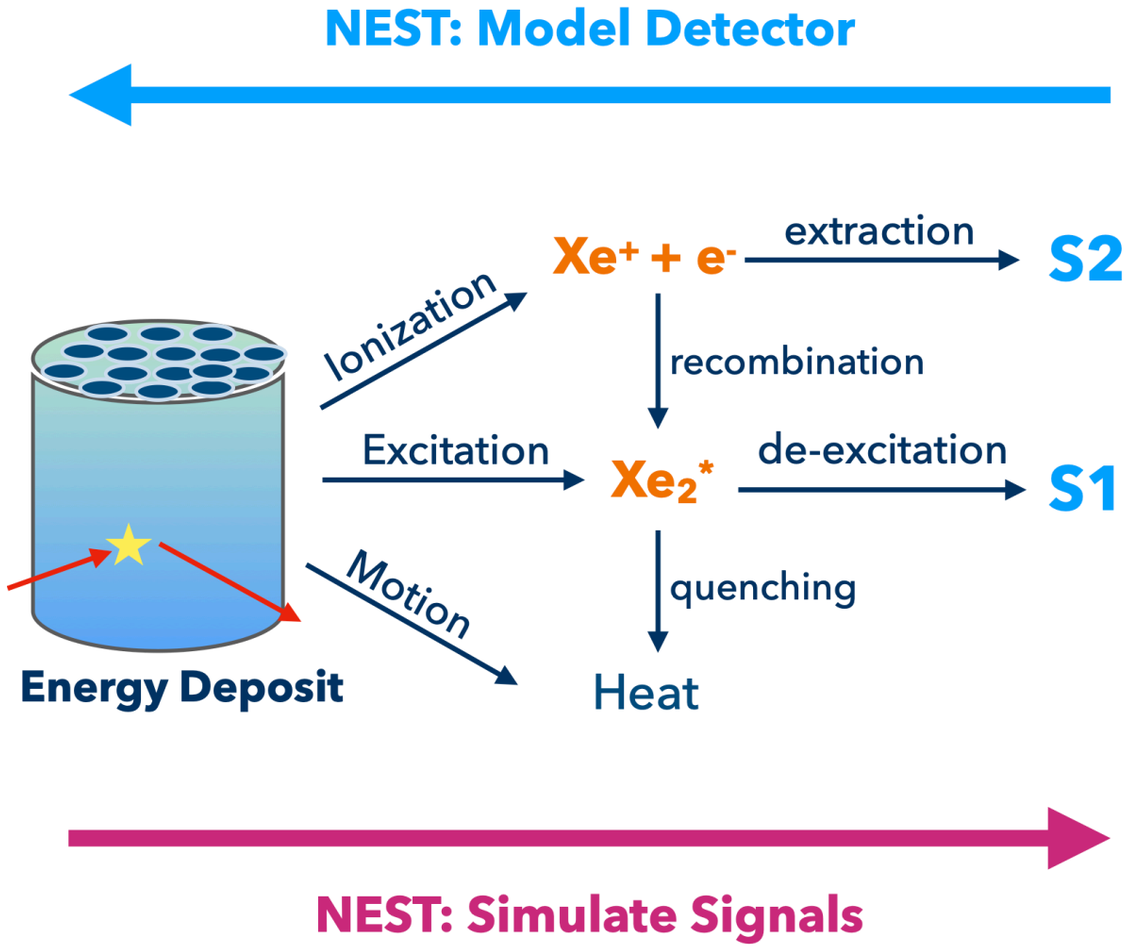

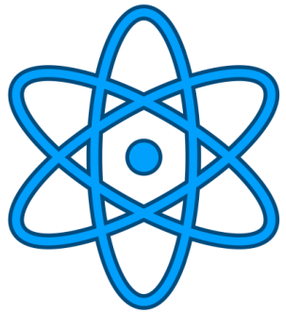

Macroscopic

- ❖ Fields (drift, gap)
- ❖ Density, Temp, Phase
- ❖ Geometry, PMTs…

Microscopic

- ❖ Particle types
- ❖ Recombination, dE/dx
- ❖ Nex/Ni

ER	NR	Other
Photons (γ)	Neutrons	α (alphas)
β^- , μ^- (leptons)	Heavy Nuclei	^{83m}Kr
expanding…	WIMPs	Protons

Slide by Sophia Andaloro, APS meeting April 2021

https://nest.physics.ucdavis.edu

Light and charge yields from NEST: Xenon

Light yields: ERs

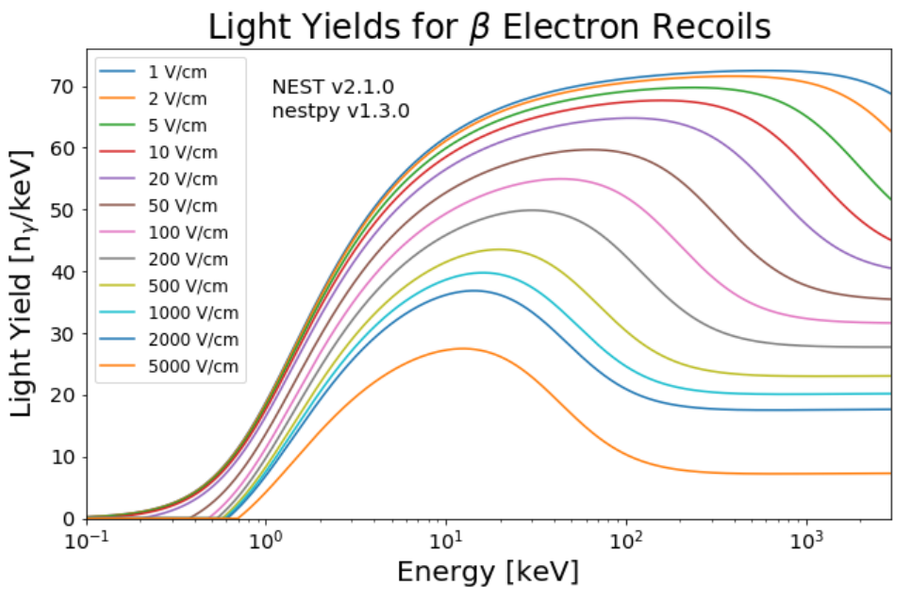

Light yields: NRs

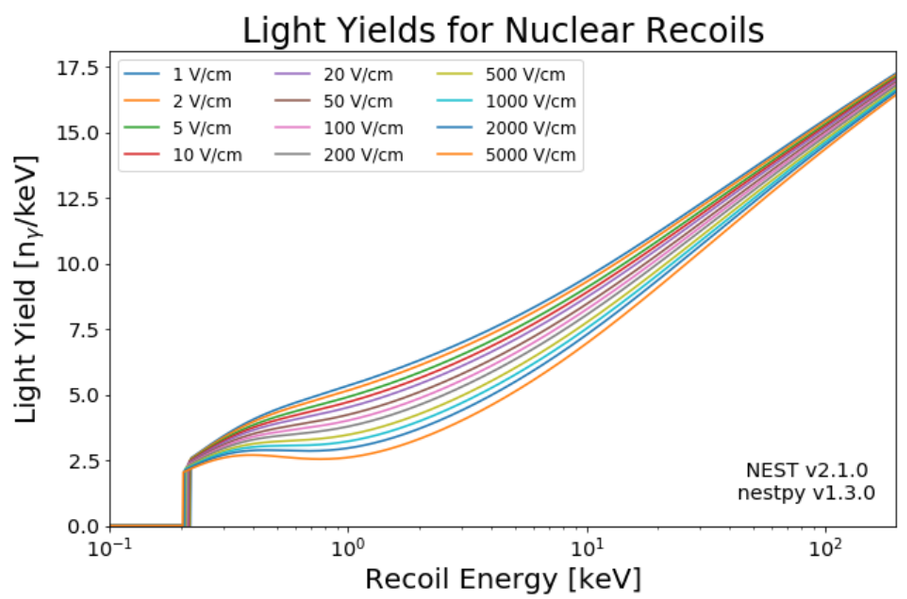

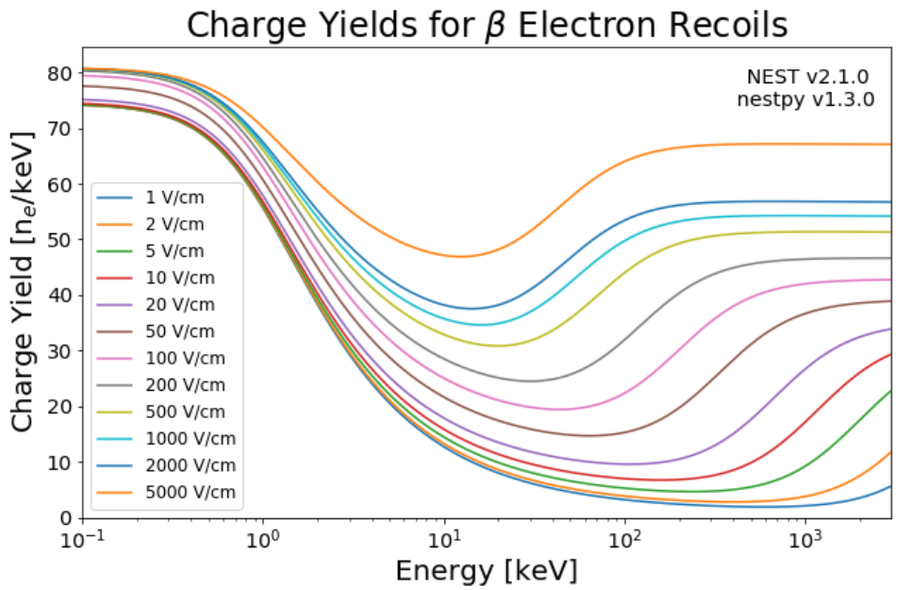

Charge yields: ERs

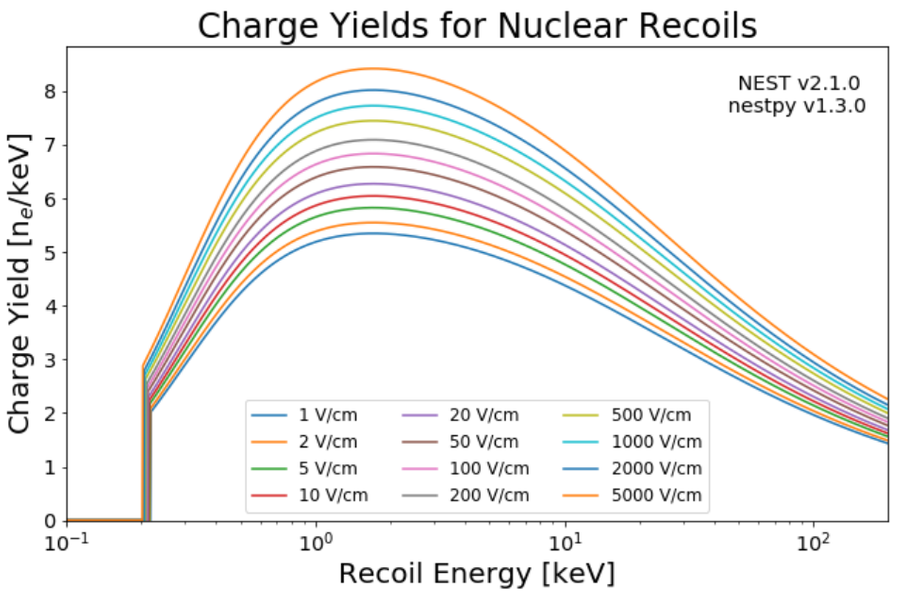

Charge yields: NRs

https://nest.physics.ucdavis.edu

Light and charge yields from NEST: Argon

Light yields: ERs

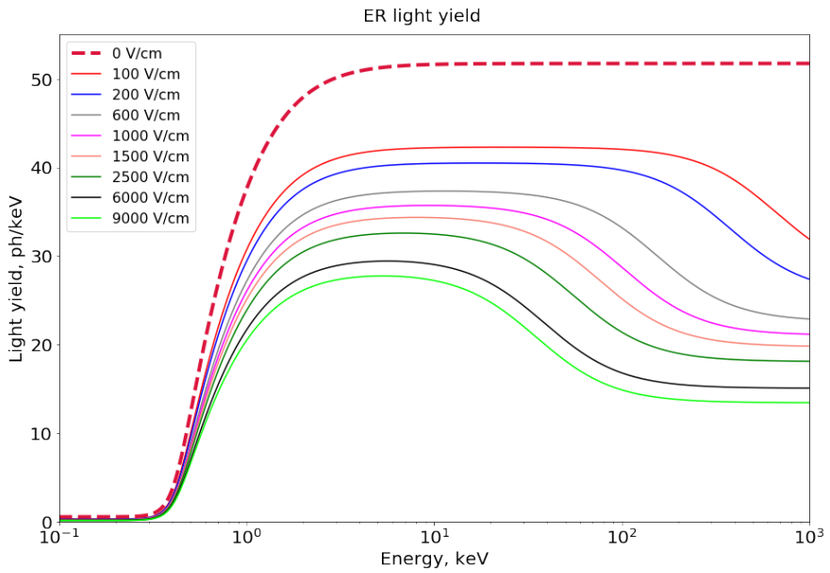

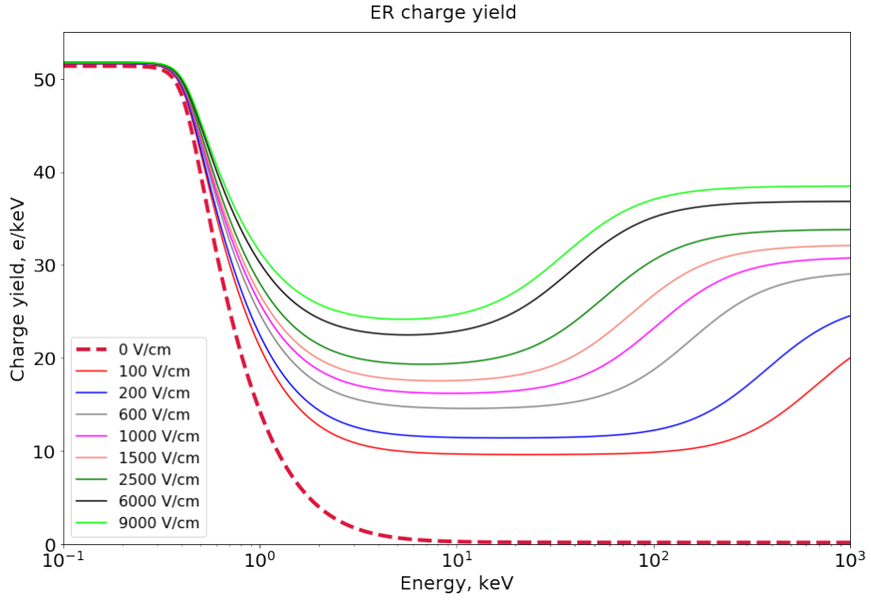

Charge yields: ERs

Light yields: NRs

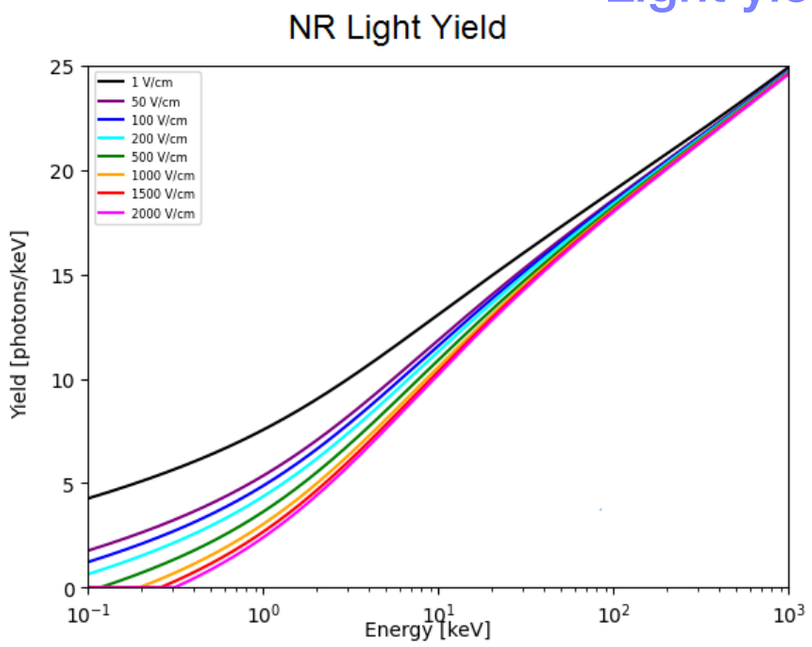

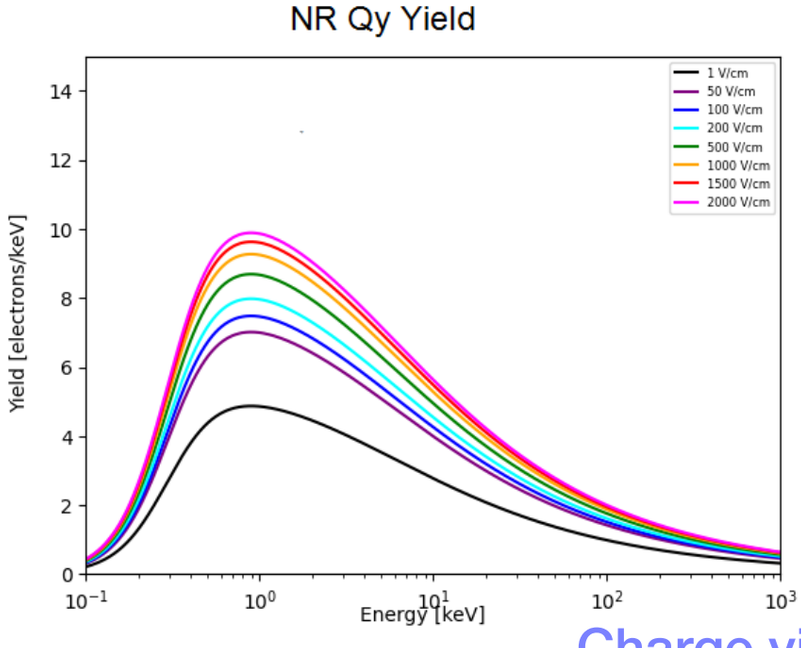

Charge yields: NRs

https://nest.physics.ucdavis.edu

Ly and Qy from NEST against data: Xenon ER β

lower drift fields

higher drift fields

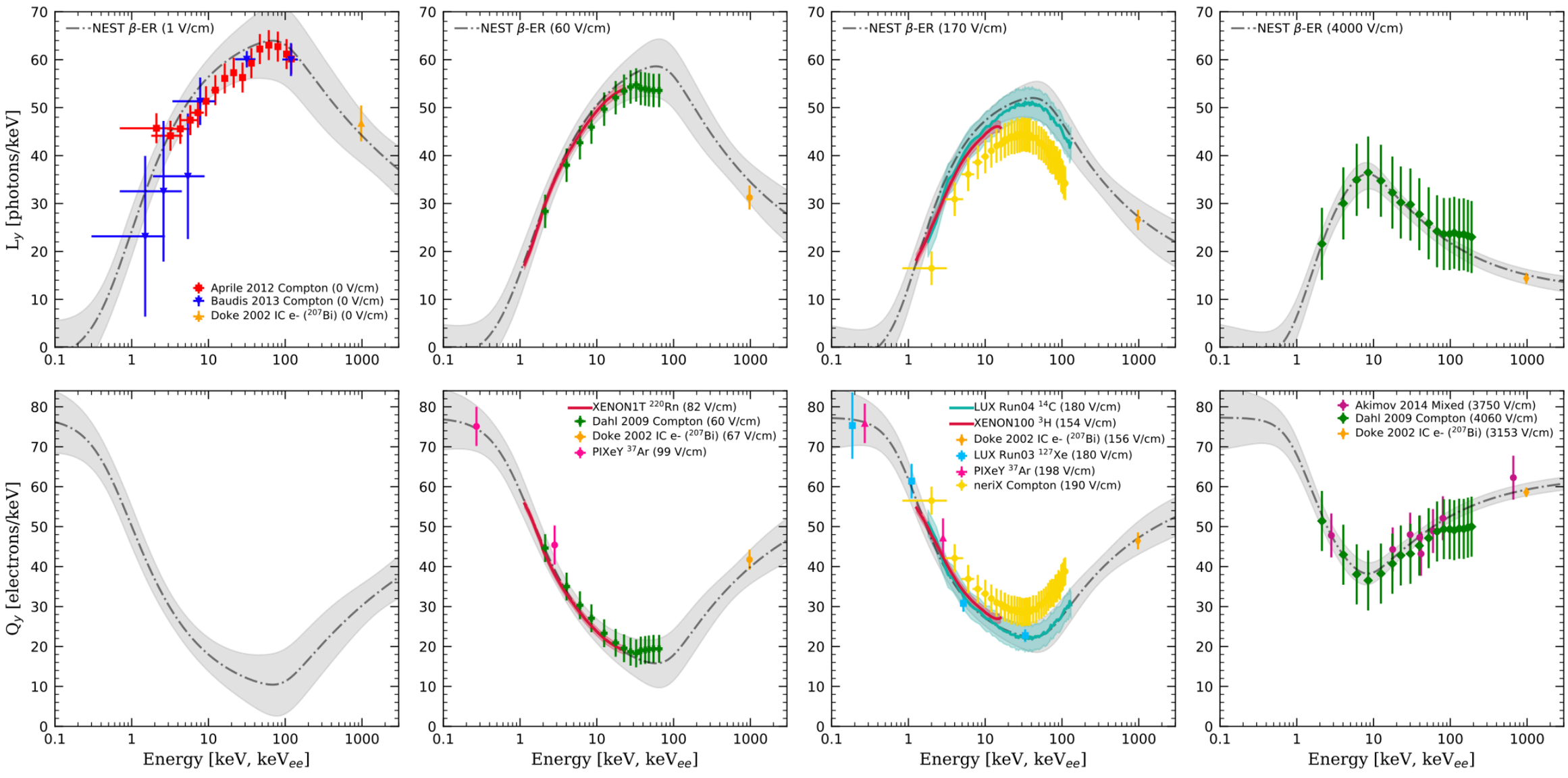

arXiv:2211.10726

Ly and Qy from NEST against data: Xenon NR

lower drift fields

higher drift fields

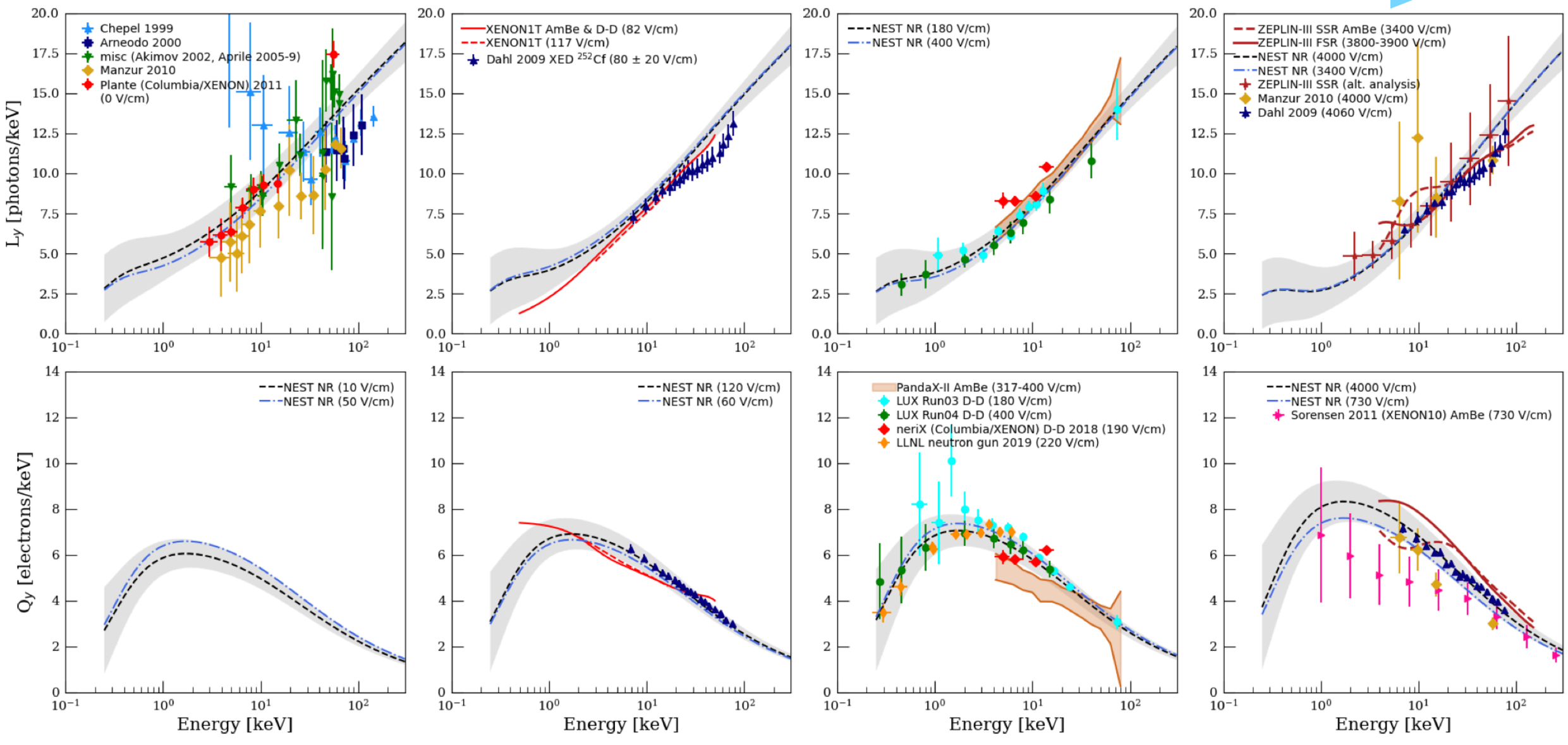

arXiv:2211.10726

Electron attachment and light absorption

- To achieve a high collection efficiency for both ionisation and scintillation signals, the concentration of impurities in the liquid has to be reduced and maintained to a level below 1 part per 10^9 (part per billion, ppb) oxygen equivalent
  - The scintillation light is strongly reduced by the presence of water vapour
  - The ionisation signal requires both high liquid purity (in terms of substances with electronegative affinity, SF_6, N_2O, O_2, etc) and a high field (typically ~ 100 V/cm)
- Attenuation lengths of ~1 m for electrons and photons were already achieved > 1m and are necessary for multi-tonne-scale experiments

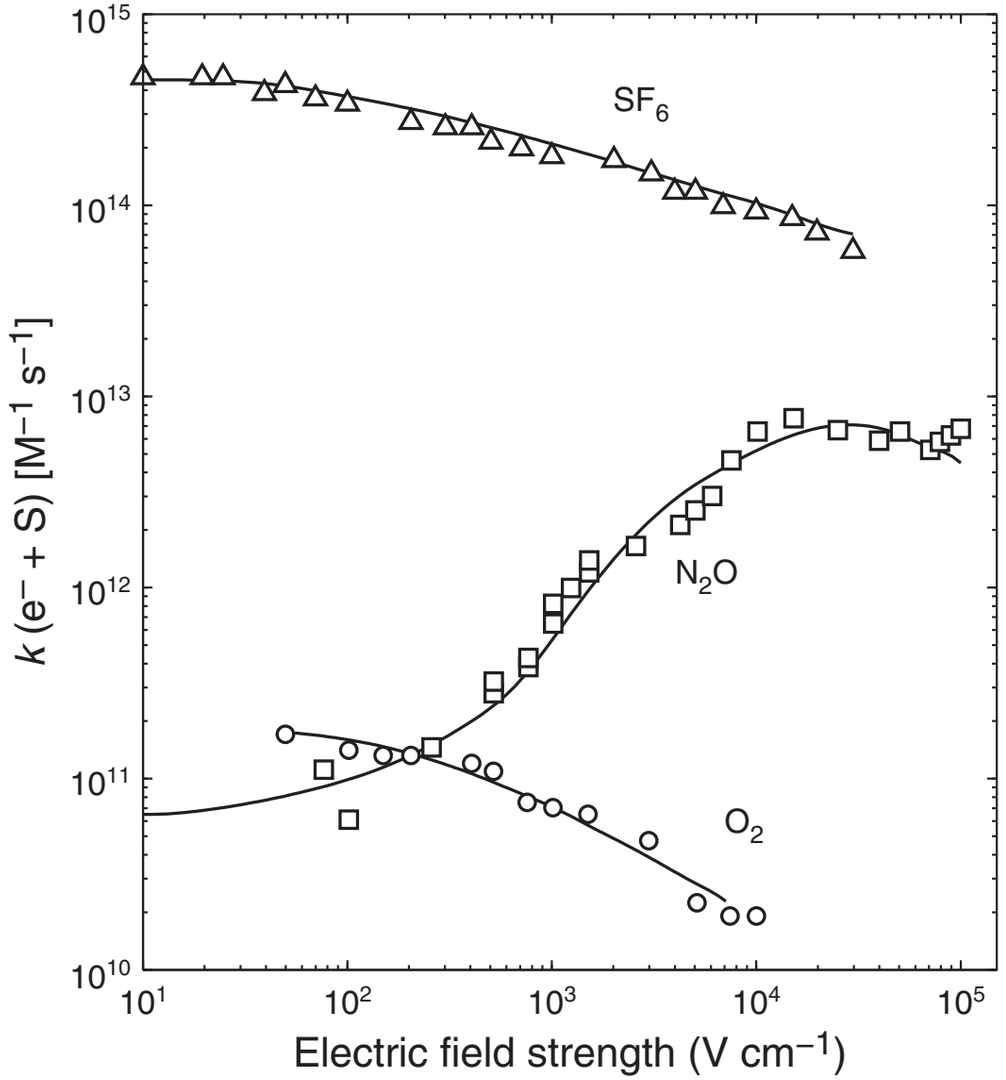

Fig. 21.4. Rate constant for the attachment of electrons in liquid xenon (T = 167 °K) to several solutes: (△) SF_6, (□) N_2O, (○) O_2 [174].

The electron drift lifetime in noble liquids

- The purity of the noble liquid is commonly expressed via the "electron lifetime" τ_e
  - the time over which the number of drifting electrons N_e is reduced by a factor e:

$$N_e(t) = N_e(t_0)\, e^{-t/\tau_e}$$

- The electron lifetime is related to the concentration of impurities (C_i) and their constants of attachment (k_i), as follows:

$$\tau_e = \frac{1}{\sum_i k_i C_i} = \frac{1}{k_{O_2} C_{O_2}}$$

  - where often the O_2-equivalent impurity concentration C_{O2} is used as benchmark (O_2 usually the dominant contributor)

- The O_2-equivalent mole fraction (x_{O2}) is expressed in ppb (parts per billion):

$$\frac{1}{\tau_e} = k_{O_2} C_{O_2} = k_{O_2} x_{O_2} \frac{\rho}{M}$$

  - where ρ is the density of the noble liquid and M the molar mass. The constant of electron attachment k_{O2} depends on the drift field (it decreases with increasing field), and it is given in [$ppb^{-1}\mu s^{-1}$]

The electron drift lifetime in noble liquids

- In general, electronegative impurities in noble liquids increase over time due to the continuous desorption from materials
- To achieve very low concentrations and high electron lifetimes, continuous removal of impurities is required
  - by gas purification through high-temperature (400 °C) zirconium getters (using highly-efficient liquid-gas heat exchangers to minimise the heat input)
  - by liquid purification through filters which contain pellets with high-surface area copper, which binds the impurities on the surface

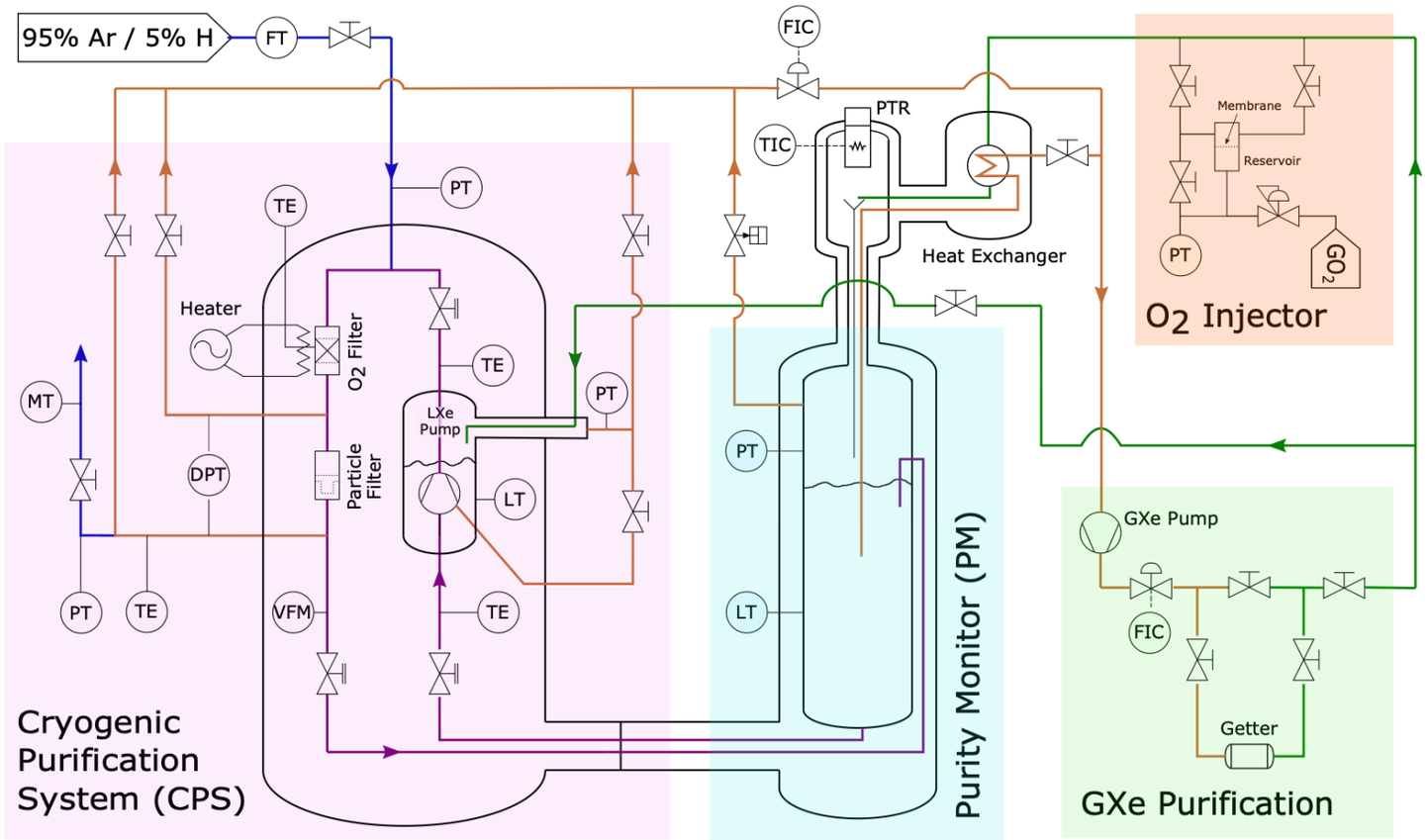

Example: Xeclipse, a xenon purification system at Columbia University (demonstrator for XENONnT at LNGS), Plante, Aprile, Howlett, Zhang, arXiv:2205.07336

How to measure the electron drift lifetime

- The electron lifetime" τ_e is usually measured with purity monitors. The concept:
  - release a cloud of electrons, drift the cloud a fixed distance through a uniform electric field
  - measure the size of the cloud at the beginning and at the end via the induced current on a cathode and anode as the e^- drift from and towards these, respectively
  - electrodes are equipped with grids to shield them from the effects of the e^- cloud except when the e^- are drifting in the space in between
  - **determine τ_e from the ratio of the induced currents and their separation in time which is the drift time t_d**

$$\frac{Q_A}{Q_C} = e^{-t_d/\tau_e}$$

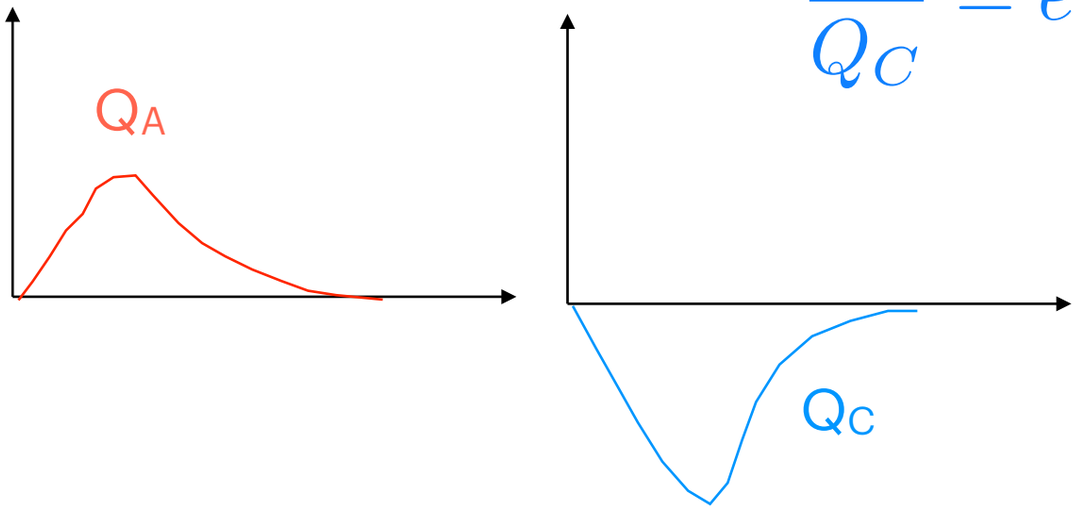

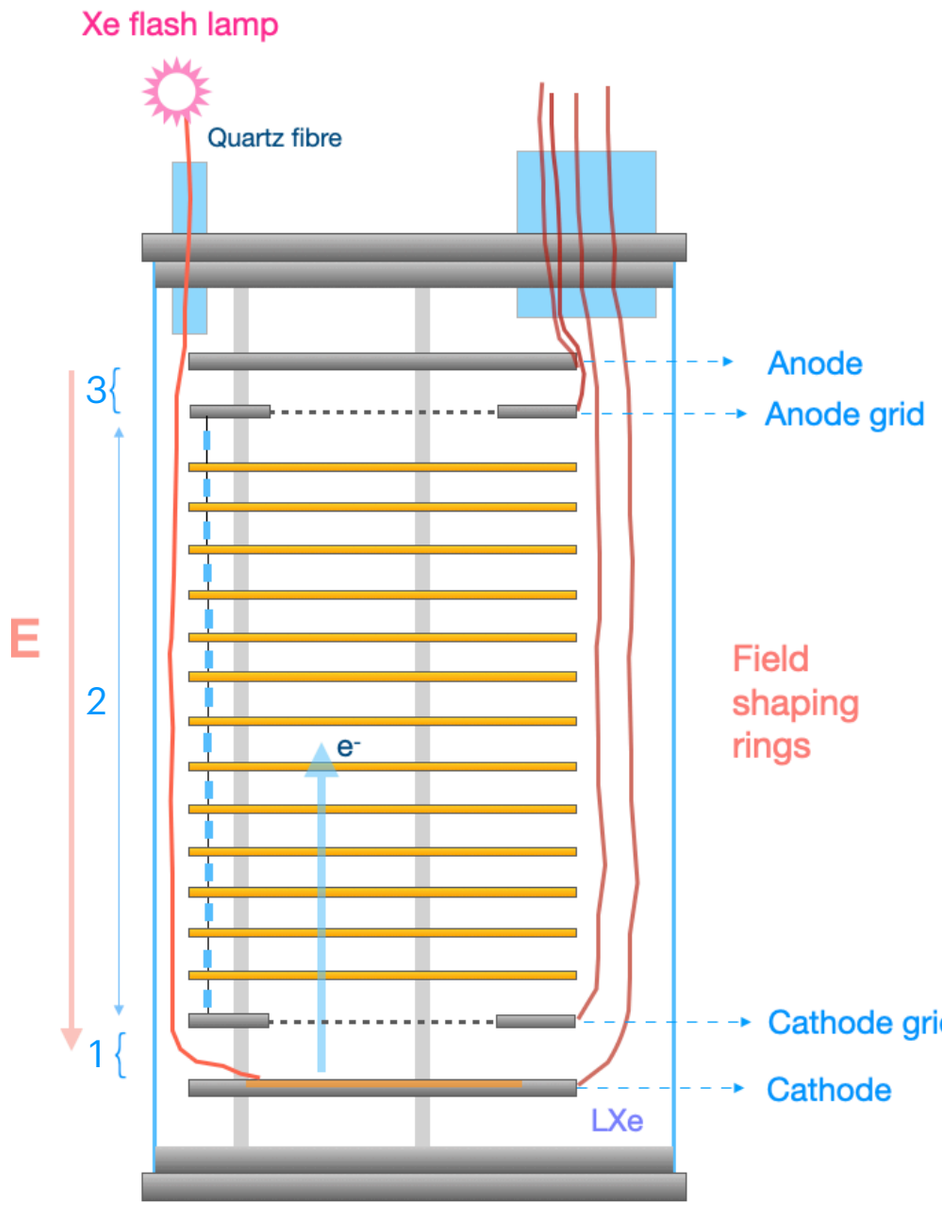

Example: a purity monitor for liquid xenon

- Drift length: 530 mm
- Electron cloud: produced from in-house made, thin film Au photocathode (on quartz substrate) via pulsed xenon flash lamp (Hamamatsu L7685)
- Charge readout on top (Q_A) and bottom (Q_C)
- Electrons are absorbed as they drift upwards (in region 2) towards the anode
- Ratio of signals: $\propto$ electron lifetime τ_e

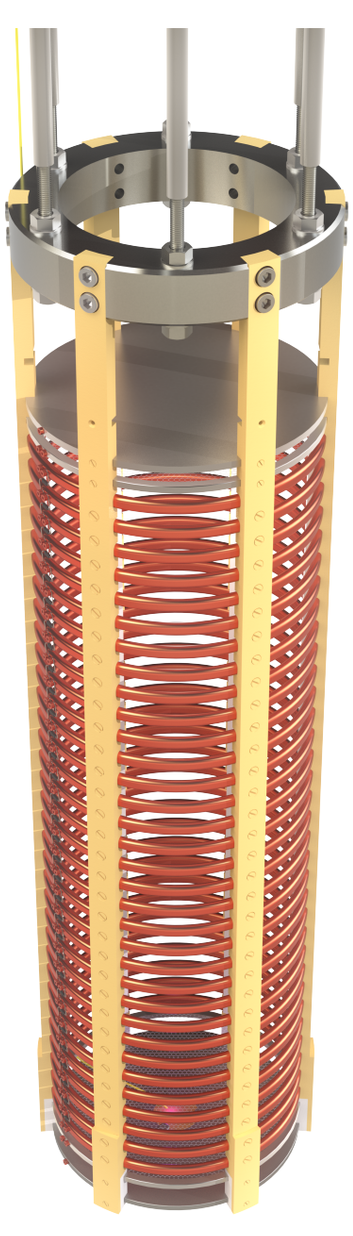

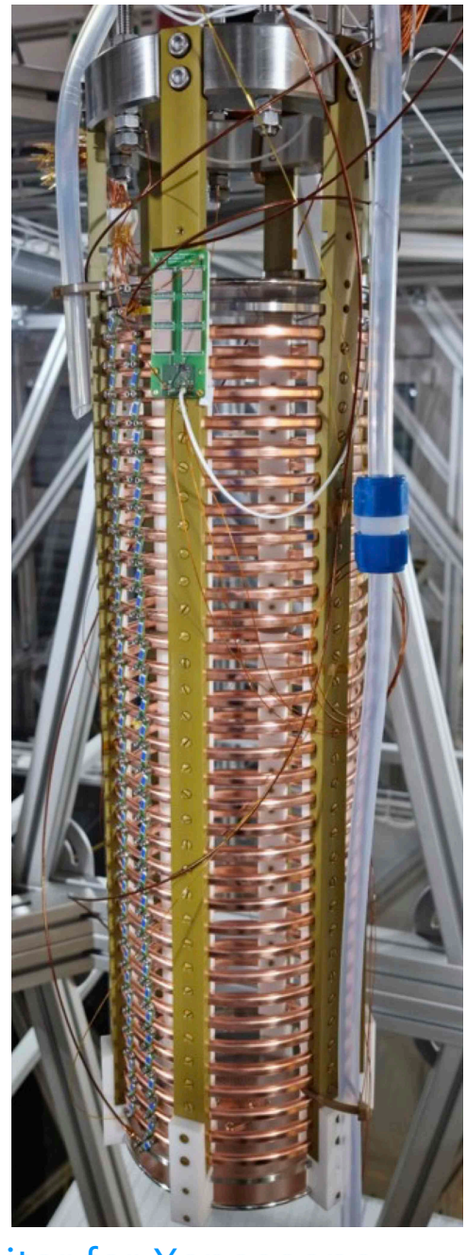

Purity monitor for Xenoscope
(PhD thesis of Yanina Biondi, UZH)

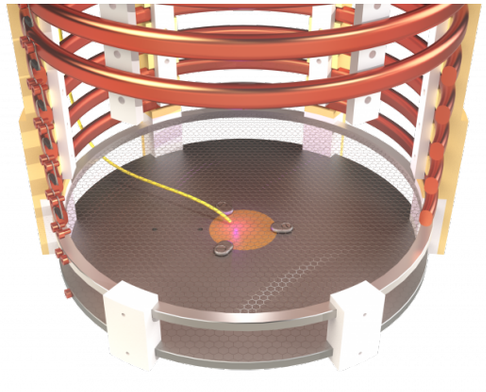

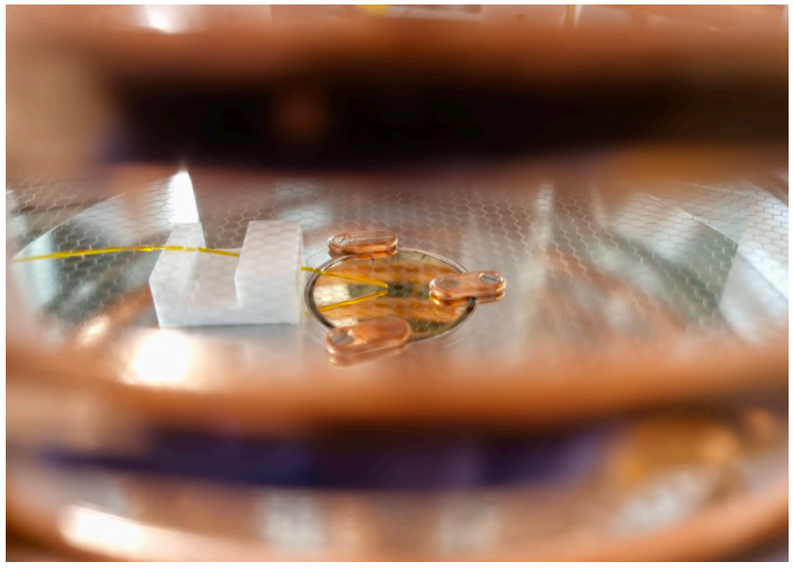

Purity monitor signal readout

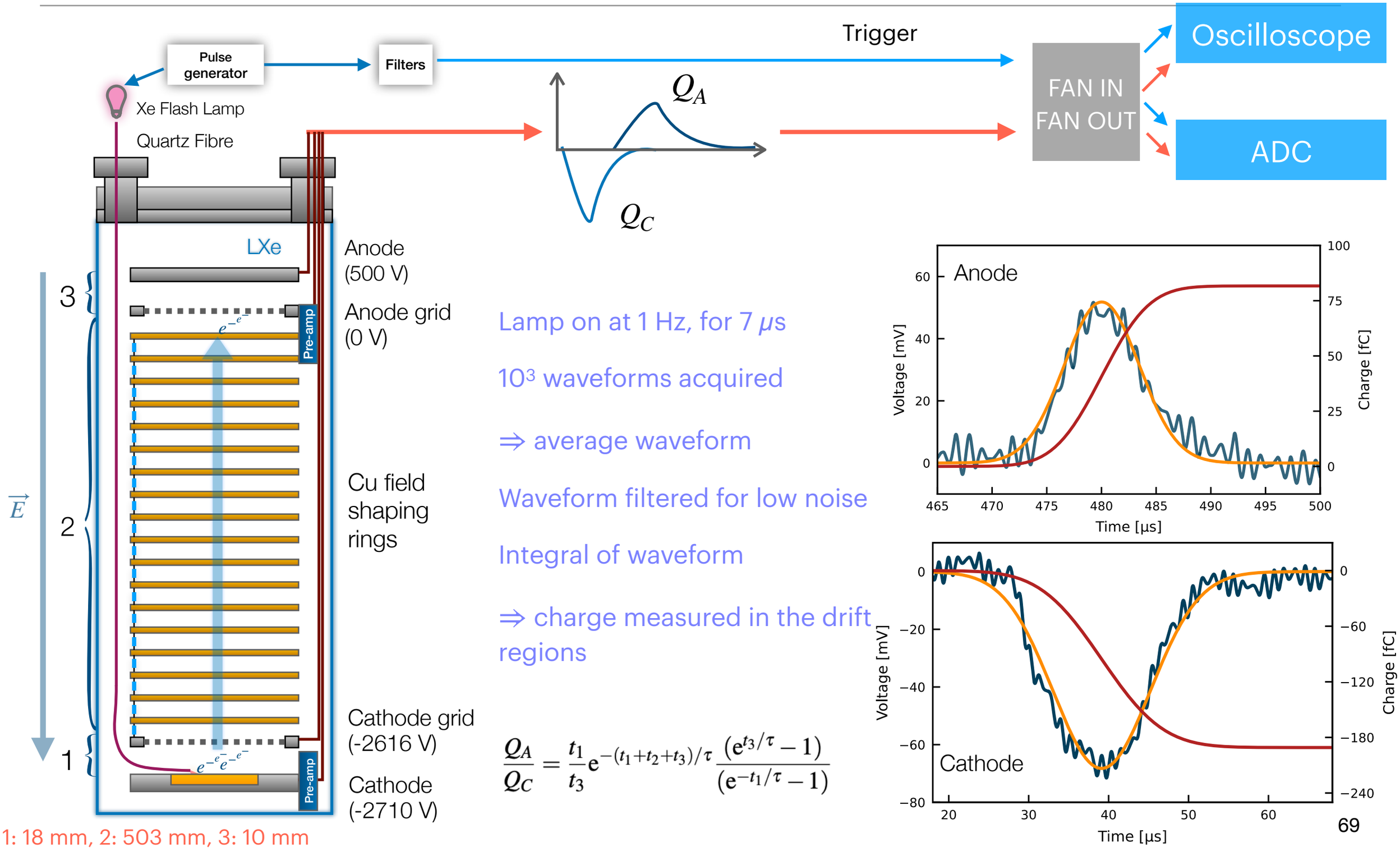

Lamp on at 1 Hz, for 7 μs

10^3 waveforms acquired

⇒ average waveform

Waveform filtered for low noise

Integral of waveform

⇒ charge measured in the drift regions

$$\frac{Q_A}{Q_C} = \frac{t_1}{t_3} e^{-(t_1+t_2+t_3)/\tau} \frac{(e^{t_3/\tau}-1)}{(e^{-t_1/\tau}-1)}$$

Electron lifetime determination

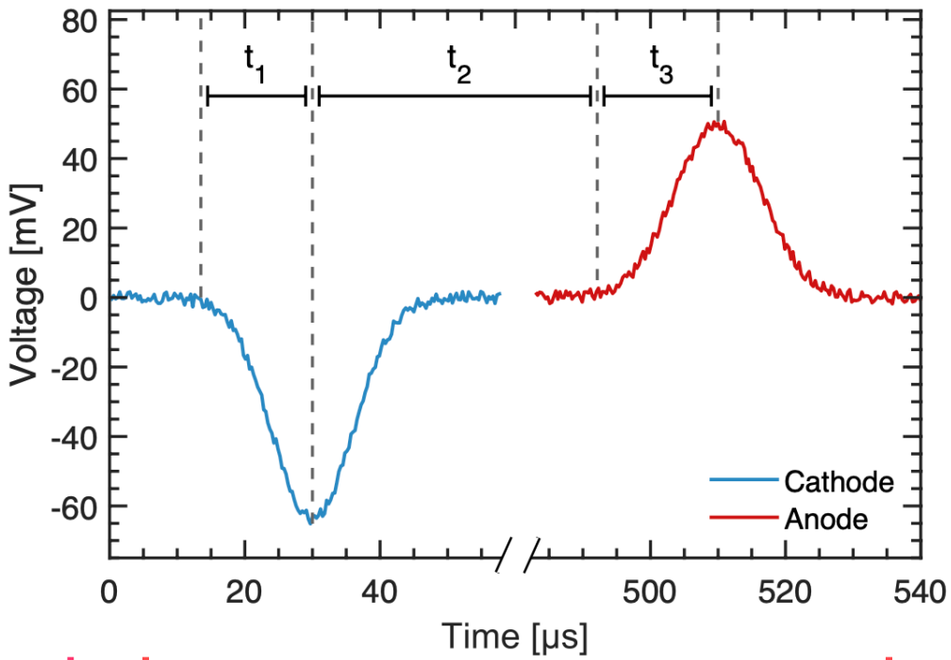

cathode signal

anode signal

- Run: 88 d with 343 kg LXe, three different Xe flow regimes

30 slpm ≡ 252 kg/h 35 slpm ≡ 294 kg/h 40 slpm ≡ 353 kg/h

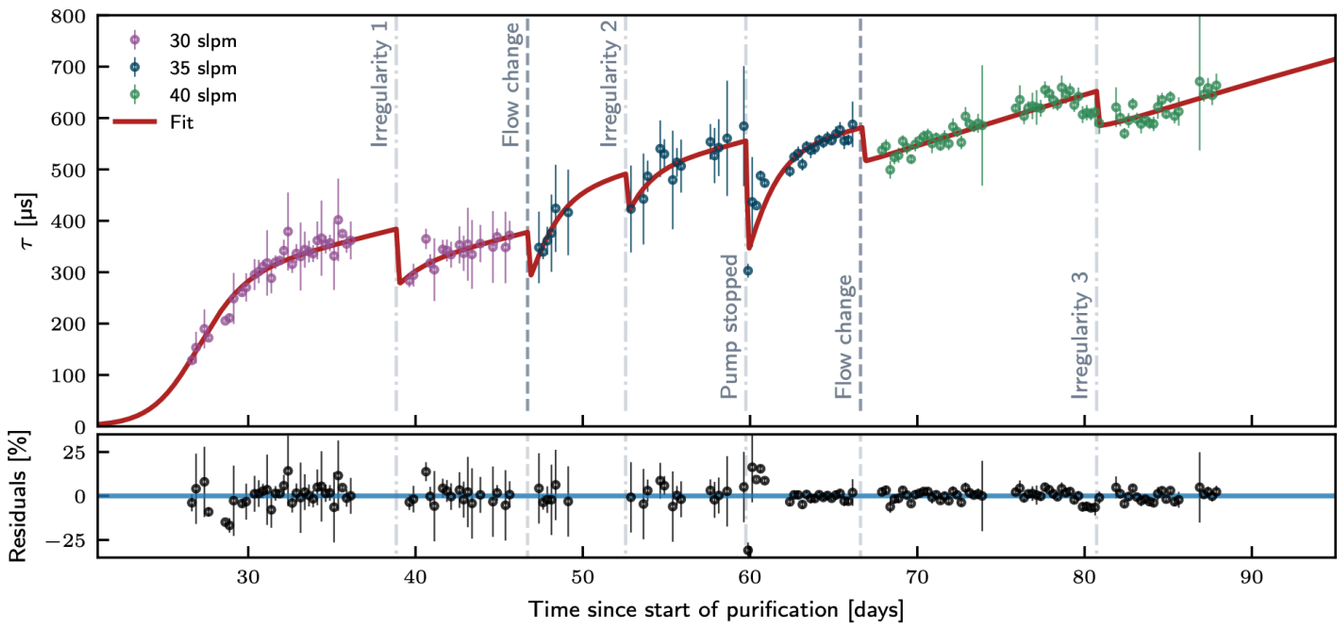

- Waveforms: acquired by oscilloscope and ADC
- Charges: integrals of the current pulses
- The e-lifetime (with $\Delta t = t_2$, rise times t_1, t_3): $\tau_e \approx \frac{1}{\ln(Q_A/Q_C)} \left(t_2 + \frac{t_1 + t_3}{2} \right)$

LB et al., *Eur.Phys.J.C* 83 (2023) 8, 717

Energy resolution

- We had looked at the way energy is deposited in a noble liquid target, by particle interactions:

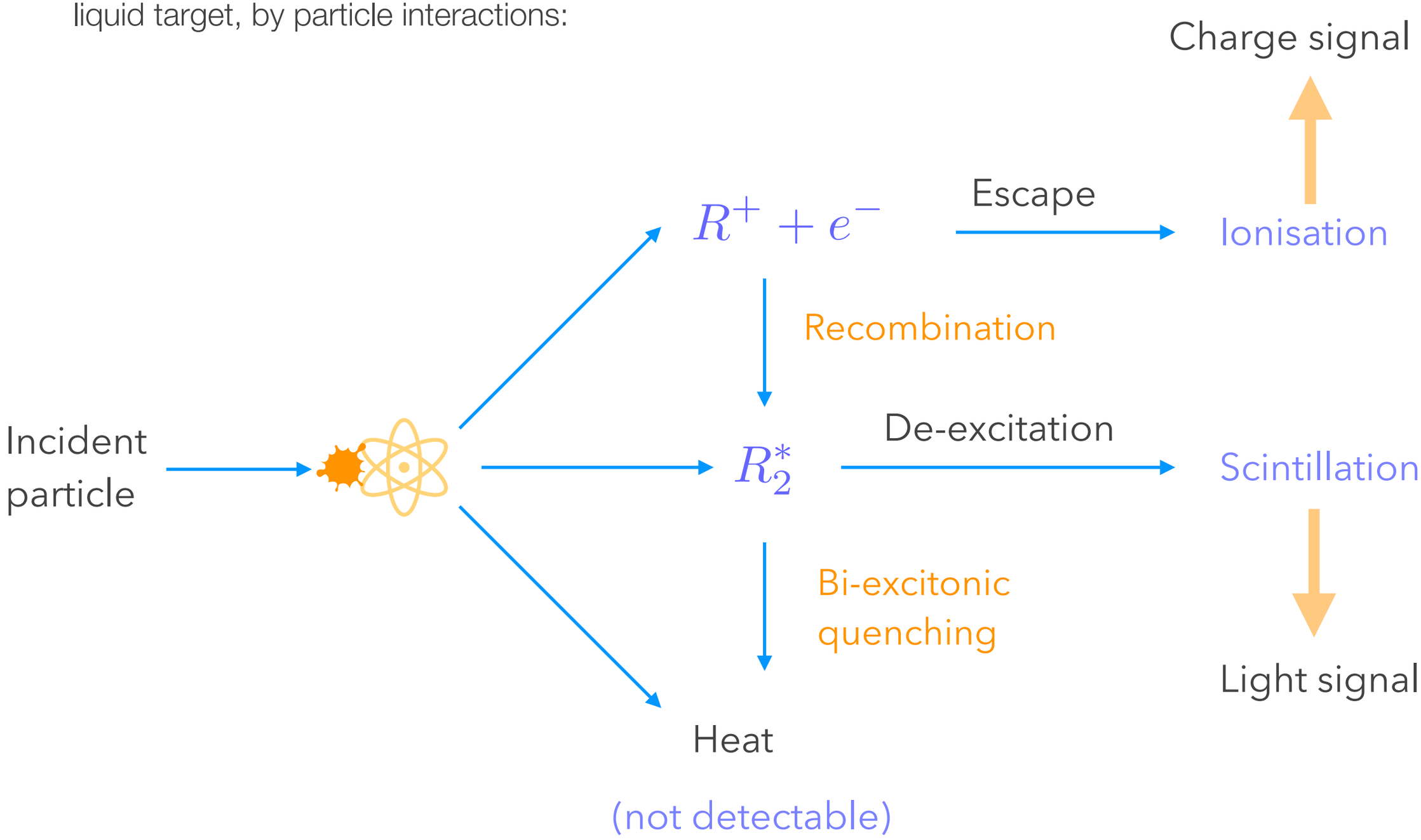

Energy resolution

- With the energy deposition being described as

$$E_0 = (N_{ph} + N_q) \cdot W$$

➡ where W was the average energy required to produce a single excited or ionised atom (and for NRs we must also consider the "quenching factor" f_n)

- As we shall see, in two-phase TPCs, the observed light and charge signals are called S1 and S2, respectively, and these are related to the detector-specific gains g_1 and g_2. We usually write:

$$E_0 = \left(\frac{S1}{g_1} + \frac{S2}{g_2} \right) \cdot W$$

- with g_1 = total photon detection efficiency, g_2 = charge amplification factor. These are determined by using mono-energetic lines from various calibration sources.
  - g_1 and g_2 are typically given in terms of number of photoelectrons (PE) per quantum, or in terms of detected photons (phd) per quantum
  - typical values: g_1 = 0.15 PE/photon (XENON1T), 0.11 phd/photon (LUX), g_1 = 0.16 PE/photon (DarkSide-50); g_2 = 10 PE/electron (XENON1T) , g_2 = 12 phd/electron (LUX), g_2 = 23 PE/electron (here per extracted electron, DarkSide-50)

Energy resolution

- The mean light and charge yields (L_y and Q_y) are then defined as:

$$L_y \equiv \frac{S1}{E_0} \qquad Q_y \equiv \frac{S2}{E_0}$$

- and are estimated by 2D Gaussian fits to mono-energetic lines, from the measured S1 and S2

- Knowing L_y, Q_y from these mono-energetic lines, one can measure the energy resolution (usually with an empirical fit to a number of measurements at different energies). The relative resolution scales as:

$$\frac{\sigma}{E} \propto \frac{a}{\sqrt{E}} + b$$

Example XENON100

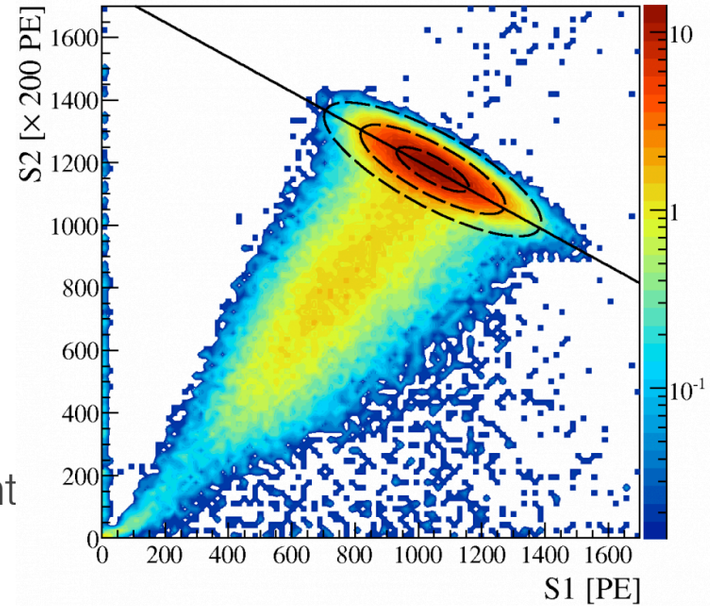

anti-correlation of charge and light signals

Example LUX

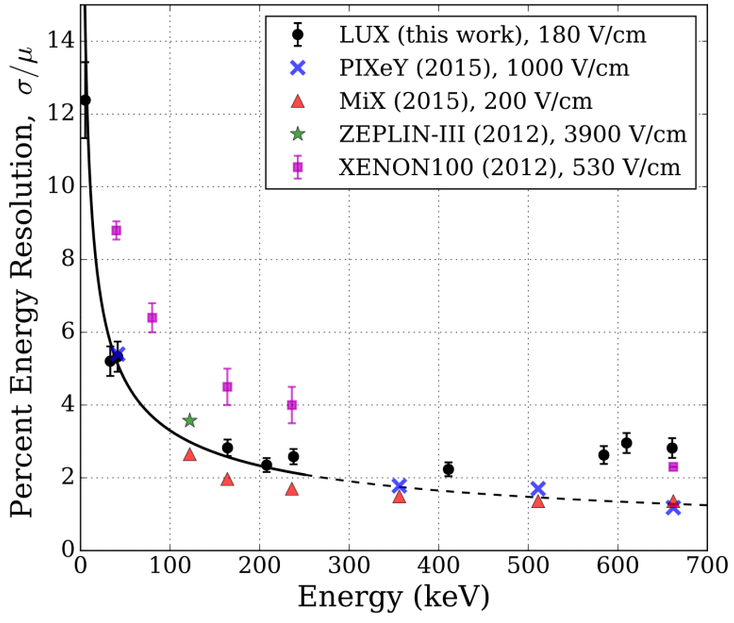

Example XENON100

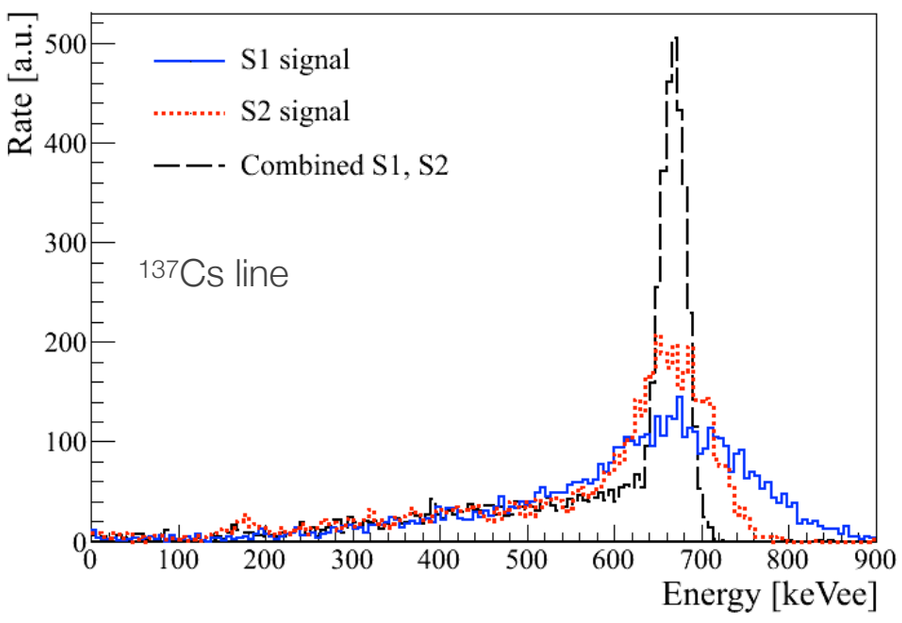

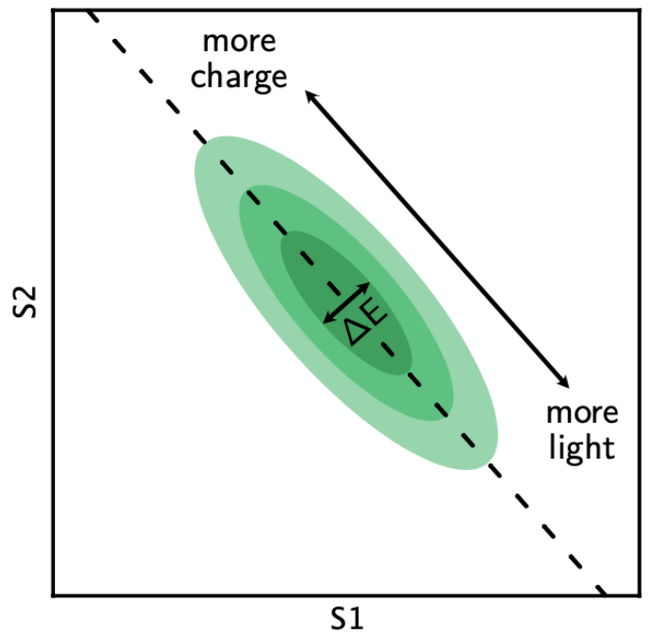

The Doke plot

- One can rewrite the previous equation as follows:

$$Q_y = -\frac{g_2}{g_1} L_y + \frac{g_2}{W}$$

- Since we can measure S1 and S2 for clear spectral features, and E_0 is known, we can then estimate g_1 and g_2 from a so-called *Doke plot*: a plot of Qy (=S2/E_0) versus Ly (=S1/E_0)

- From a linear fit one can extract g_1, g_2, and once these are known, reconstruct the energy of an event:

$$E_0 = \left(\frac{S1}{g_1} + \frac{S2}{g_2}\right) \cdot W$$

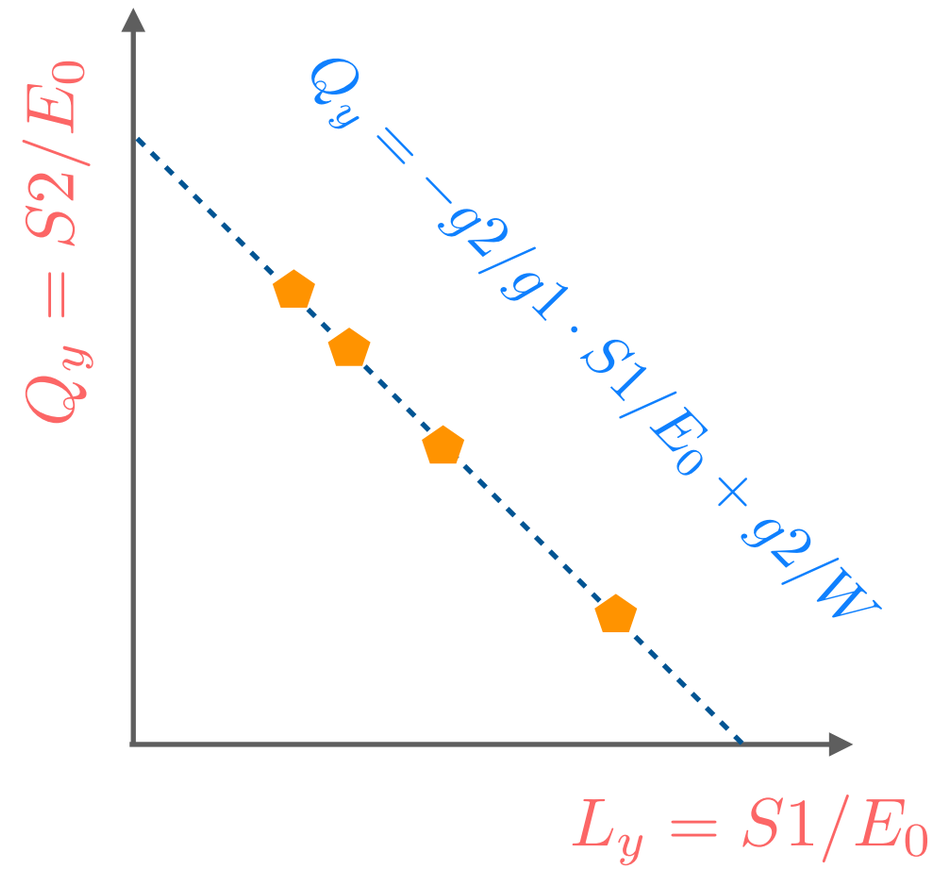

- Hence g1 and g2 are simply the proportionality factors between produced number of photons and electrons, and detected ones, for each signal
  - for S1: mostly the efficiency of detecting photons
  - for S2: it includes the extraction efficiency, secondary amplification, etc

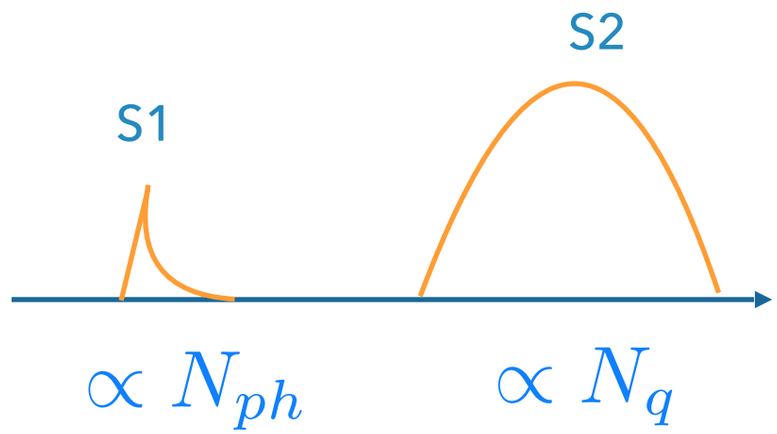

$$N_{ph} = N_{ex} + r \cdot N_i \quad N_q = (1 - r) \cdot N_i$$

The Doke plot

- One can rewrite the previous equation as follows:

$$Q_y = -\frac{g_2}{g_1} L_y + \frac{g_2}{W}$$

- Since we can measure S1 and S2 for clear spectral features, and E_0 is known, we can then estimate g_1 and g_2 from a so-called *Doke plot*: a plot of Qy (=S2/E_0) versus Ly (=S1/E_0)

- From a linear fit one can extract g_1, g_2, and once these are known, reconstruct the energy of an event:

$$E_0 = \left(\frac{S1}{g_1} + \frac{S2}{g_2}\right) \cdot W$$

- Hence g1 and g2 are simply the proportionality factors between produced number of photons and electrons, and detected ones, for each signal
  - for S1: mostly the efficiency of detecting photons
  - for S2: it includes the extraction efficiency, secondary amplification, etc

Example Doke plot from XENON1T

$Q_y = S2/E_0$

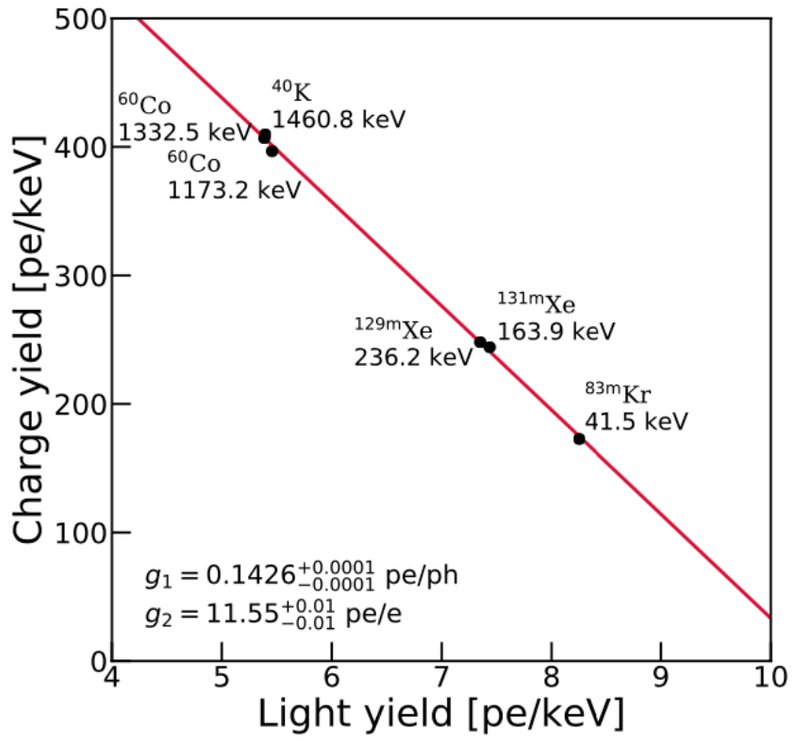

$L_y = S1/E_0$

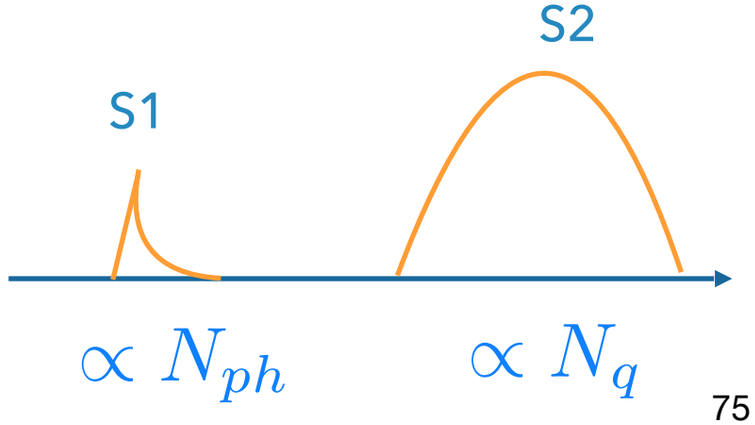

Particle discrimination in noble liquids

- Pulse shape of prompt scintillation signal (in liquid argon)
  - the ratio of light from singlet and triplet depends on dE/dx (~ 10:1 for NRs:ERs)
- Charge versus light (in LAr and LXe)
  - the recombination probability, and thus the S2-to-S1 ratio depends on dE/dx

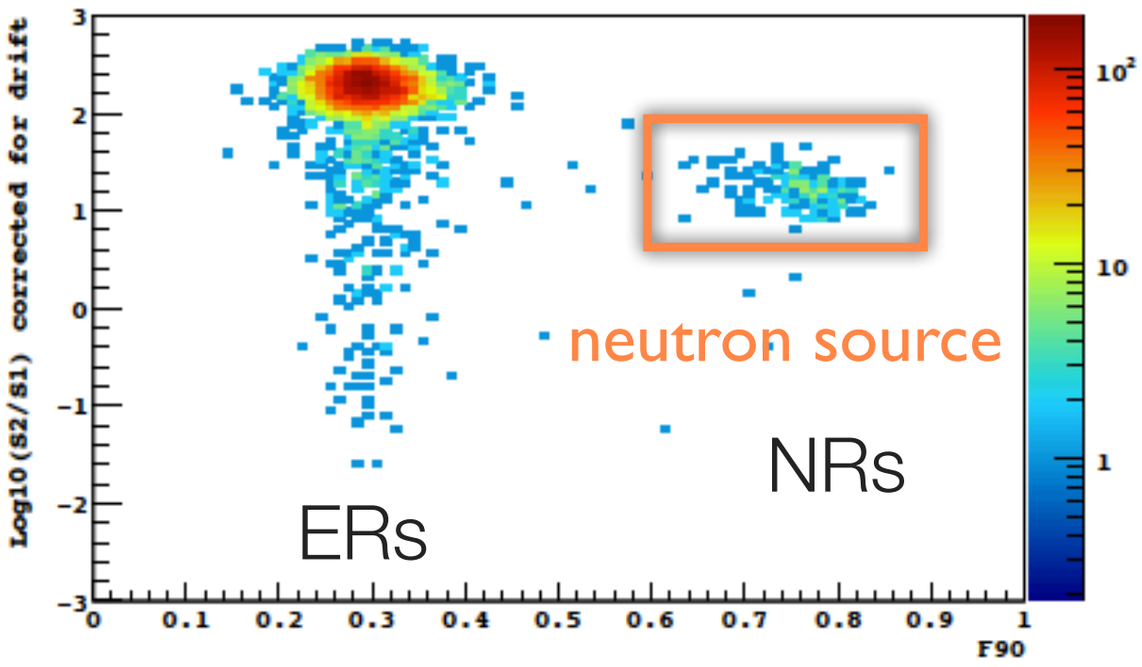

Example for LAr (DarkSide-10)

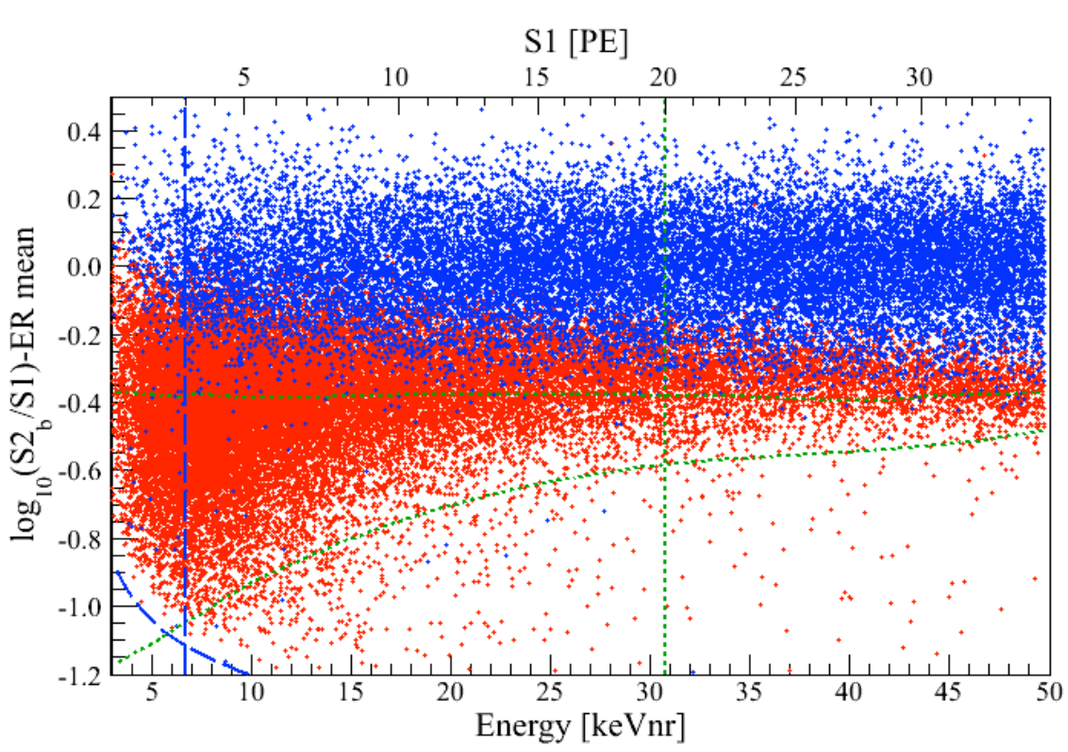

Example for LXe (XENON100)

Pulse shape discrimination in liquid argon

- Lifetime difference between the excimer's singlet (~ 6 ns) and triplet (~ 1.4-1.6 μs) states
- Singlet and triplet photons are well-separated in time, and the ratio for individual events can be estimated with high precision: the expectation value of the ratio depends on the linear energy transfer of the interacting particle (fewer triplet excimers are produced at higher LET)
  - Intensity ratio of fast/slow component: ~ 0.3 for ERs and in the range 1.3 - 3.3 for NRs
  - PSD methods thus usually use the ratio of prompt scintillation light to the total light; as an example f_{90} = fraction of S1 light detected in the first 90 ns of a pulse
  - low f_{90} values (<0.5) ≋ ERs, high f_{90} values (> 0.5) ≋ NRs

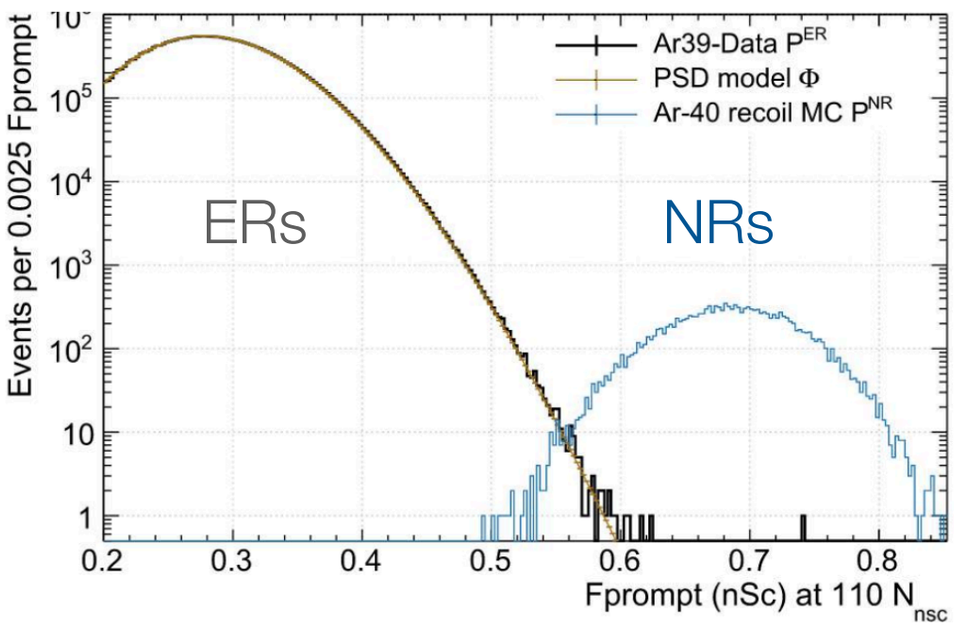

ER (^{39}Ar beta decays) vs NR discrimination in DEAP-3600, EPJ-C 81, 2021

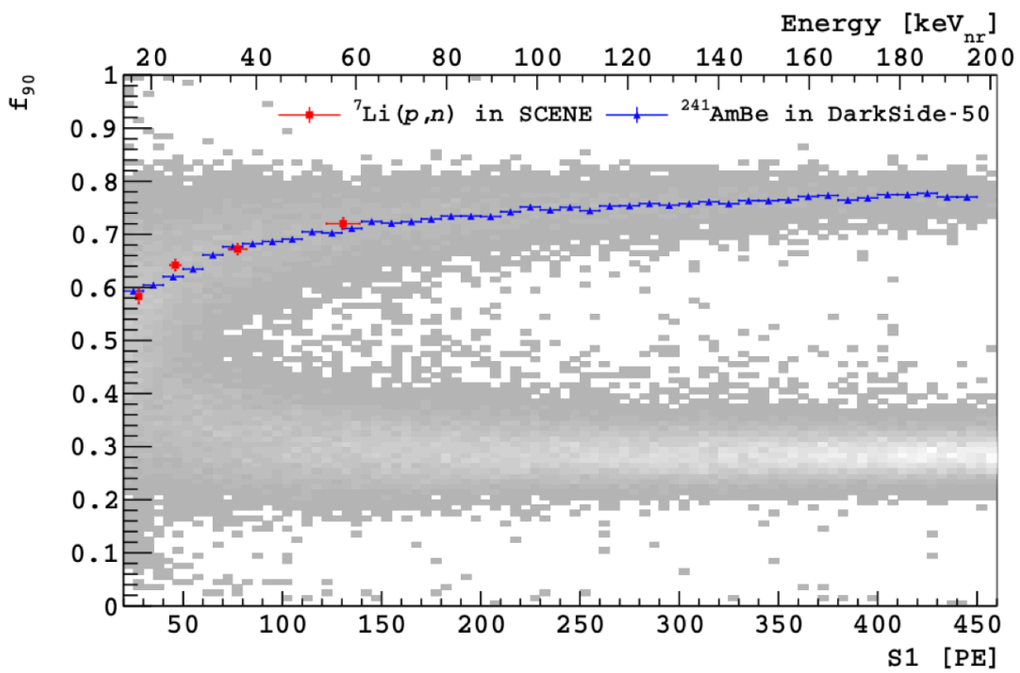

Median f_{90} values from SCENE and from high-activity AmBe data in DarkSide-50

Cryogenic noble liquid detectors: some challenges

- Cryogenics: efficient, reliable and cost effective cooling systems
- Detector materials: compatible with low-radioactivity and purity requirements
- Intrinsic radioactivity: ^{39}Ar and ^{42}Ar in LAr, ^{85}Kr in LAr and LXe, ^{222}Rn emanation and diffusion

- Light detection:
  - efficient VUV photosensors, directly coupled to liquid (low T and high P capability, high purity), effective UV reflectors and wavelength shifters (WLS) (in LAr)
  - light can be absorbed by H_2O and O_2: continuous recirculation and purification
- Charge detection:
  - requires $\ll$ 1ppb (O_2 equivalent) for e^--lifetime > 1 ms (commercial or custom-made purifiers and continuous circulation, in gas and/or liquid phase)
  - electric drift fields: few100 V/cm required for maximum yield for MIPs; for alphas and NRs the field dependence is much weaker, challenge to detect a small charge in presence of HV

Types of DM noble liquid detectors

Single phase, light readout

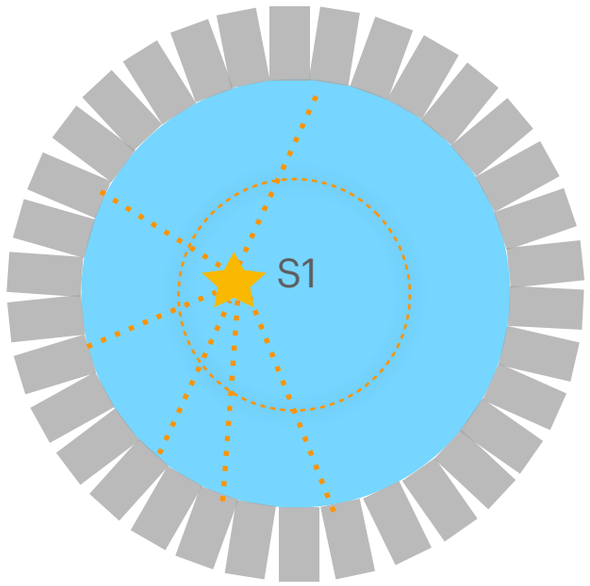

- High light yields, simple geometry, no E-fields
- Scintillation with PMTs
- LAr: DEAP-3600
- LXe: XMASS (until 2019)

Dual-phase TPC with light readout

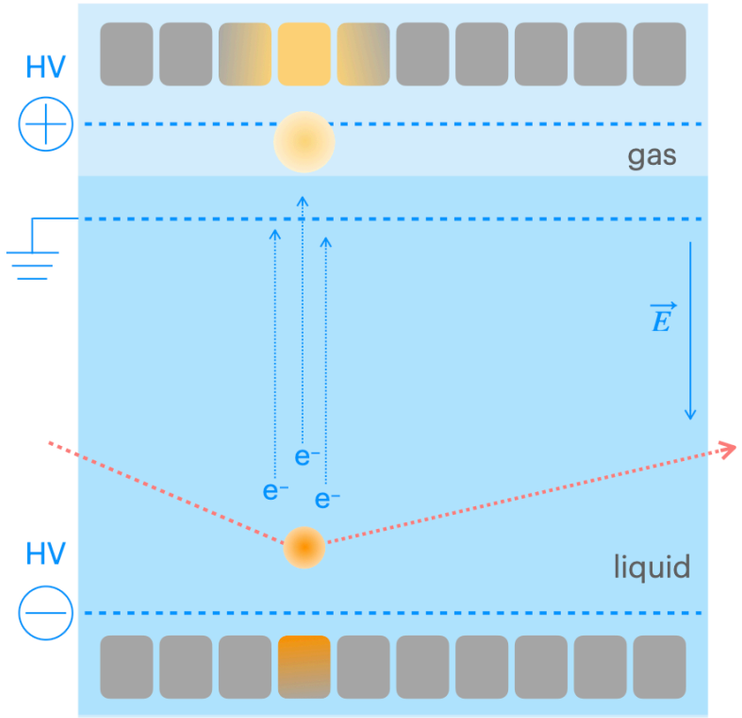

- Light and charge with PMTs
- 3D position resolution, improved energy resolution, discrimination based on S2/S1
- LAr: DarkSide-50 (until 2019), DS20k
- LXe: LZ, PandaX-4T, XENONnT

Superfluid ^{4}He, phonon readout

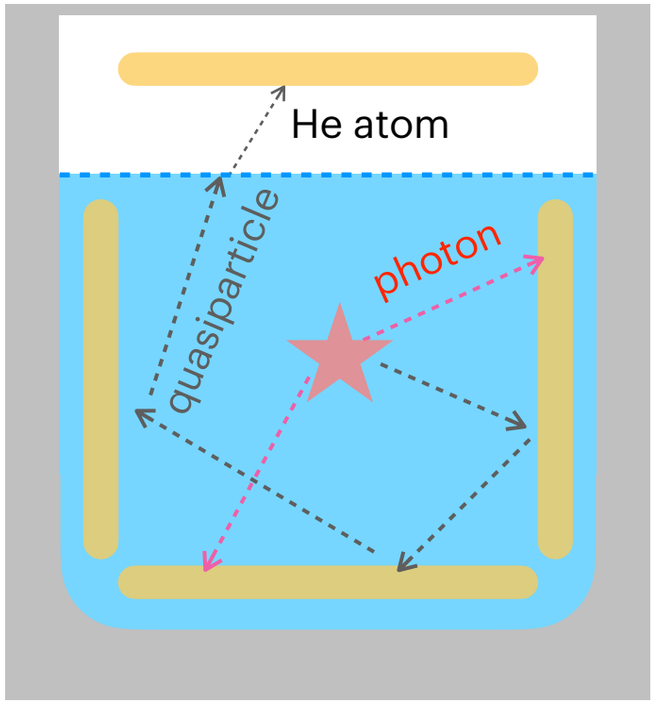

- R&D phase for light DM
- Signals: phonons and rotons; detect excitations down to ~ 1 meV (via ejection of ^{4}He atom), TES/MMC readout
- HeRALD, DELight

Single phase detectors

- Observe the prompt scintillation light in a large, homogeneous volume of liquid argon or xenon
- Particle discrimination via pulse shape analysis (in LAr)
- Advantages
  - High light yield (4-π coverage with photosensors; e^--ion recombination)
  - Simpler detector geometry, no electric fields and high-voltage, cheaper
  - Large, homogeneous target with ultra-low backgrounds
- Disadvantages
  - No particle discrimination in LXe
  - Position resolution typically few cm
  - Very low energy thresholds (via "S2-only" signal) not possible
- Example of past/existing experiments
  - LAr: DEAP-3600 at SNOLAB, MiniCLEAN at SBOLAB (until 2019)
  - LXe: XMASS at Kamioka (until 2019)

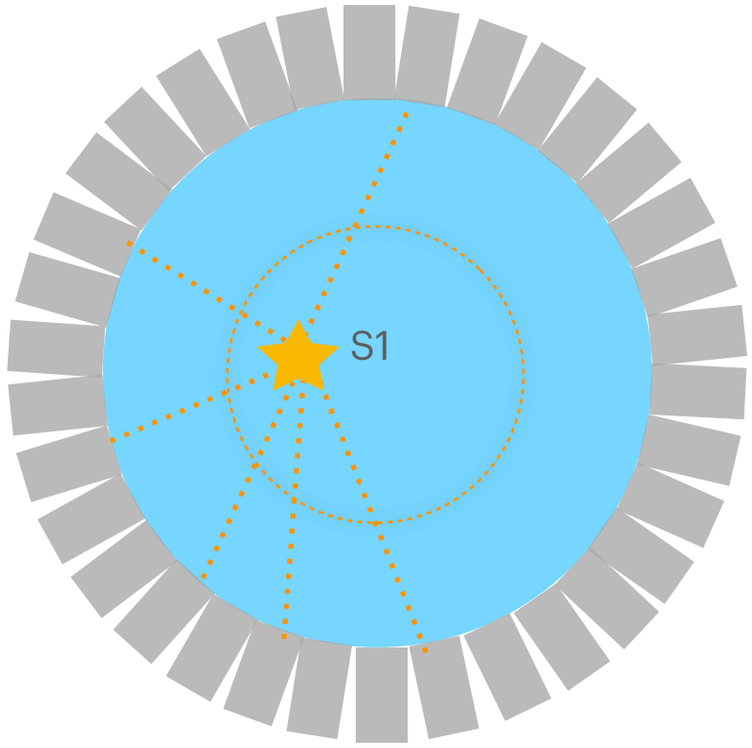

Single phase, light readout

Two-phase TPCs

- Observe the prompt scintillation light and electroluminiscence in a large, homogeneous volume of liquid argon or xenon
- Particle discrimination via the ratio of charge to light yield and in addition via pulse shape analysis (in LAr)
- Advantages
  - Three dimensional position reconstruction
  - Improved energy resolution & lower energy threshold ("S2-only")
  - Improved single versus multiple scatters discrimination
- Disadvantages
  - Complex detector geometry
  - Electric fields and high-voltage FTs, large, uniform electrodes
  - Precise control of liquid level needed
- Example of past/existing experiments
  - LAr: DarkSide-50 at LNGS (until 2019)
  - LXe: LZ at SURF, PandaX-4T at Jinping, XENONnT at LNGS

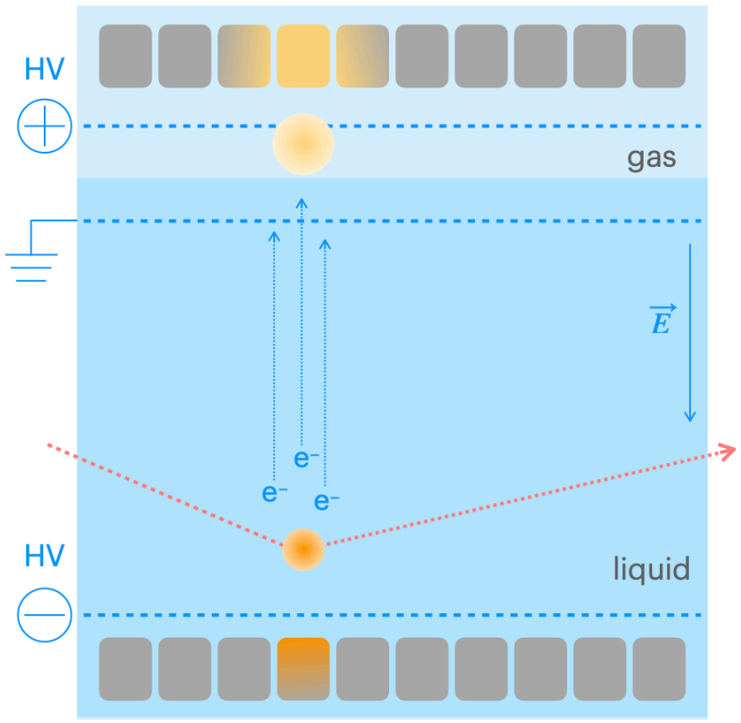

Two-phase TPC with light readout

Two-phase detection principle

- Time projection chambers
  - Signals detected with arrays of photosensors
  - energy determination based on light (S1) & charge (S2) signals
  - 3D position resolution, which allows for fiducialisation
  - S2 over S1⇒ ER versus NR discrimination
  - Identification of single versus multiple interactions
  - Pulse shape information (LAr) ⇒ ER versus NR discrimination

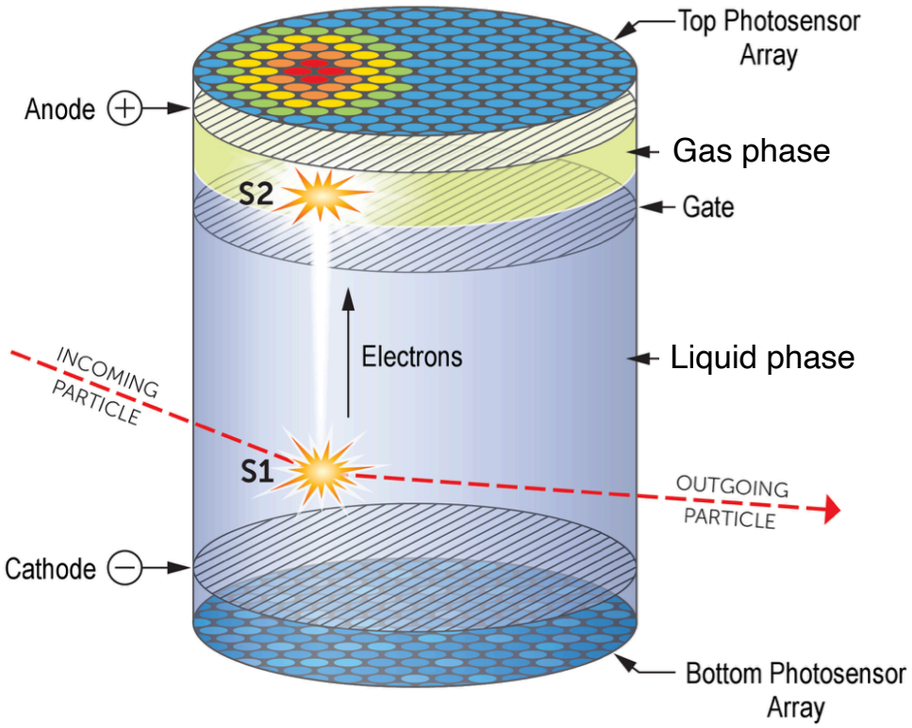

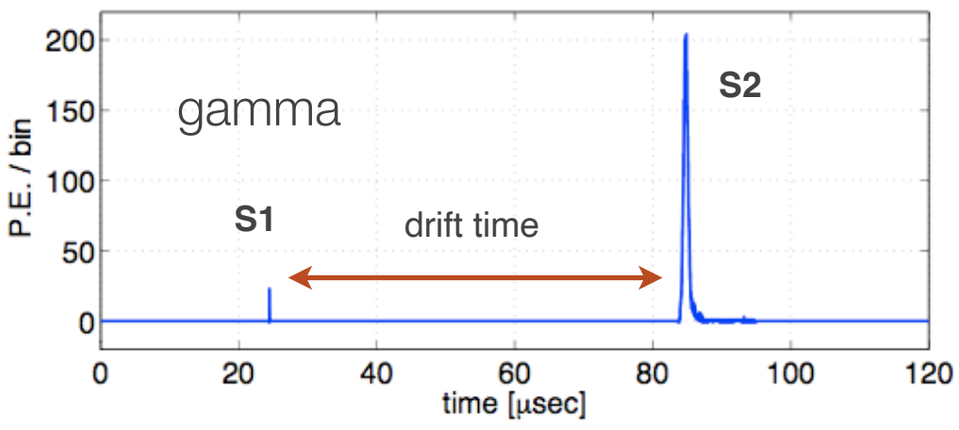

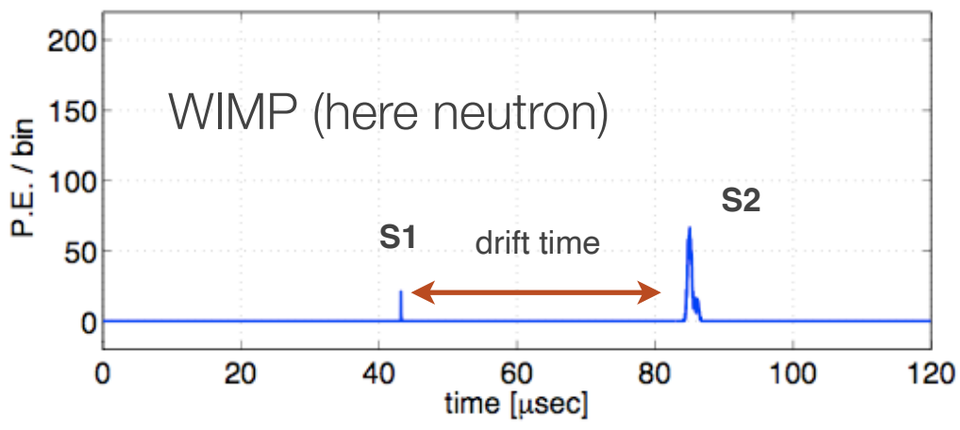

The fraction of electrons escaping recombination with positive ions: higher for ERs than for NRs
⇒ for a given initial energy deposit, the S2 signal is higher for ERs compared to NRs

Liquid noble technology for dark matter

- Leading sensitivity at intermediate/high DM masses since ~2007
- Liquid detectors
  - scalable ⇒ large target masses
  - readily purified ⇒ ultra-low backgrounds
  - high density ⇒ self-shielding
- SI and SD (^{129}Xe, ^{131}Xe) interactions
- Many other science opportunities (second order weak decays, solar and SN neutrinos, etc)

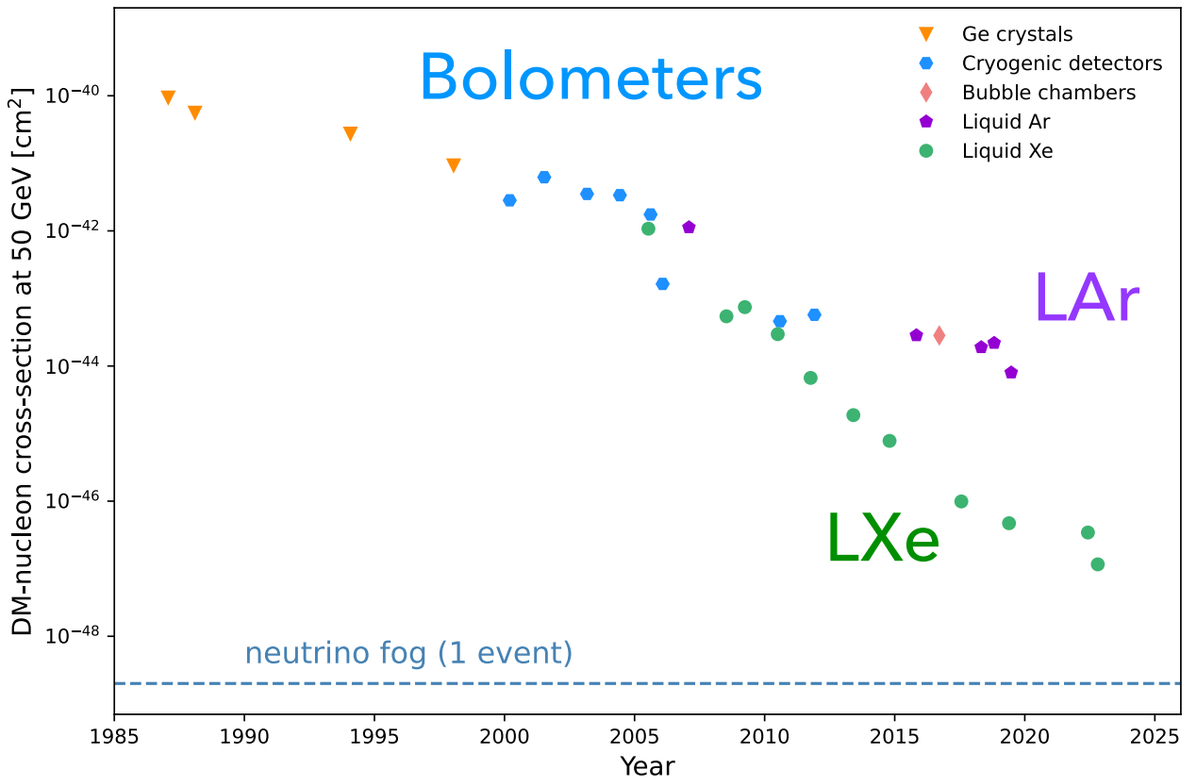

Liquid argon detectors

- DEAP-3600 at SNOLAB: 3300kg LAr (1 tonne fiducial), 255 PMTs
  - Data taking since 2016
  - WIMP search with blinded data ongoing; detector upgrades in progress
- DarkSide-50 at LNGS: 50 kg LAr, depleted in ^{39}Ar (33 kg fiducial), 38 PMTs
  - Data taking: 2013-2019
  - New constraints on light DM: S2-only analysis (0.6 keV_{nr} threshold $\equiv$ 4 e^-)

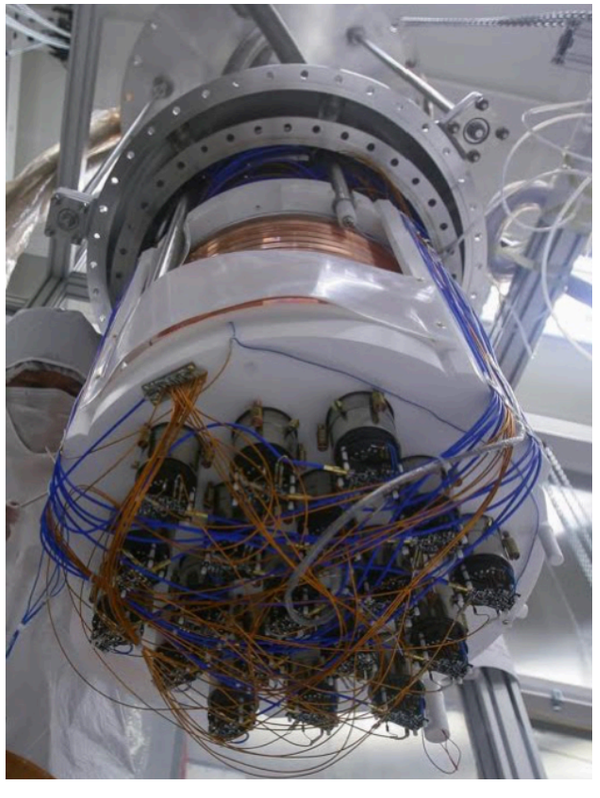

Liquid argon detectors

- DEAP-3600 at SNOLAB: 3300kg LAr (1 tonne fiducial), 255 PMTs
  - Data taking since 2016
  - WIMP search with blinded data ongoing; detector upgrades in progress
- DarkSide-50 at LNGS: 50 kg LAr, depleted in ^{39}Ar (33 kg fiducial), 38 PMTs
  - Data taking: 2013-2019
  - New constraints on light DM: S2-only analysis (0.6 keV_{nr} threshold ≡ 4 e^-)

DEAP-3600, PRD 100, 022004

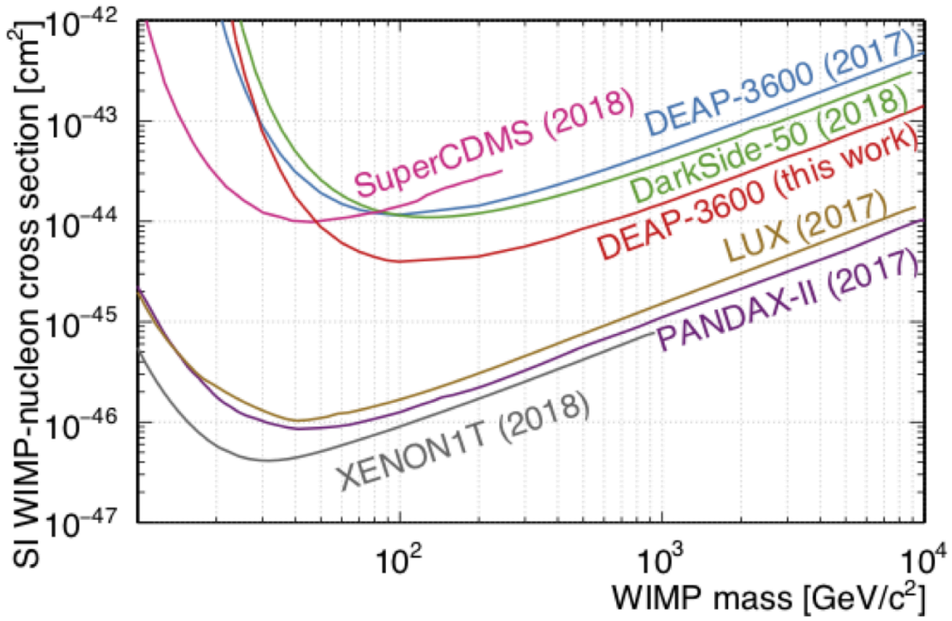

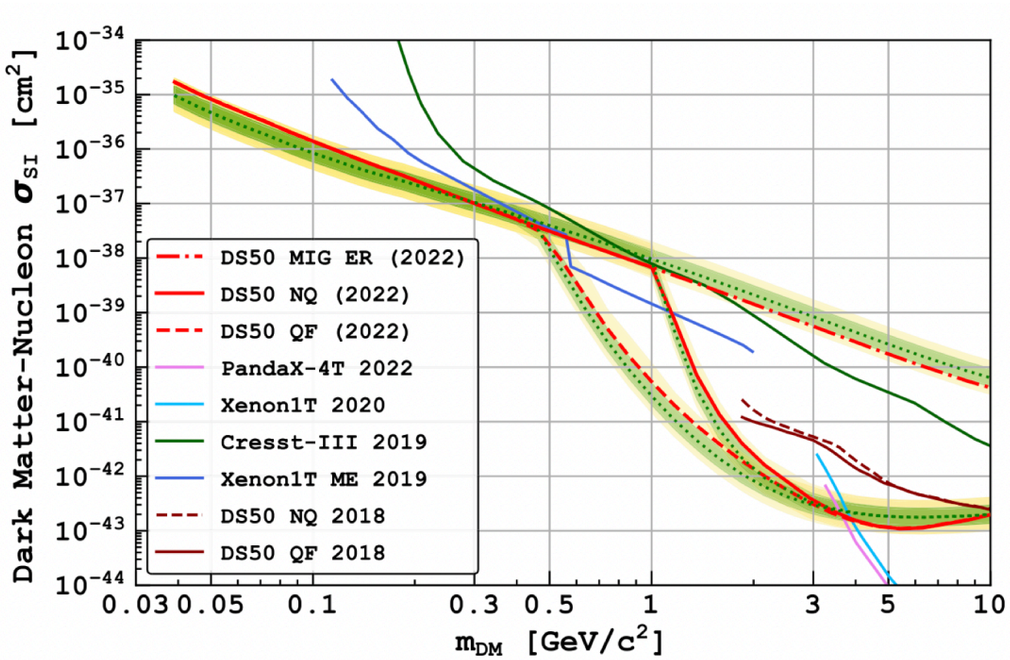

DarkSide-50, PRL 130 (2023) 10

Future liquid argon detectors

- Global Argon Dark Matter Collaboration
  - DarkSide-20k: 51.1 t underground LAr (20 t fiducial volume) in octagonal TPC with SiPM arrays
  - Cryostat currently under construction in Hall C at LNGS
  - First commissioning expected end of 2026
  - Argo: 400 t LAr (300 t fiducial), likely at SNOLAB

DarkSide-20k

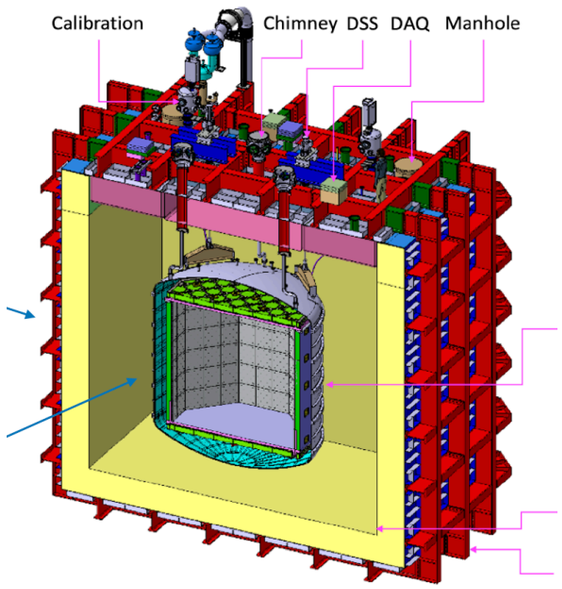

ARGO

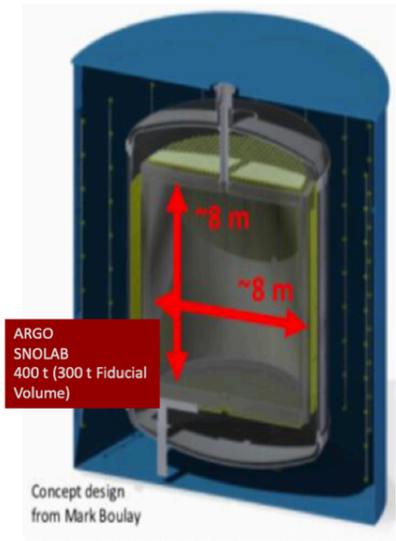

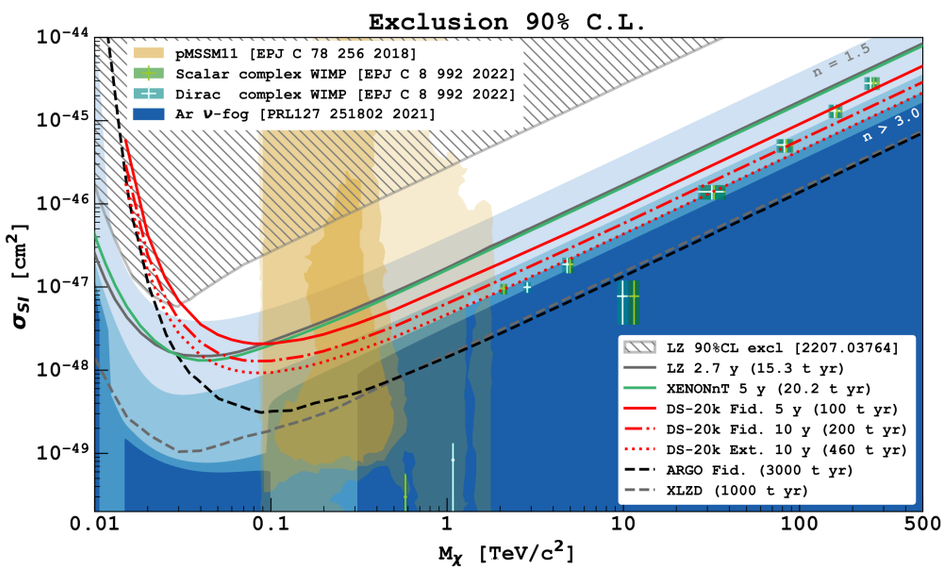

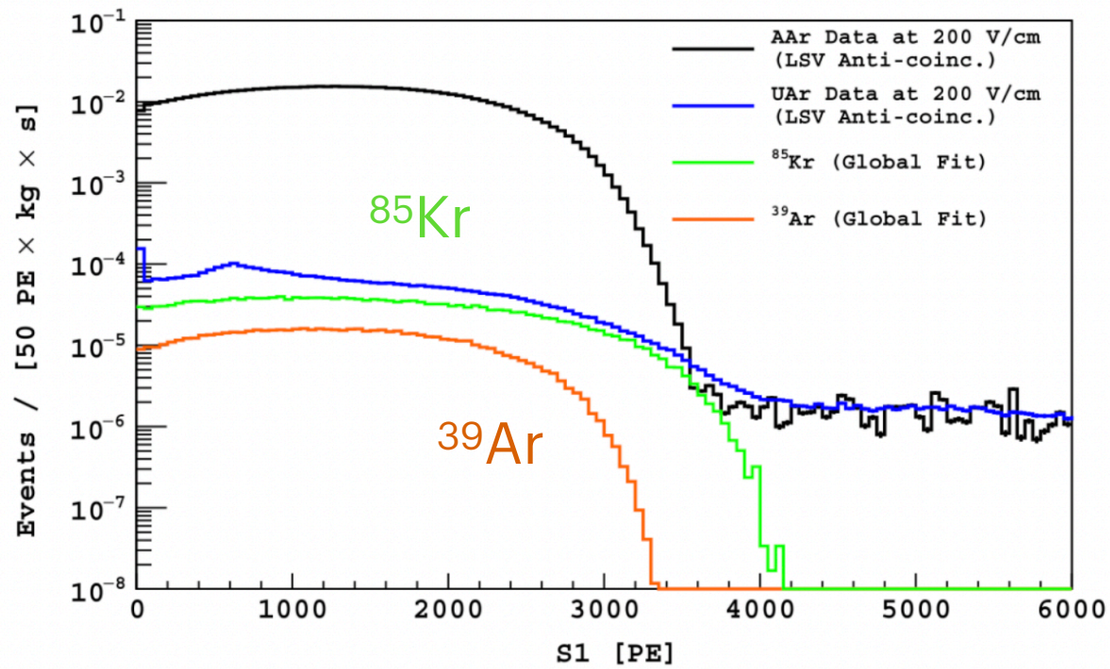

Underground argon, DarkSide-50, PRD 93, 2016

Liquid xenon detectors

- LZ at SURF, PandaX-4T at JinPing, XENONnT at LNGS
- Detector scales: 10 t (LZ), 6 t (PandaX-4T) and 8.6 t LXe (XENONnT) in total xenon mass
  - TPCs with 2 arrays of 3-inch PMTs
  - Kr and Rn removal techniques
  - Ultra-pure water shields, n & μ vetos
  - External and internal calibration sources
- Status: PandaX-4T first result in 2021 from commissioning run, LZ first results from run in 2022, XENONnT first results from SR0 in 2021/22; all experiments taking data

LUX-ZEPLIN

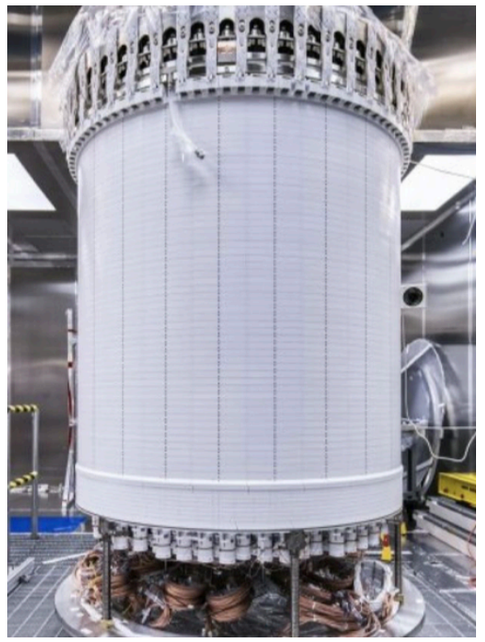

XENONnT

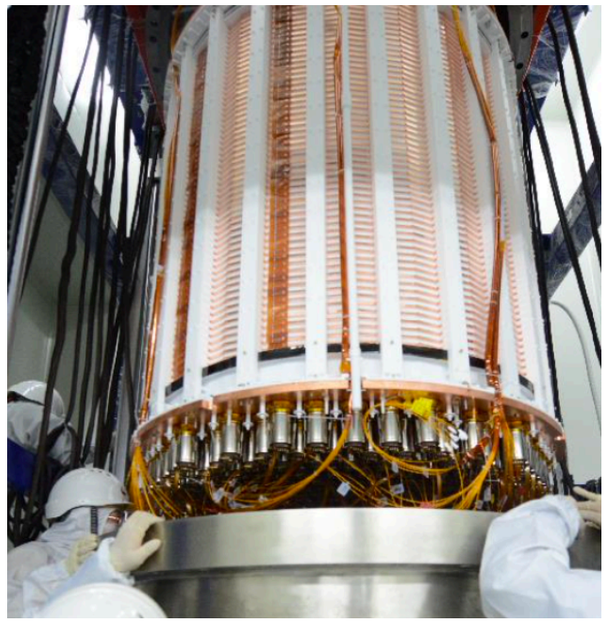

PandaX-4T

Future liquid xenon detectors

- DARWIN/XLZD
  - DARWIN: 50 t LXe (40 t active target) at LNGS; ~1900 3-inch PMTs (baseline design); Gd-doped water n and μ vetoes
  - R&D and prototyping in progress
  - XLZD: 75 t LXe (60 t active target), several labs are considered
- PandaX-xT: 47 t LXe (43 t active target) at JinPing; 2 arrays of 2-inch PMTs, Cu cryostat

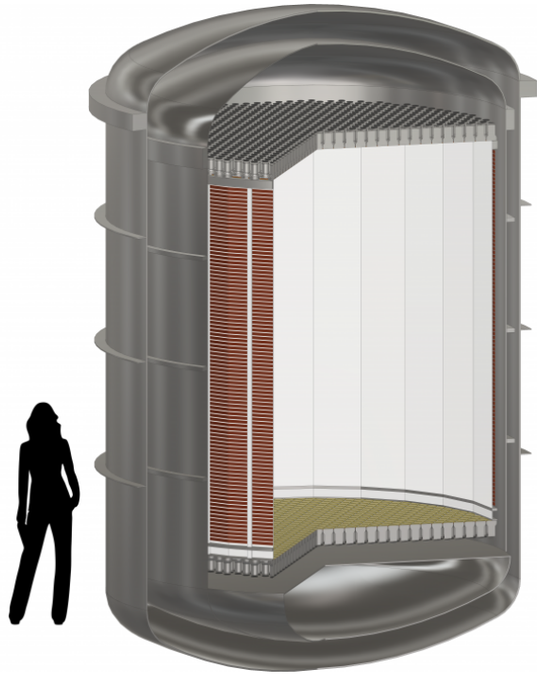

DARWIN collaboration
JCAP 1611 (2016) 017

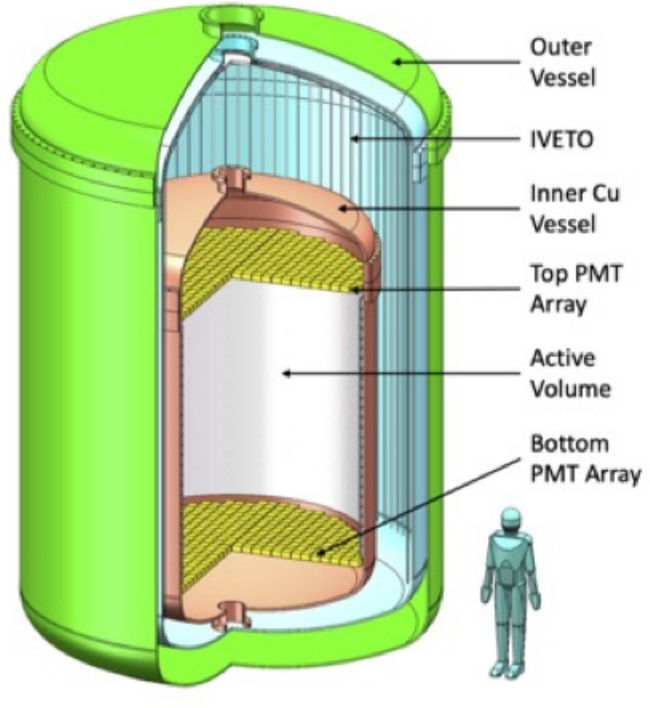

PandaX collaboration
arXiv: 2402.03596

Cross section versus mass (time)

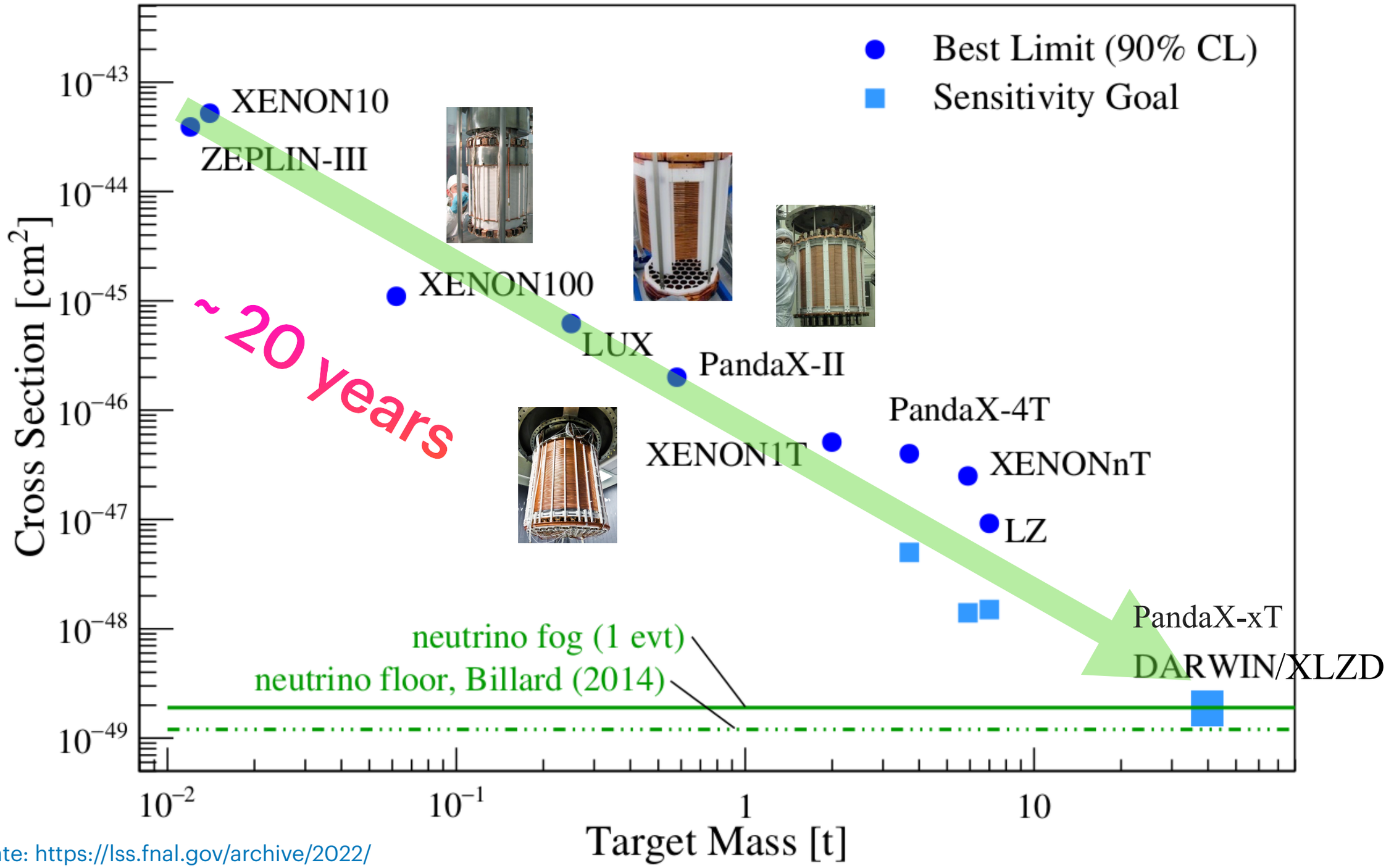

Update: https://lss.fnal.gov/archive/2022/conf/fermilab-conf-22-180-v.pdf

Background rates versus mass (time)

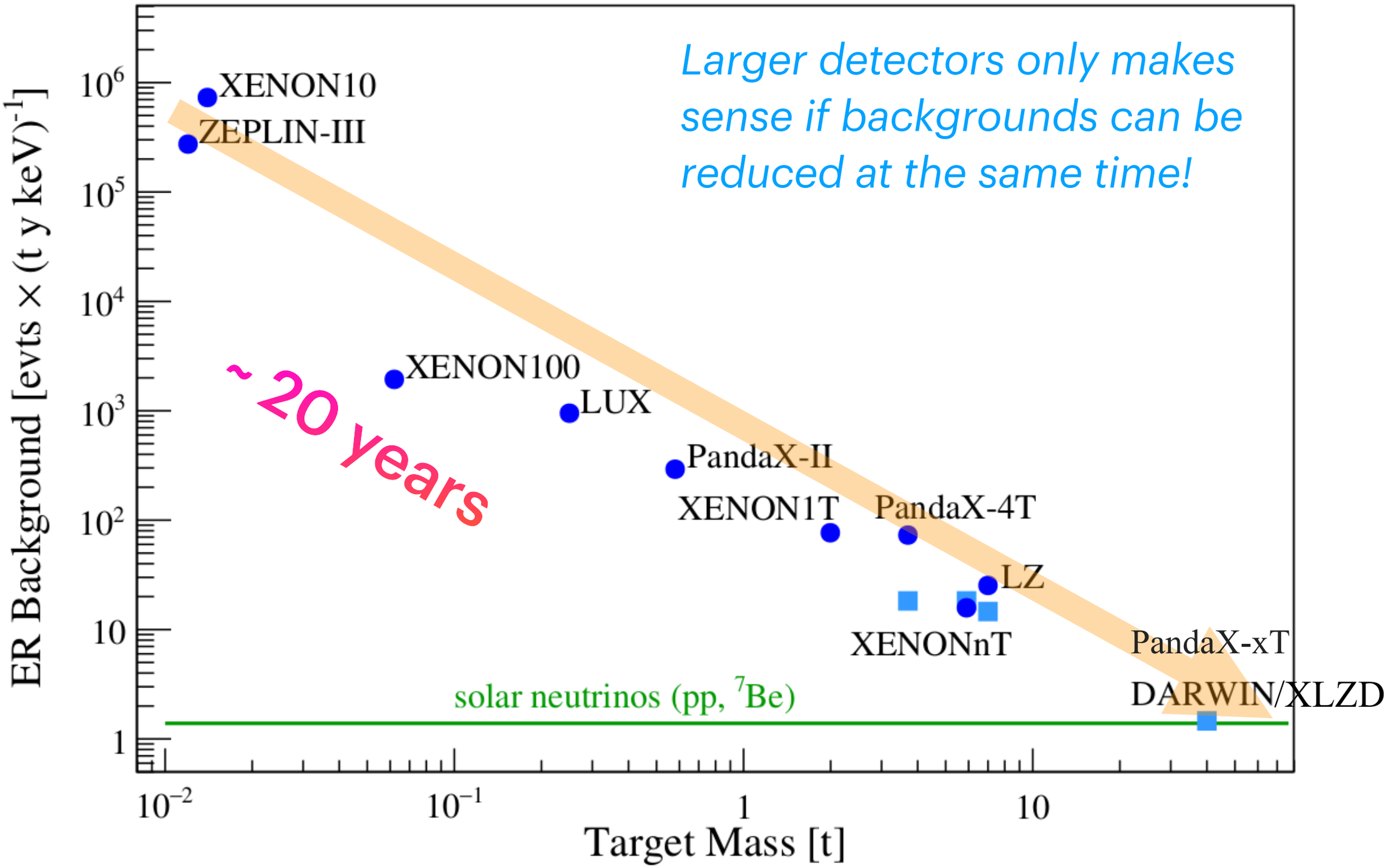

Update: Journal of Physics G 50 (2023)

DM cross sections versus time

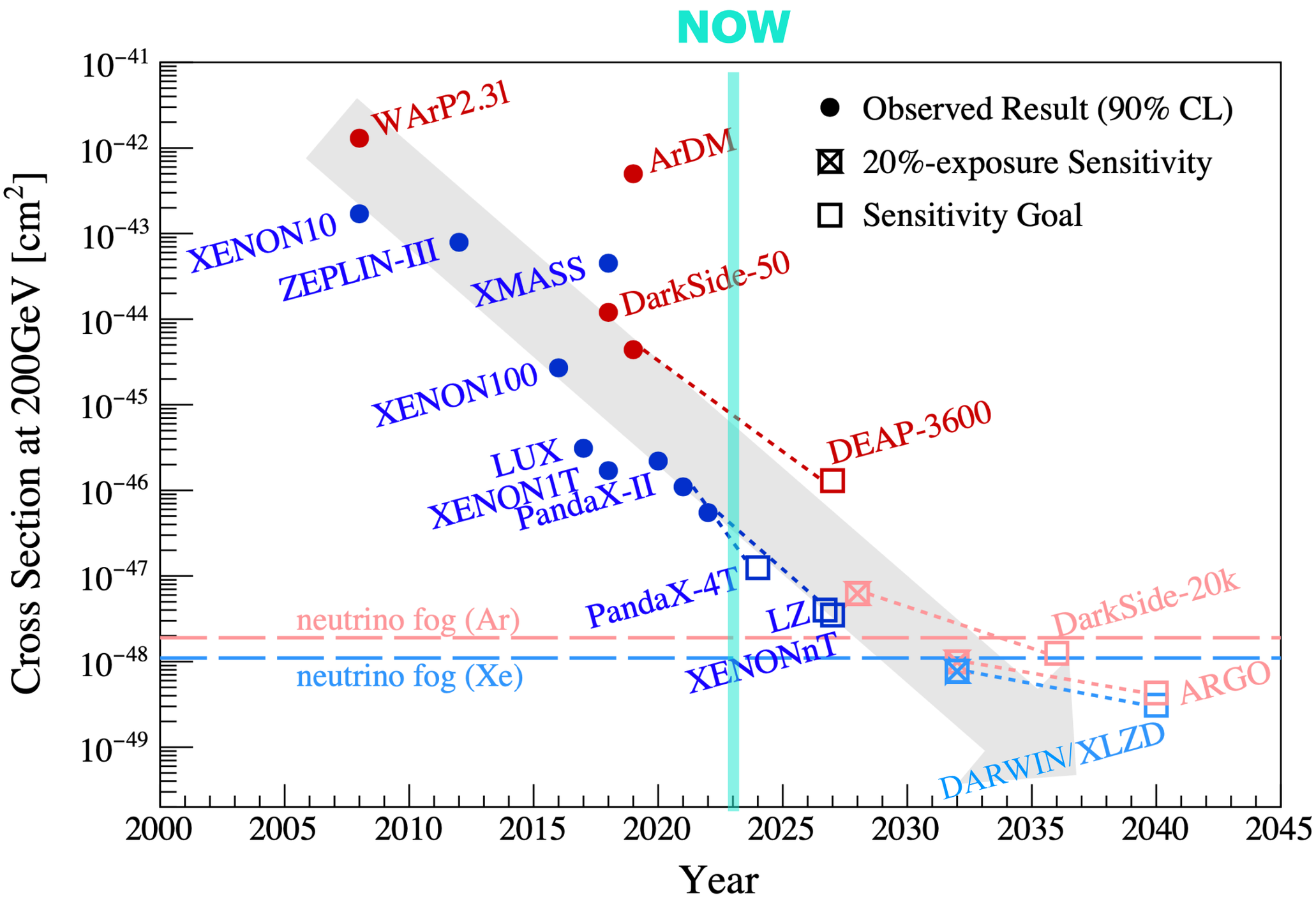

Snowmass, Topical Group on Particle Dark Matter Report, arXiv: 2209.07426

Size matters

- LUX-ZEPLIN and XENONnT: 1.5 m e^- drift and ~ 1.5 m diameter electrodes
- **DARWIN/XLZD: 2.6 - 3.0 m ⇒ new challenges**
  - Design of electrodes: robustness (minimal sagging/ deflection), maximal transparency, reduced e^- emission
  - Electric field: ensure spatial and temporal homogeneity, avoid charge-up of PTFE reflectors
  - High-voltage supply to cathode design, avoid high-field regions
  - Liquid level control
  - Cryogenic purification (^{222}Rn and ^{85}Kr below solar pp neutrino level)
- Electron survival in LXe: > 10 ms lifetime
- Diffusion of the e^--cloud: size of S2-signals

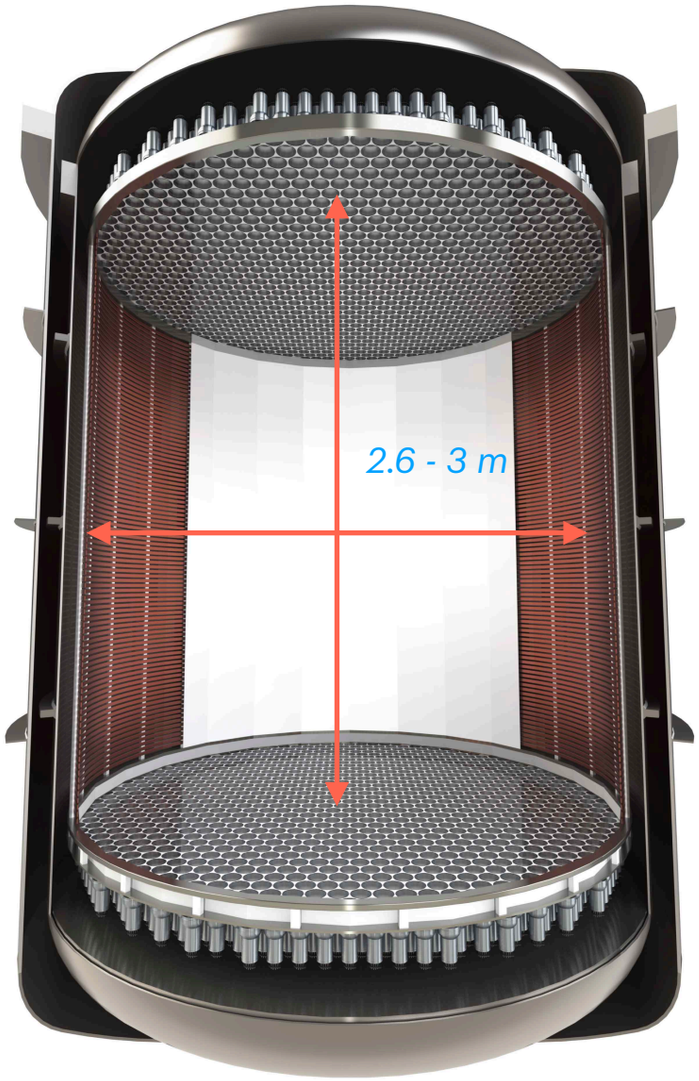

DARWIN/XLZD

R&D topics

Detector design and time projection chamber

- demonstrate e^- drift over large distances, electrodes with 2.6 m diameter; high-voltage feedthroughs
- study alternative designs: sealed/hermetic TPC (to prevent radon diffusion into inner volume), single-phase TPC (simplify detector design, mitigate single e^- background)
- cryostat design: stability, reduce amount of material (hence gamma and neutron emitters) close to TPC

Photosensors

- baseline: VUV-sensitive, low-radioactivity PMTs (established technology, low dark count rate of ~ 0.02 Hz/mm^2)
- study low-field SiPMs, digital SiPMs & hybrid photosensors; also, low-noise, low heat dissipation, low-radioactivity readouts

Target and background control

- fast purification for large e^- lifetime, large distillation columns for low ^{222}Rn and ^{85}Kr levels
- "radon-free" circulation pumps; coating techniques to avoid radon emanation ((electrochemical, sputtering, epoxy based); storage and recuperation of large amounts of xenon
- identification of low-radioactivity material components

Detector demonstrators

- Full scale demonstrators in z and in x-y:
  - Xenoscope, 2.6 m tall TPC and Pancake, 2.6 m ø TPC in double-walled cryostats
  - Both facilities available to the collaboration/consortium for R&D purposes
  - LowRad to demonstrate large-scale cryogenic distillation at Münster

Vertical demonstrator: *Xenoscope*

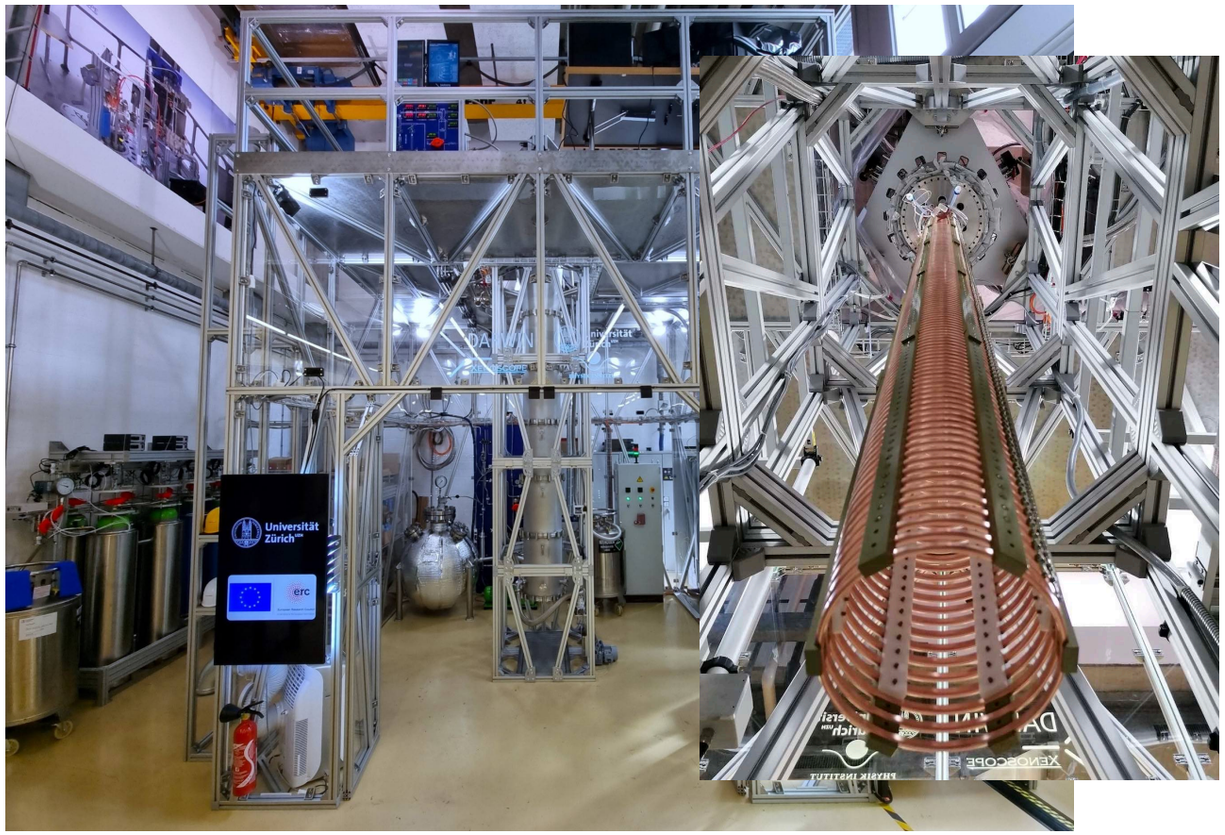

L. Baudis et al, JINST 16, P08052, 2021

Horizontal demonstrator: *Pancake*

Test electrodes with 2.6 m Ø

Superfluid 4-Helium detectors

- Detection of prompt UV ($h\nu = 16$ eV) and IR photons and of ballistic triplet excimers ($\tau \sim 13$ s) with MMC or TES-calorimeters
- Phonons liberate ^{4}He atoms from the surface (phonon energy ~ 1 meV > binding energy)
- **DELight and HeRDALD:** R&D stage with small prototypes operating

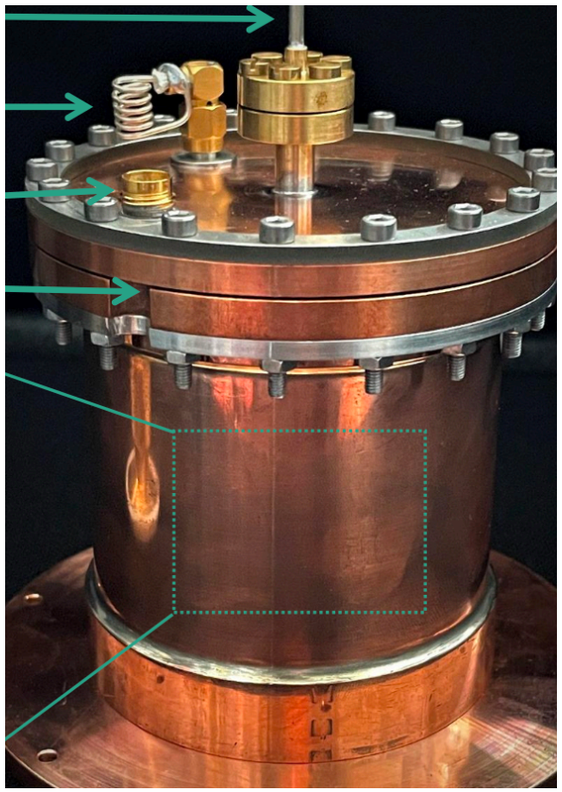

DELight, SciPost 12 (2023)

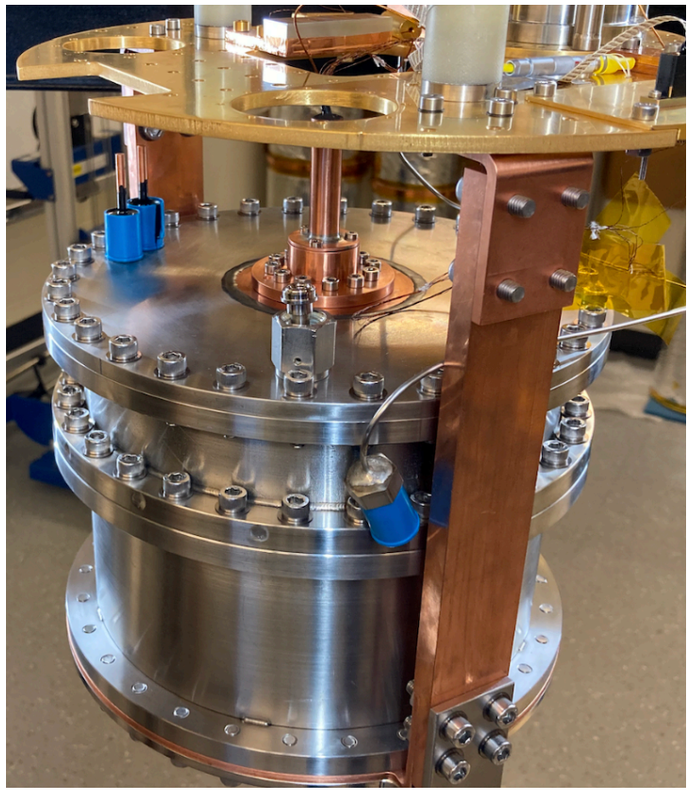

HeRALD, 2307.11877

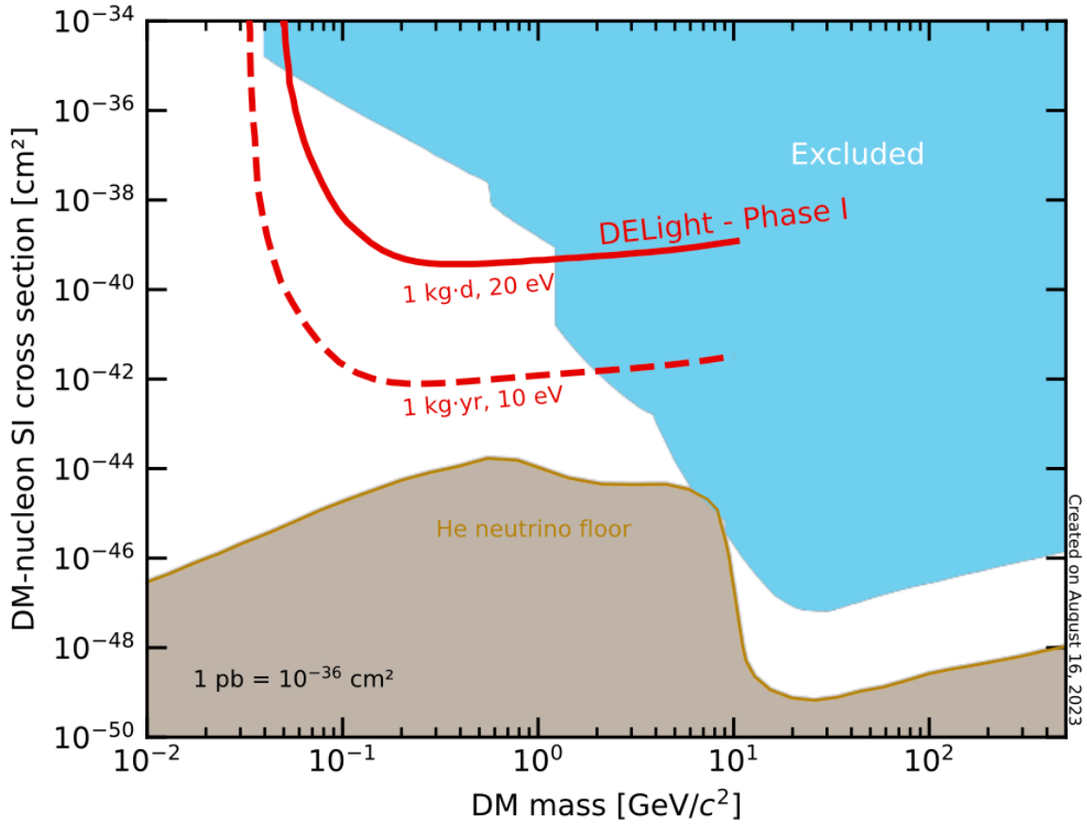

SUMMARY

- **Nature of dark matter in the Universe:** still an enigma
- **World-wide concerted efforts:** direct, indirect and accelerator searches
- **Direct DM detection experiments:** must cover an enormous range in dark matter masses & cross sections
- **Principal challenges**: reduce energy thresholds further (with existing and new technologies & materials), reduce/ understand backgrounds, increase target masses
- **Main goals:** discover a new, dark species & explore the parameter space until solar and cosmic neutrinos will dominate event rates
- Explore **a variety of DM candidates** (WIMPs, LDM, ALPs, dark photons, etc) & break new grounds in neutrino physics, solar axions, etc

2033 (??) PARTICLE LISTINGS

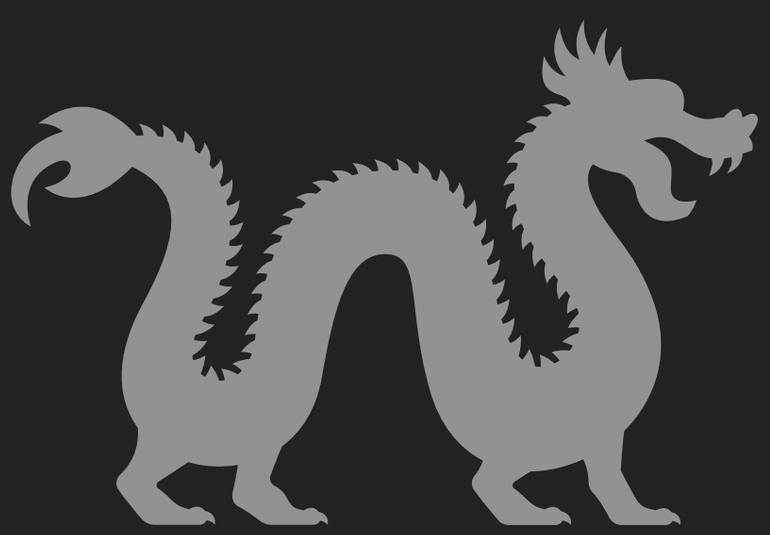

- Mass =?
- J = ?
- $\tau >$?
- $\sigma(\chi + \bar{\chi} \rightarrow SM + SM) =$?
- $\sigma(\chi + SM \rightarrow \chi + SM) =$?
- ...